

Recent and Ongoing Developments in LS-DYNA

John O. Hallquist, Thomas Borrvall, Thomas Klöppel

Jason Wang, Cheng-Tang Wu, Inaki Caldichoury,

Xinhai Zhu, Yun Huang, and Isheng Yeh



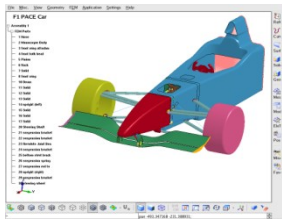
14th LS-DYNA International Conference

June 2016, Detroit, Michigan

Outline

- Introduction
- Developments Sweden Thomas Borrvall
- Developments Germany Thomas Klöppel
- Particle Methods Jason Wang
- Meshfree Methods Cheng-Tang Wu
- ICFD, CFD, Electromagnetics Inaki Caldichoury
- Metal Forming Xinhai Zhu
- Frequency Domain Yun Huang
- Control Systems & Summary Isheng Yeh

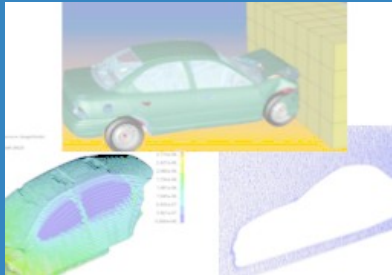
LSTC Products



LS-PrePost


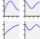




Dummies & Barriers

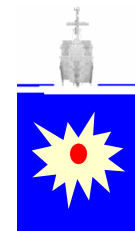


LS-DYNA



-  Surface
-  2D Interpolator
-  Accuracy
-  Sensitivity

LS-OPT/LS-TaSC



USA



No additional license cost

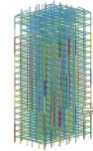
LS-DYNA Applications

Development costs are spread across many industries



Automotive

Crash and safety
NVH & Durability
FSI



Structural

Earthquake safety
Concrete structures
Homeland security



Aerospace

Bird strike
Containment
Crash



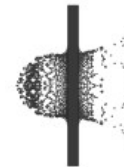
Electronics

Drop analysis
Package analysis
Thermal



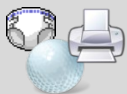
Manufacturing

Stamping
Forging
Welding



Defense

Weapons design
Blast and Penetration



Consumer Products



Biosciences

LS-DYNA - Current Capabilities

Includes coupled Multi-Physics, Multi-Scale , and Multi-Stage in one Scalable Code



Explicit/Implicit



Heat Transfer



ALE & Mesh Free

i.e., EFG, SPH, Airbag Particle



User Interface

Elements, Materials, Loads



Acoustics, Frequency Response,
Modal Methods



Discrete Element Methods



Incompressible Fluids



CESE Compressible Fluids

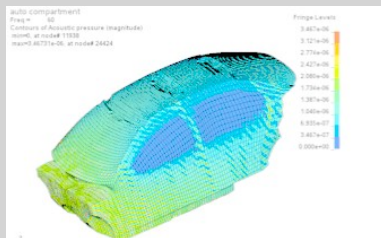
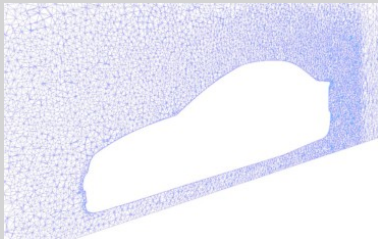


Electromagnetics



Control Systems

LS-DYNA - One Code, One Model



Single Model for Multiple Disciplines

Manufacturing, Durability, NVH, Crash, FSI

Multi-physics and Multi-stage

Structure + Fluid + EM + Heat Transfer

Implicit + Explicit

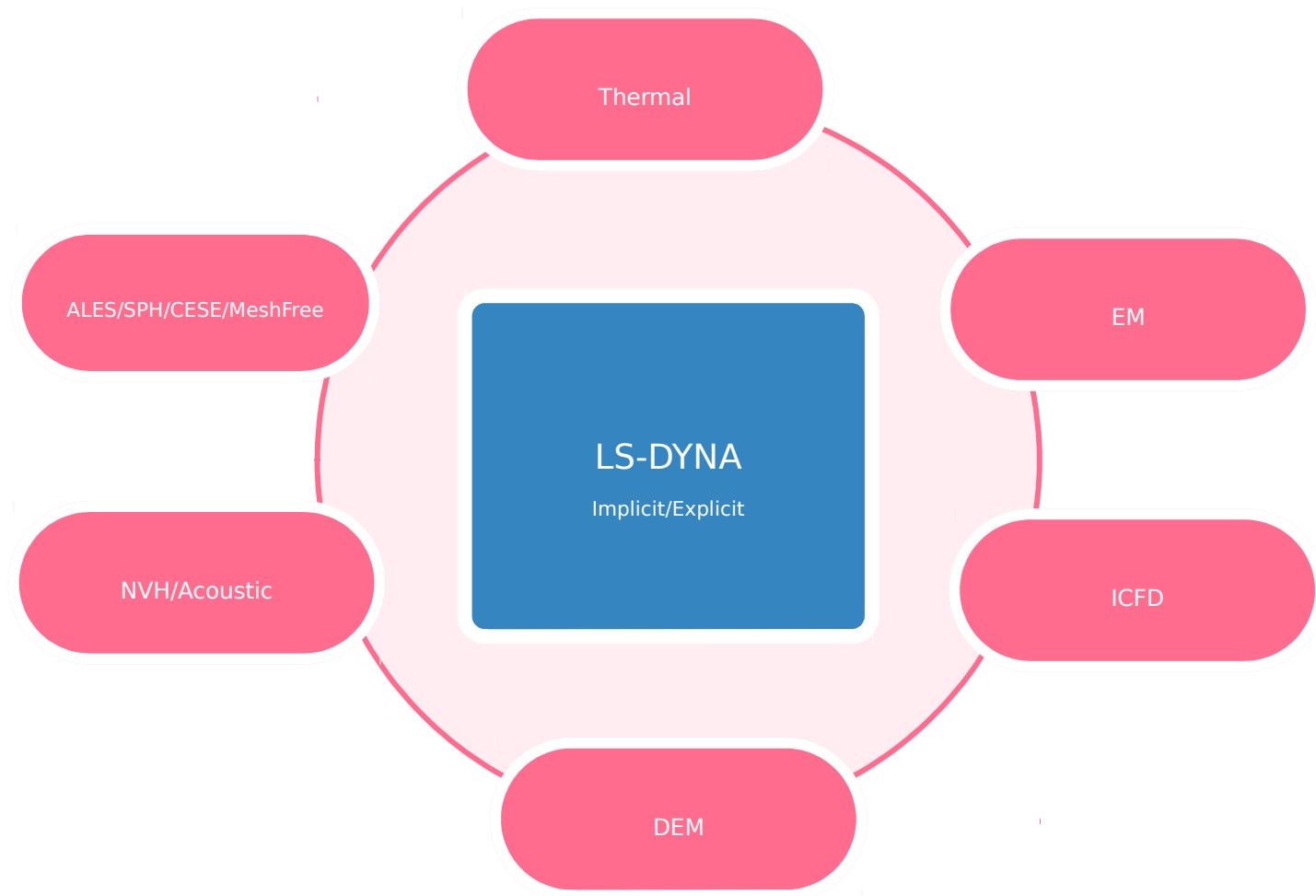
Multi-scale

Failure predictions, i.e., spot welds

Multi-formulations

linear + nonlinear + peridynamics + ...

Strong Coupled Multi-Physics Solver



Computers that can handle multiphysics simulations are becoming affordable
Scalability is rapidly improving for solving multi-physics Problem

European Developments

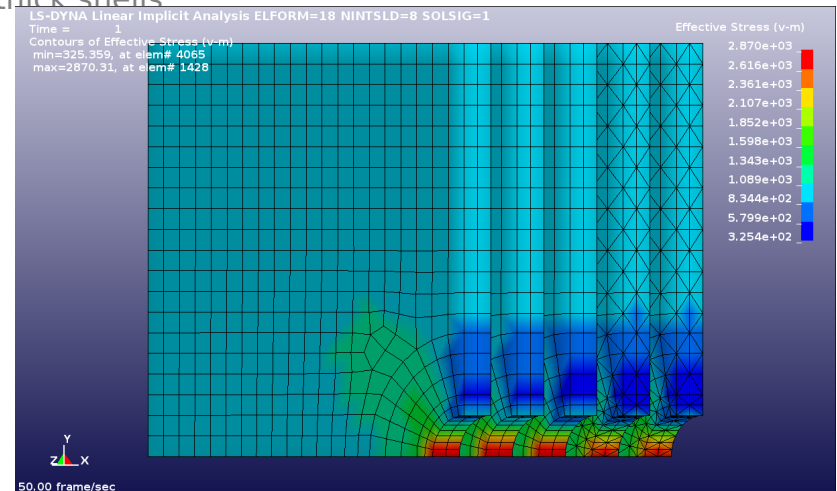
Thomas Borrvall Sweden

Jesper Karlsson

Anders Jernberg

Mortar Contact for Lagrangian/Classical FEM

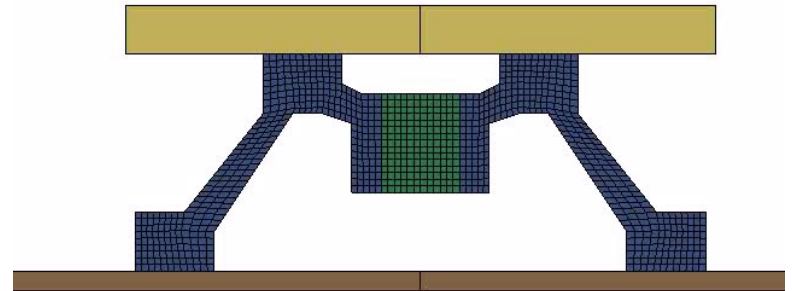
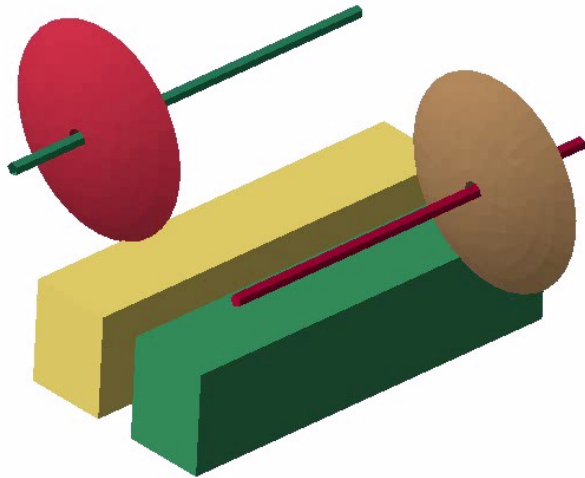
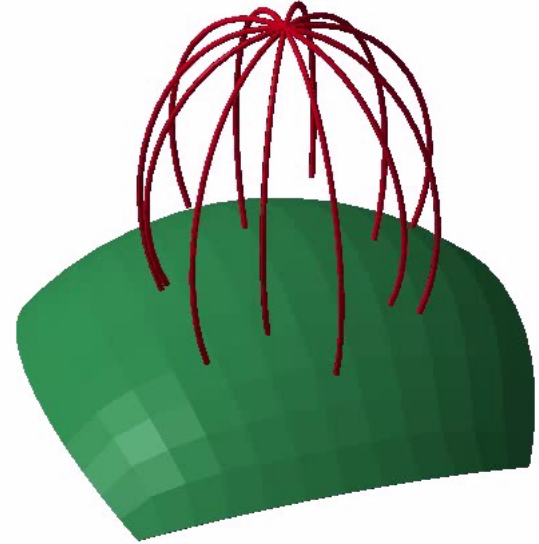
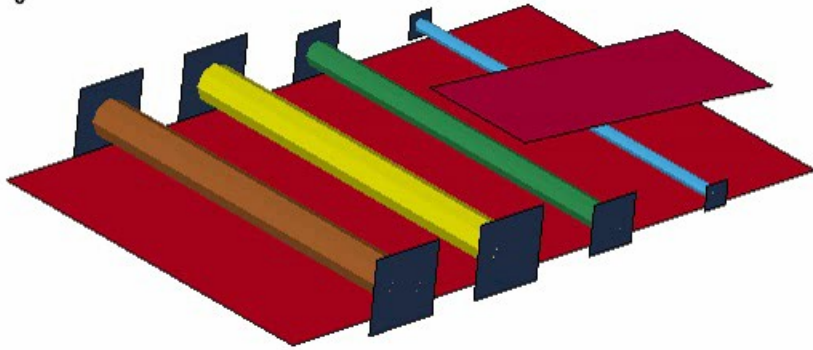
- Goal to make it simple and universal with minimal options
 - Additional CPU time for increased accuracy
- Features and recent developments
 - Segment to Segment with Accurate Contact Stress Integration
 - Element Types Supported
 - Solids, Shells, Beams, Thick Shells, 2D solids (2D in SMP Implicit *only*)
 - Physical Geometry Contact
 - Flat edges on shells
 - Beams are cylinders with flat ends
 - Couples to rotations for beams to exert moments
 - Contact with sharp edges on solids and thick shells
 - Friction
 - Table, part and dynamic friction
 - Wear
- Ongoing work
 - Implicit
 - High Order Element support
 - Explicit
 - Bucket sort frequency
 - SMP parallelism and Hybrid support



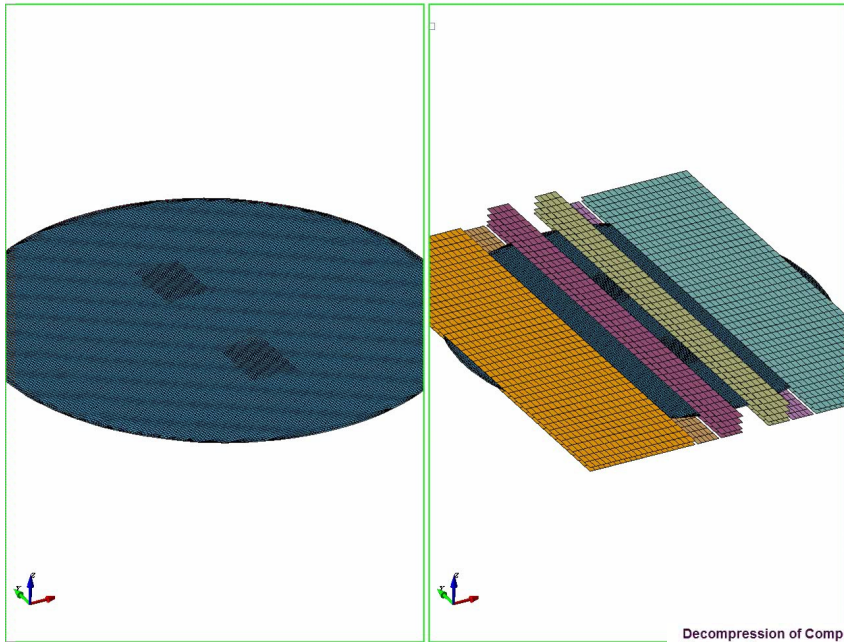
Implicit Examples



LS-DYNA keyword deck by LS-PrePost
Time = 0

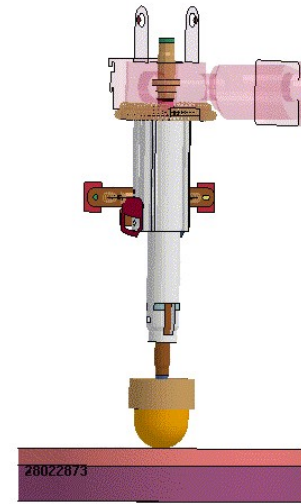


Explicit Examples

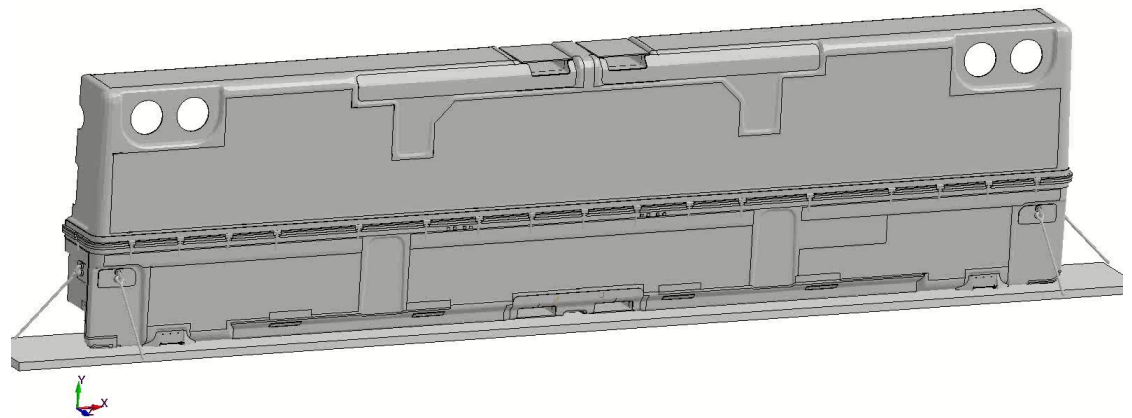


Decompression of Composite Container
Time = 0

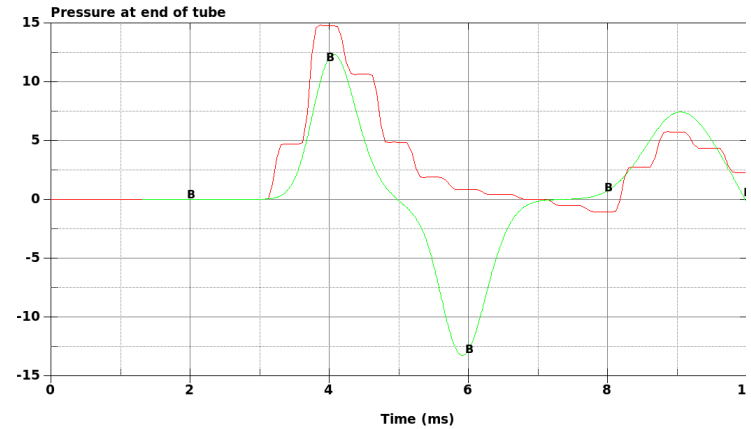
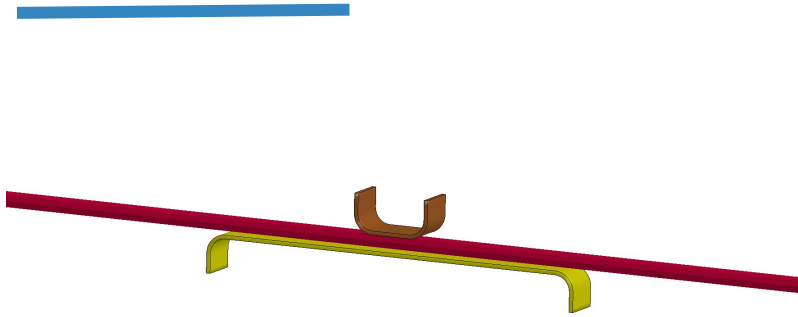
Time = 0



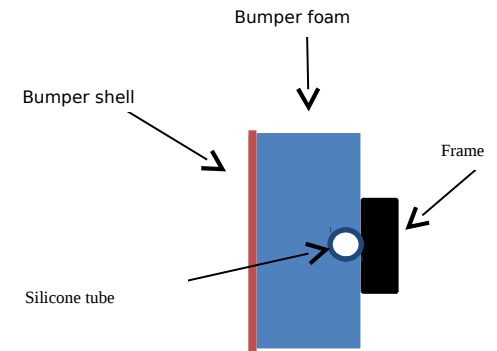
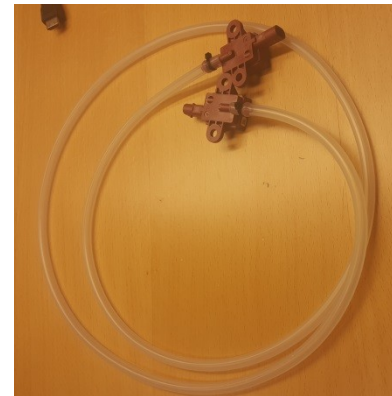
Jensen et al,
"Broad-Spectrum Stress and Vibration Analysis of
Large Composite Container"



Pressure Tube

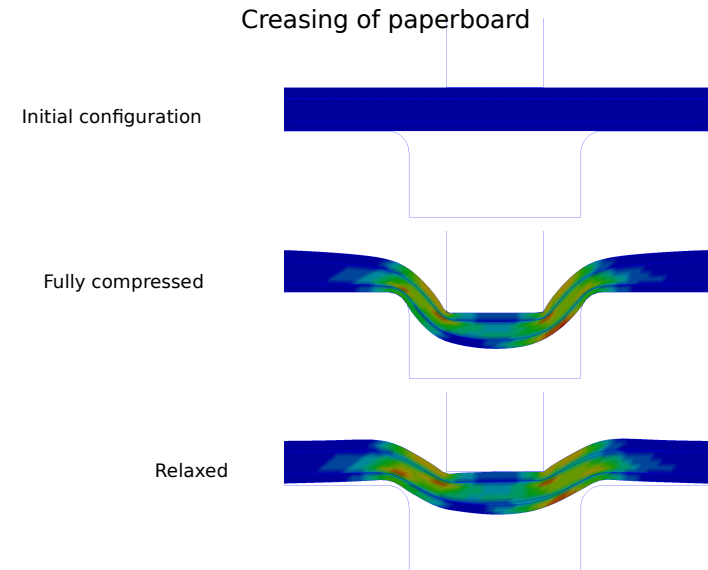
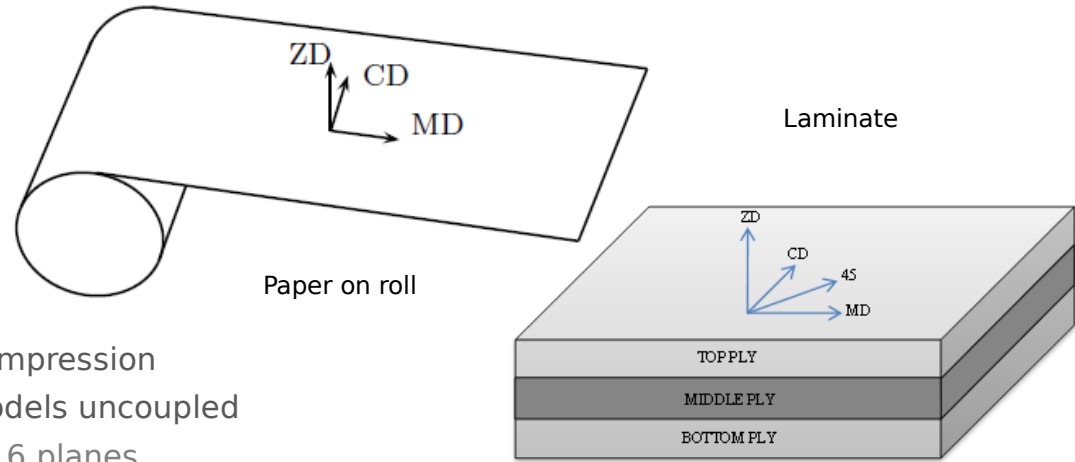


- ***DEFINE_PRESSURE_TUBE**
 - Air filled silicone tube embedded in bumper foam
 - Pressure sensors at tube ends detects crash
- Acoustic approximation of 1D compressible Euler for pipes with varying cross section area
- Tube defined by beam elements, area changes due to contact penetration



Paperboard Modeling

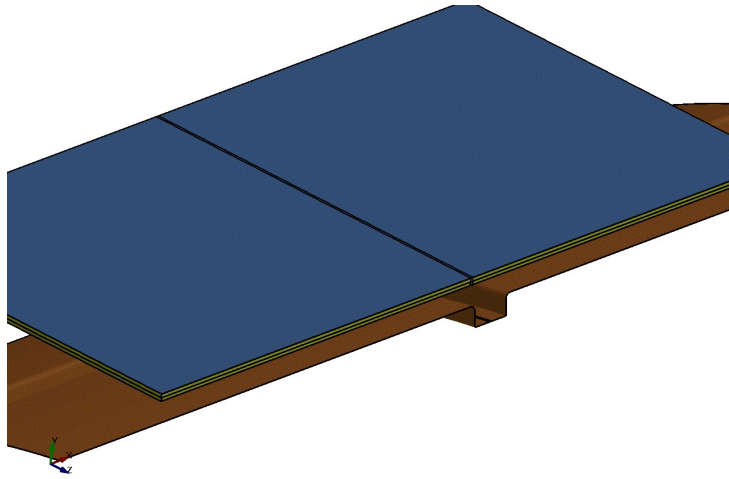
- For shell or solid modeling
- ***MAT_PAPER (*MAT_274)**
 - Hyp(er/o)elastic-plastic orthotropic model
 - Out-of-plane elasticity non-linear in compression
 - In-plane and out-of plane plasticity models uncoupled
 - In-plane yield surface consists of 6 planes (tension/compression in MD,CD,MD/CD)
 - Out-of-plane yield surfaces in compression and transverse shear
- ***MAT_COHESIVE_PAPER (*MAT_279)**
 - For modeling delamination in conjunction with *MAT_PAPER and shells
 - In-plane and out-of-plane models uncoupled
 - Normal compression nonlinearly elastic
 - Normal tension and tangential traction given by elastoplastic traction-separation law



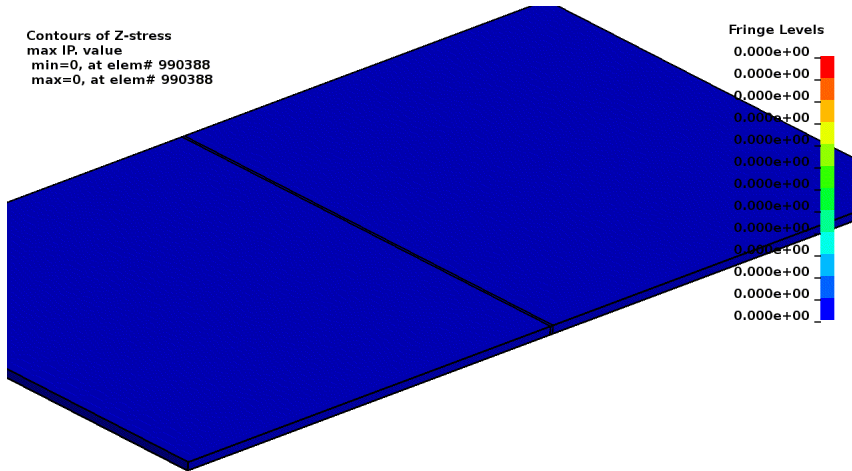
Jesper Karlsson,

"Two New Models for Paperboard Materials"

Rotational Creasing Simulation and Forming



Contours of Z-stress
max IP. value
min=0, at elem# 990388
max=0, at elem# 990388



Fringe Levels
0.000e+00
0.000e+00
0.000e+00
0.000e+00
0.000e+00
0.000e+00
0.000e+00
0.000e+00
0.000e+00
0.000e+00
0.000e+00
0.000e+00
0.000e+00
0.000e+00



Implicit Development – General Overview

- Linear Solvers

- Linear Algebra team constantly working on efficiency related issues
- Expand range of applications
- *Nonsymmetric solver available*

- Nonlinear Solver

- *New default in R9.0*
- Minimize total number of iterations and stiffness reformations
 - BFGS
 - Robust line search
 - Cut-back strategies
 - Tolerances

- Features

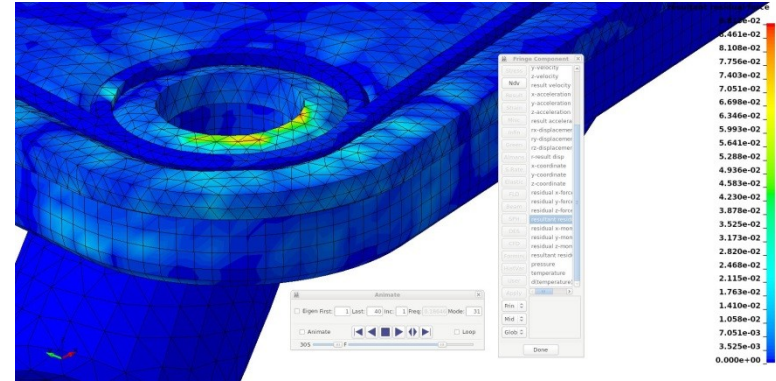
- Think different
 - Accurate Modeling improves robustness and convergence
 - Speed not as important as in explicit analysis

- Output

- Facilitate debugging
 - Binary d3iter (graphical) and ascii message (text)
 - Implstat in LS-PrePost

- Documentation

- Appendix P and Theory Manual
 - Implicit Guide
 - Nonlinear implicit and mortar contact theory



```

Contact sliding interface           1
Number of contact pairs           16209

Maximum penetration is 0.5027372E+00 between
elements 219492 and 94935 on this processor

Maximum relative penetration is 0.1005474E+03 % between
elements 219492 and 94935 on this processor
*** Warning Penetration is close to maximum before release

Contact sliding interface           2
Number of contact pairs           11932

Maximum penetration is 0.5007380E+00 and occurs
on some other processor

Maximum relative penetration is 0.1001476E+03 % and occurs
on some other processor
*** Warning Penetration is close to maximum before release

Contact sliding interface           3
Number of contact pairs           0

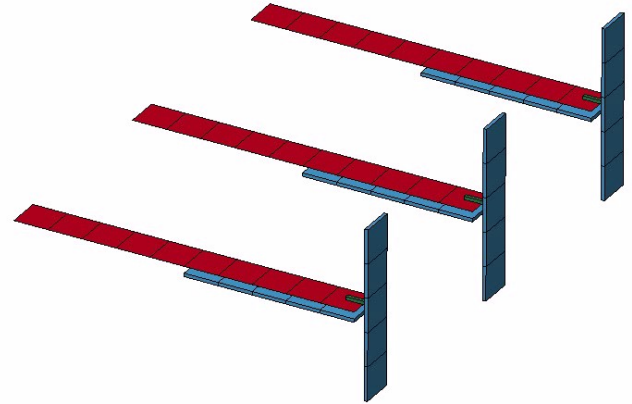
Contact sliding interface           4
Number of contact pairs           776

Maximum penetration is 0.3886436E+00 between
elements 205048 and 224238 on this processor

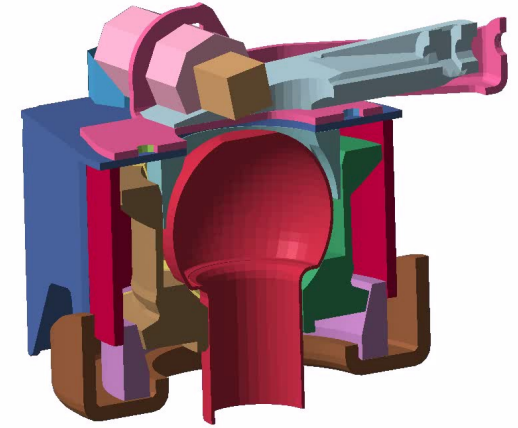
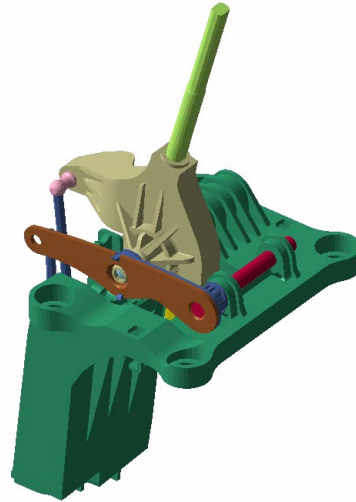
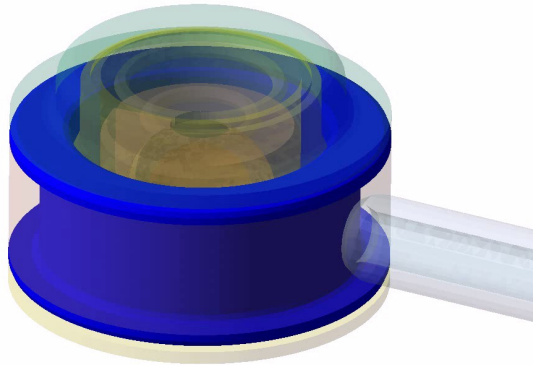
Maximum relative penetration is 0.7772871E+02 % between
elements 205048 and 224238 on this processor
    
```

Implicit Accuracy

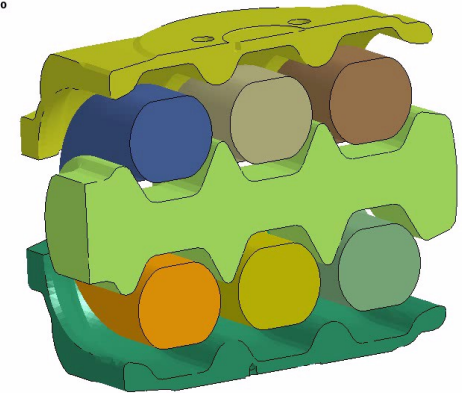
- Implicit accuracy option
IACC=1 on
*CONTROL_ACCURACY
 - Higher accuracy in selected material models
 - Fully iterative plasticity
 - Tightened tolerances
 - Strong objectivity and consistency in selected tied contacts
 - Physical (only ties to degrees of freedoms that are "real") - bending/torsion whenever applicable
 - Finite rotation
 - Strong objectivity and increased accuracy in selected elements
 - Finite rotation support for hypoelasticity
- In line with the general philosophy "Increased accuracy implies better convergence"



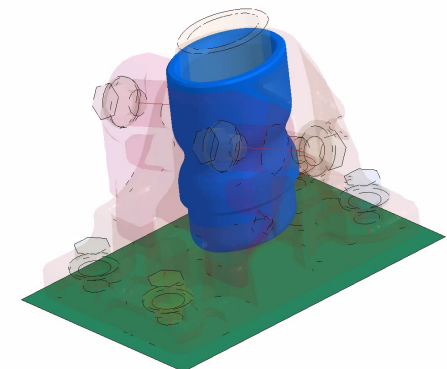
Typical Implicit Applications



Time = 0



Time = 0
Contours of Pressure
reference shell surface
min=-1.44862e-16, at elem# 7029847
max=1.17269e-16, at elem# 7020664



Fringe Levels
7.000e-01
6.189e-01
5.377e-01
4.566e-01
3.755e-01
2.943e-01
2.132e-01
1.320e-01
5.091e-02
-3.023e-02
-1.114e-01

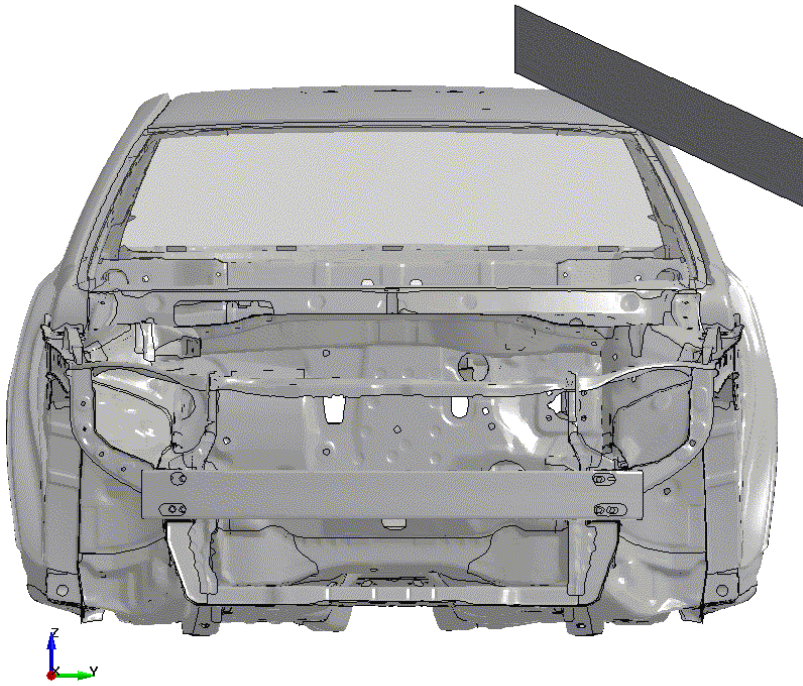
- Characterized by
 - Contacts
 - High order elements
 - Rubbers
 - Prestress
 - Inteferece
 - Initial stress/force

Courtesy of Kongsberg Automotive, Thule Sweden,
Volvo GTT and Dellner Couplers



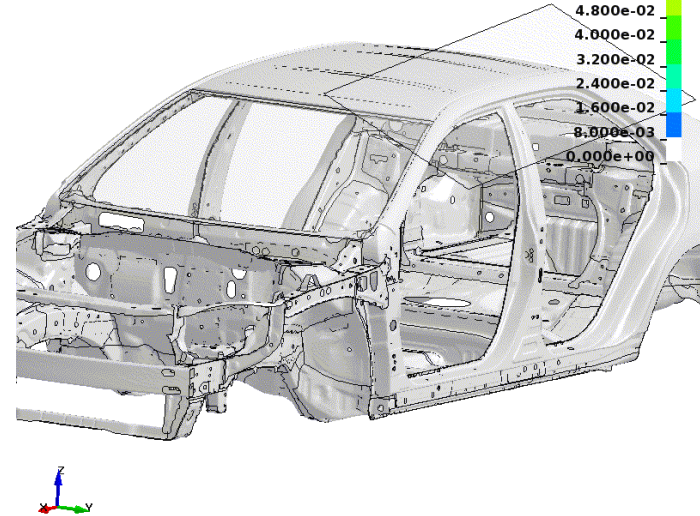
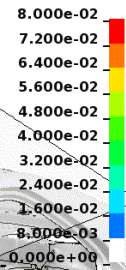
Implicit Roof Crush

LS-DYNA keyword deck by LS-PrePost
Time = 0

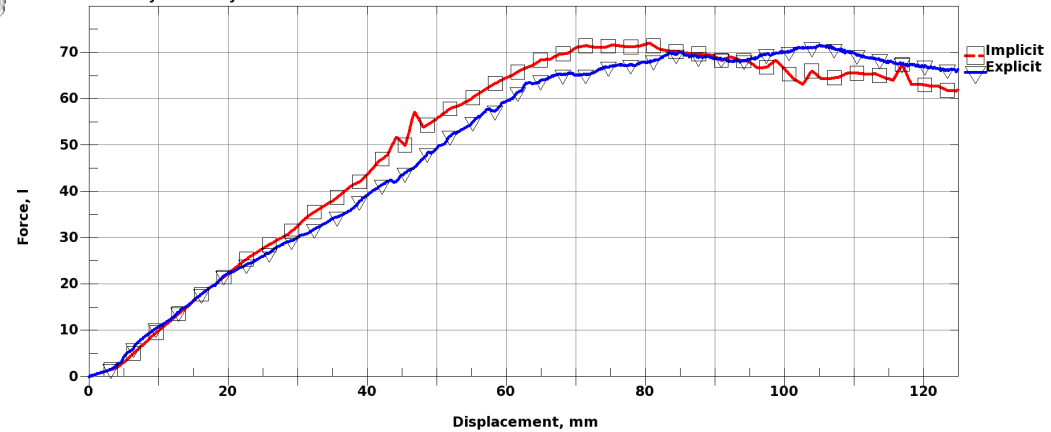


LS-DYNA keyword deck by LS-PrePost
Time = 0
Contours of Effective Plastic Strain
max IP. value
min=0, at elem# 50000001
max=0, at elem# 50000001

Effective Plastic Strain



2012 Toyota Camry NCAC model - Static Roof-Crush test



- No speed up
- Robust
- Comparable to explicit

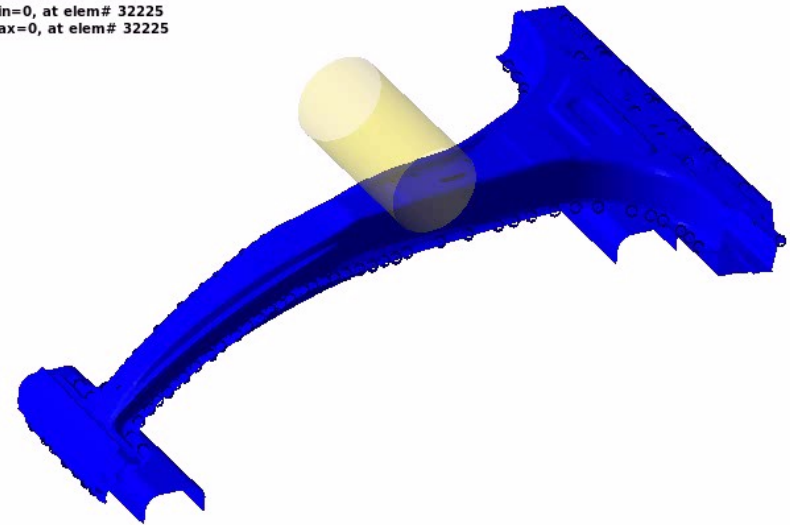
Satish Pathy and Thomas Borrvall,

"Quasi-Static Simulations using Implicit LS-DYNA"

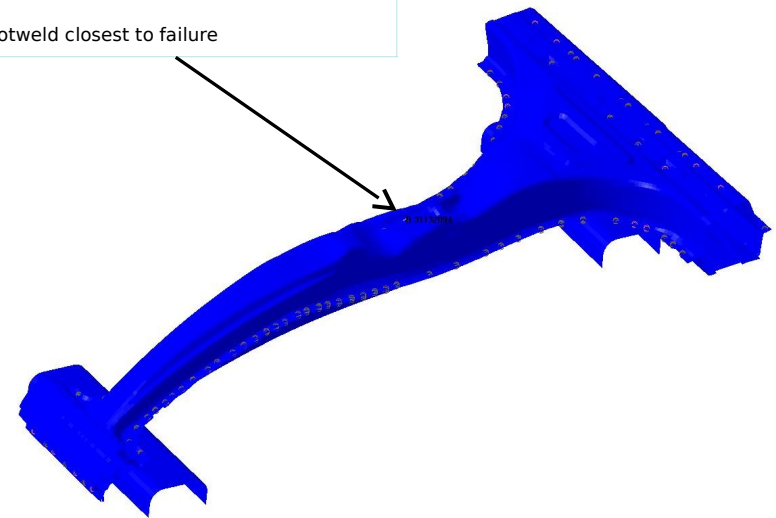
History Management

- Purpose, to facilitate and organize the post-processing of history variables in the d3plot database
- *DEFINE_MATERIAL_HISTORIES
 - Allows to customize the history variable output
 - Instability
 - Damage
 - Plastic strain rate
 - Select a certain historyvariable in a given part and material
- A given history variable # will correspond to the specific quantity listed in the keyword
 - No contamination by combination of materials
 - Effective plastic strain *is* effective plastic strain

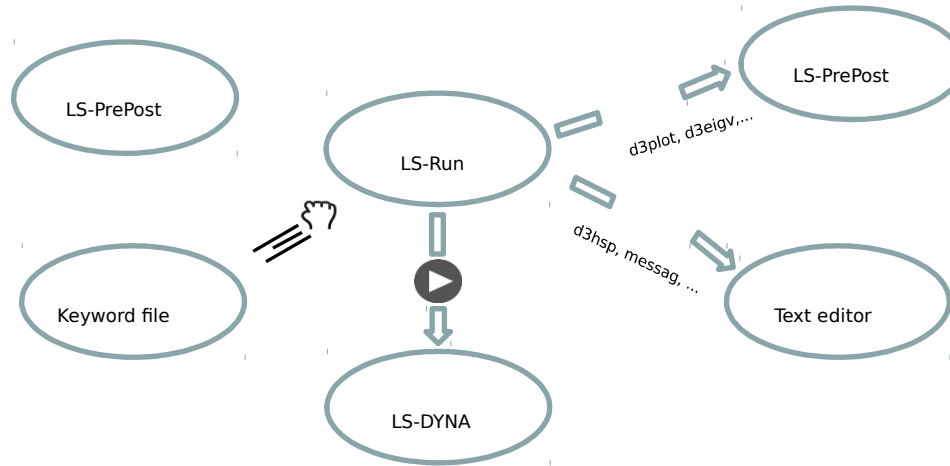
Contours of Effective Plastic Strain
max IP, value
min=0, at elem# 32225
max=0, at elem# 32225



Spotweld closest to failure



LS-Run



Parametric Command Line

Launch Jobs

ID	Input File	Run Command	Status
40	Z:\home\anders\download\beam.k	"C:\LSDYNA\program\ls-dyna_smp_d_R711_winx64_ifort131.exe"	Finished (Normal Term)
39	Z:\home\anders\download\beam.k	"C:\LSDYNA\program\ls-dyna_smp_d_R711_winx64_ifort131.exe"	Finished (Normal Term)
38	C:\Users\anders\Desktop\hemi\hemi.k	"C:\LSDYNA\program\ls-dyna_smp_d_R711_winx64_ifort131.exe"	Finished (Normal Term)
37	C:\Users\anders\Desktop\hemi\hemi.k	"C:\LSDYNA\program\ls-dyna_smp_d_R711_winx64_ifort131.exe"	Finished (Normal Term)
36	C:\Users\anders\Desktop\dynatest\airbagd	"C:\LSDYNA\program\ls-dyna_smp_d_R711_winx64_ifort131.exe"	Finished (Normal Term)
35	C:\Users\anders\Desktop\dynatest\airbagd	"C:\Users\anders\Desktop\ls run\ls-dyna_smp_s_R700_w"	Finished (Normal Term)

Administrative and View Jobs

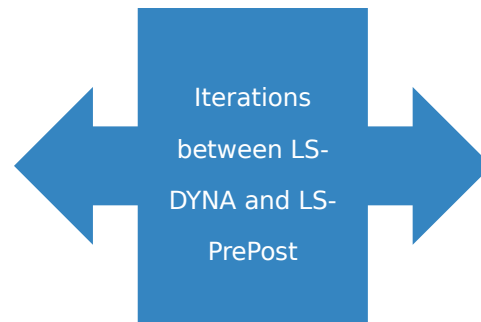
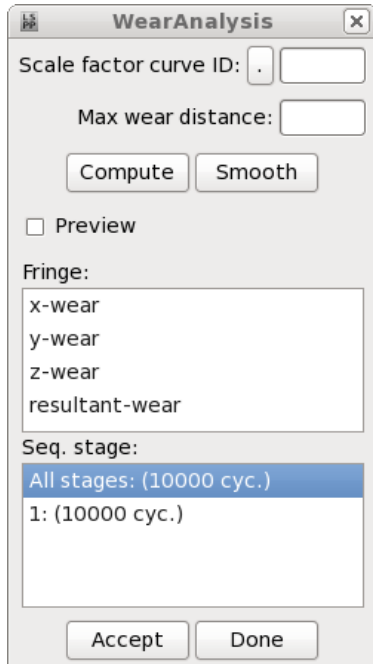
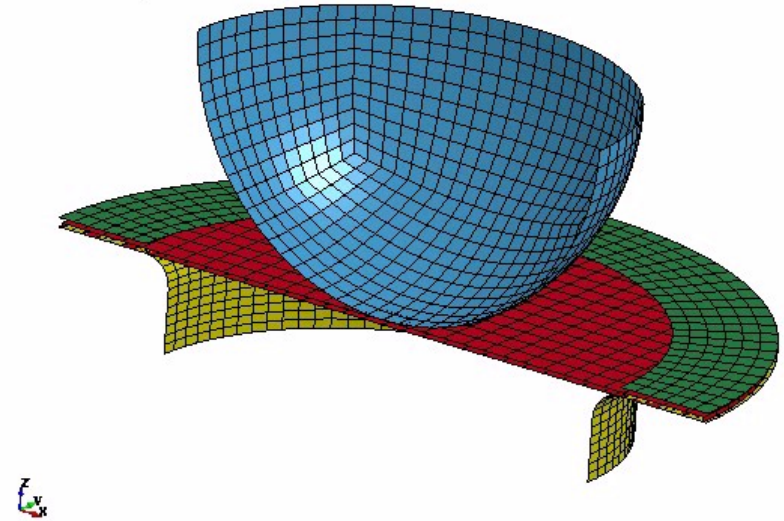
Queuing Jobs

Wear Processes

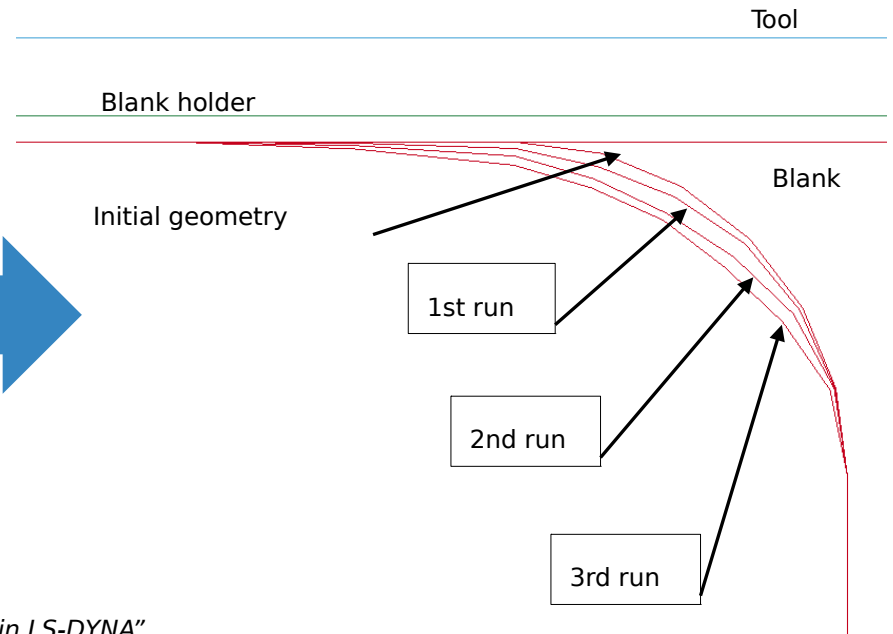
*CONTACT_ADD_WEAR

- Archard and User wear laws
- Post process wear in LS-PrePost
- Modify geometry in LS-PrePost based on wear, using *INITIAL_CONTACT_WEAR

Wear simulation example
Time = 0, #nodes=4779, #elem=4521



Borrvall et al,
"Simulation of Wear Processes in LS-DYNA"



European Developments

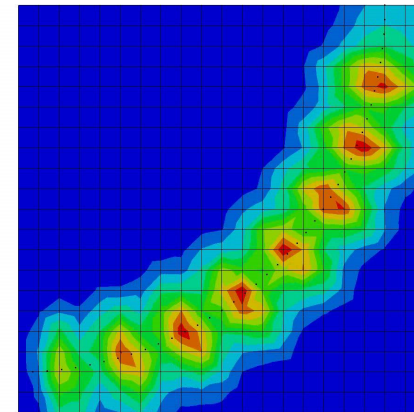
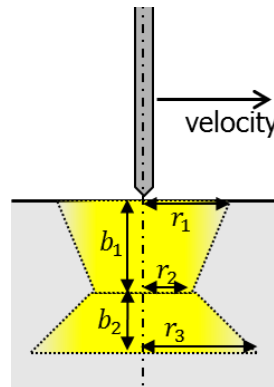
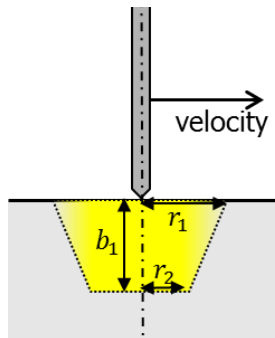
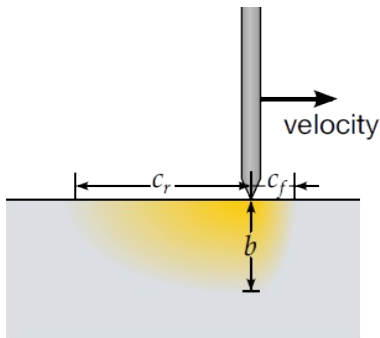
Thomas Klöppel Germany

Tobias Erhart

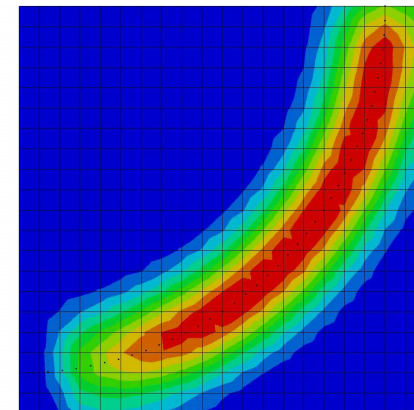
Stefan Hartmann

*BOUNDARY_THERMAL_WELD_TRAJECTORY

- Define a heat source motion along a trajectory (nodal path) with a prescribed velocity
- Works in thermal-only and coupled analyses (SMP and MPP)
- Weld beam aiming direction can be defined
 - By a constant vector
 - Normal to a segment set
 - By a second trajectory
- Applicable to solids and thermal thick shells
- User can choose from a list of pre-defined equivalent heat sources



temperature
no damping

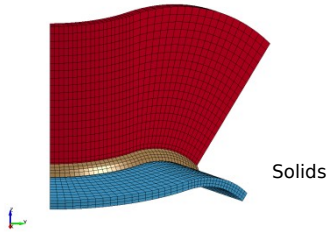


temperature
with damping

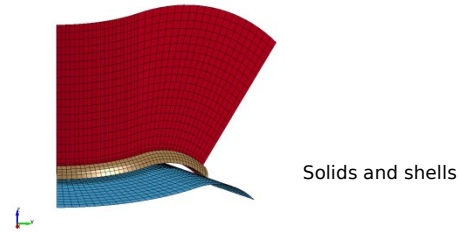
*BOUNDARY_THERMAL_WELD_TRAJECTORY

Example: Three-dimensional curved T-Joint, thermal-only analysis

LS-DYNA keyword deck by LS-PrePost
Time = 0

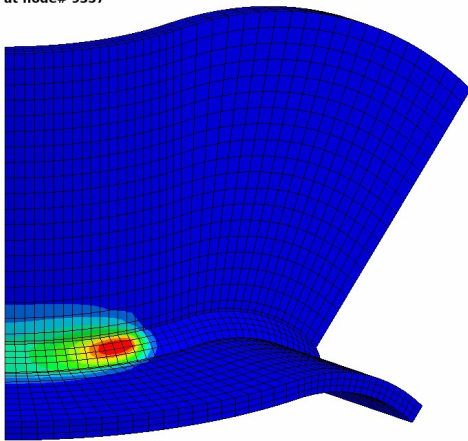


LS-DYNA keyword deck by LS-PrePost
Time = 0



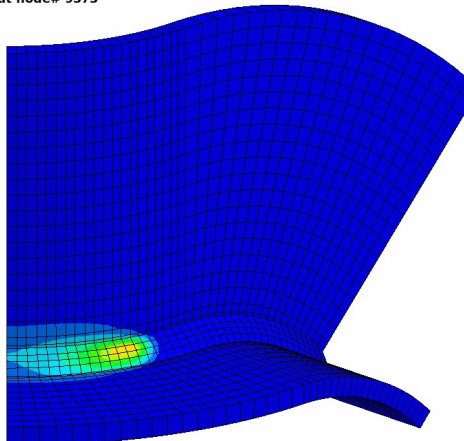
LS-DYNA keyword deck by LS-PrePost

Time = 0.99484
Contours of Temperature, outer
min=19.9881, at node# 9540
max=153.564, at node# 9357



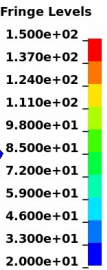
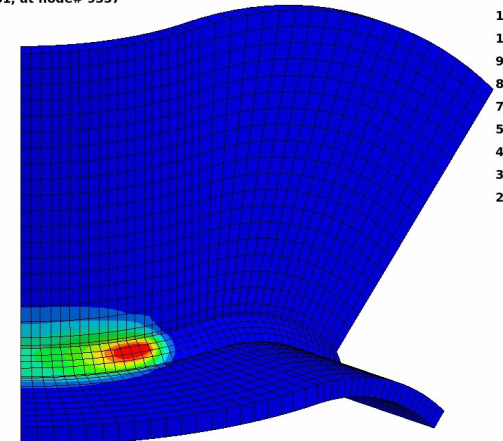
LS-DYNA keyword deck by LS-PrePost

Time = 0.99484
Contours of Temperature, outer
min=19.9777, at node# 9535
max=123.47, at node# 9373



LS-DYNA keyword deck by LS-PrePost

Time = 0.99484
Contours of Temperature, outer
min=19.9634, at node# 9535
max=154.901, at node# 9357



Welding pre-processor in LS-PREPOST

- Easy to set the weld order, properties and choose boundary conditions for each process stage
- Weld path and direction identified by beam elements
- Color green indicates completed input
- Version 4.3 in LS-PREPOST

Sequence	Welds	Struct. B.C.	Therm. B.C.		
		1	2	3	4
== Welds ==					
6 Weld Pass 1					
8 Weld Pass 2					
Springback					
== Struct. B.C. ==					
2 edge x					
3 edge z					
4 edge2 z					
5 edge y					
6 sb xyz					
7 sb xz					
8 sb z					
== Therm. B.C. ==					
Air segm.					
1 Table					

6 Weld Pass 1
8 Weld Pass 2
Springback

Path

- Pick weld path
- Pick weld start
- Pick orientation path
- Pick orientation start

Weld pool geometry

Ellipsoid

a: 4
b: 5
cf: 4
cr: 4
Ff: 1
Fr: 1
n: 3

Apply Unify DISC: 0.5

Weld stroke

Velocity: 3.33
Weld Power: 4e+006
Eff. factor: 1
Step/ele: 0.375
NCYC: 4
Cooldown Time: 5

Thermal only

Apply Unify

*MAT_254 / *MAT_GENERALIZED_PHASECHANGE

- Very general material implemented to capture micro-structure evolution in welding and heat treatment
- Up to 24 individual phases
- For any of the possible phase transformation user can chose from a list of generic phase change mechanisms:

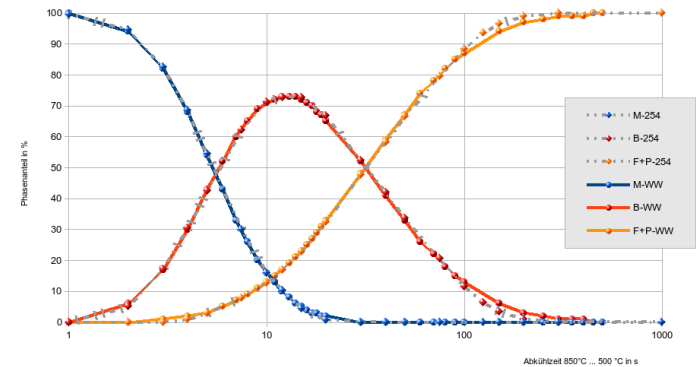
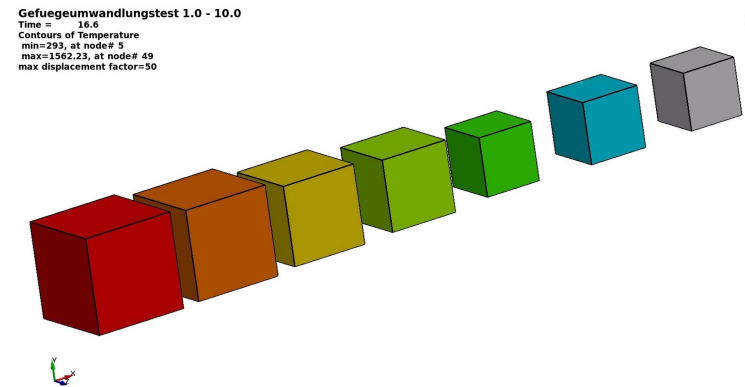
- Leblond,
- JMAK,
- Koistinen-Marburger,
- Kirkaldy,
- Oddy, ...

- Parameters for transformation law are directly given in tables

- Additional features:

- Transformation induced strains
- Transformation induced plasticity (TRIP)
- Temperature and strain rate dependent plasticity

- Ongoing development



- Curing of epoxy adhesives and implied changes of mechanical behavior
- Curing kinetics computed with the Kamal model for degree of cure α :
- Viscoelastic material with Prony-series representation

= State of cure dependence

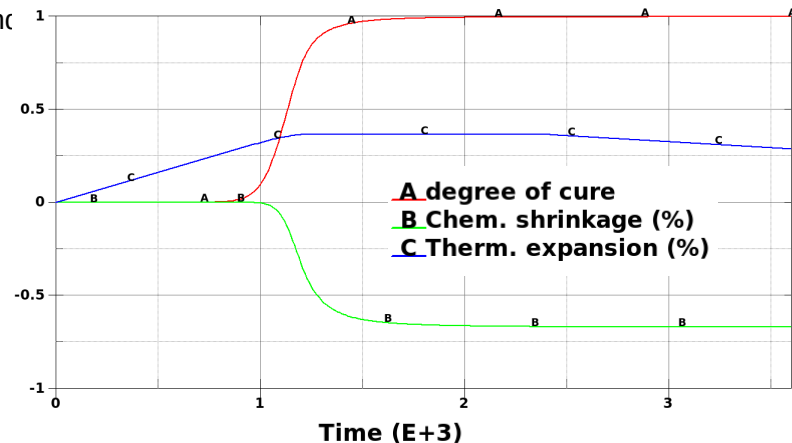
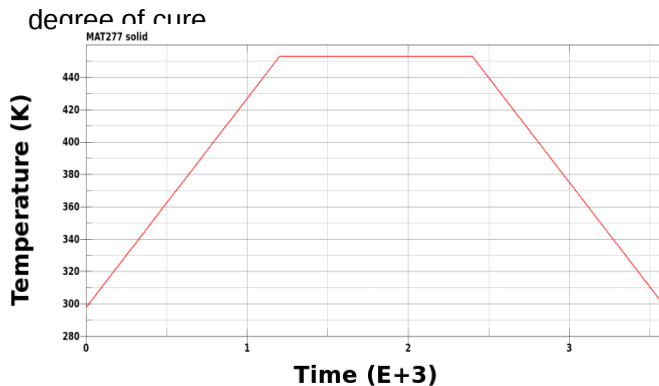
$$G(t, \alpha) = G_{\infty}(\alpha) + \sum_{i=1}^N G_i(\alpha) e^{-t/\tau_i} = G_0(\alpha) \left(1 - \sum_{i=1}^N \frac{G_i(\alpha_{1.0})}{G_0(\alpha_{1.0})} (1 - e^{-\beta_i t}) \right)$$

- WLF shift based on temperature

- WLF shift based on temperature

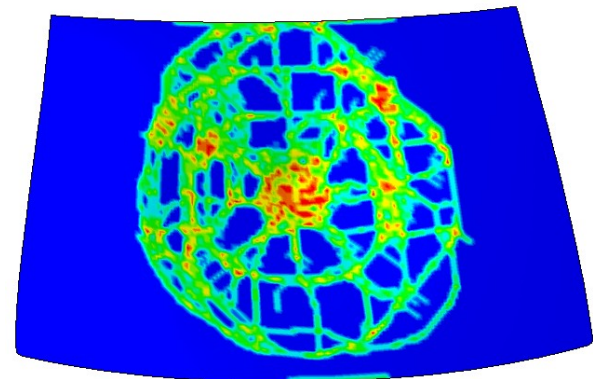
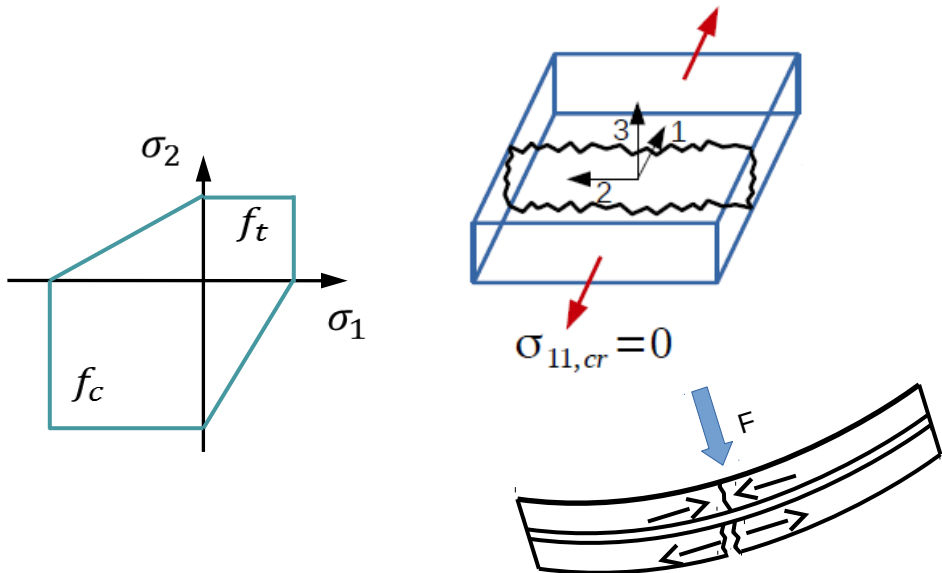
$$\tau_i(T) = a_T(T) \cdot \tau_{i,0}, \quad \ln a_T = \frac{-A(T - T_{ref})}{B + (T - T_{ref})}$$

- Chemical shrinkage as function of state of cure α
- Chemical shrinkage as function of state of cure
- Coefficient of thermal expansion as function of temperature T and degree of cure α
- Coefficient of thermal expansion as function of temperature and degree of cure α



*MAT_280 / *MAT_GLASS

- New material model for fracture of glass
- Developed as user material, now implemented as *MAT_280
- Brittle smeared fixed crack model for shell elements (plane stress)
- Failure criteria: Rankine, Mohr-Coulomb, Drucker-Prager, ...
- Incorporates up to 2 cracks, simultaneous failure over thickness, crack closure effect (no element deletion), ...



*MAT_ADD_GENERALIZED_DAMAGE (MAGD)

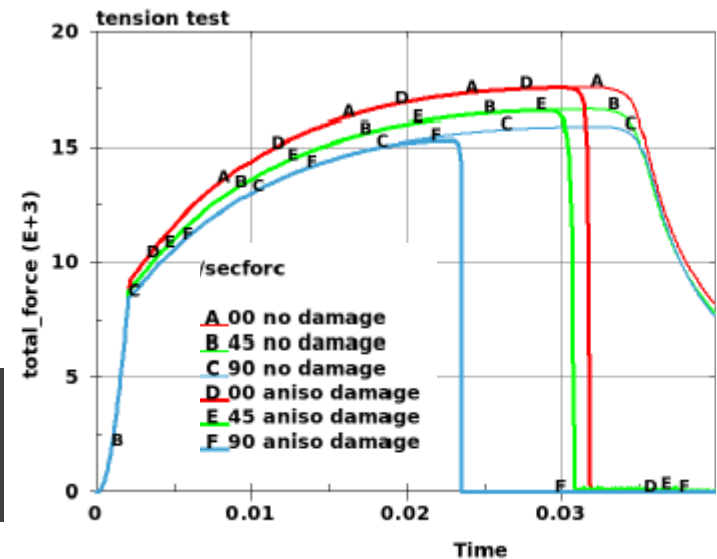
- General damage model as add-on for other material models
- Intention: non-isotropic damage as in aluminum extrusions, composites, ...
- Up to 3 history variables as damage driving quantities (“multiple GISSMO”)
- Very flexible due to input via *DEFINE_FUNCTIONS

$$\begin{bmatrix} \sigma_{11} \\ \sigma_{22} \\ 0 \\ \sigma_{12} \\ \sigma_{23} \\ \sigma_{31} \end{bmatrix} = \begin{bmatrix} D_{11} & D_{12} & 0 & D_{14} & 0 & 0 \\ D_{21} & D_{22} & 0 & D_{24} & 0 & 0 \\ 0 & 0 & D_{33} & 0 & 0 & 0 \\ D_{41} & D_{42} & 0 & D_{44} & 0 & 0 \\ 0 & 0 & 0 & 0 & D_{55} & 0 \\ 0 & 0 & 0 & 0 & 0 & D_{66} \end{bmatrix} \begin{bmatrix} \tilde{\sigma}_{11} \\ \tilde{\sigma}_{22} \\ 0 \\ \tilde{\sigma}_{12} \\ \tilde{\sigma}_{23} \\ \tilde{\sigma}_{31} \end{bmatrix}$$

```
*DEFINE_FUNCTION
```

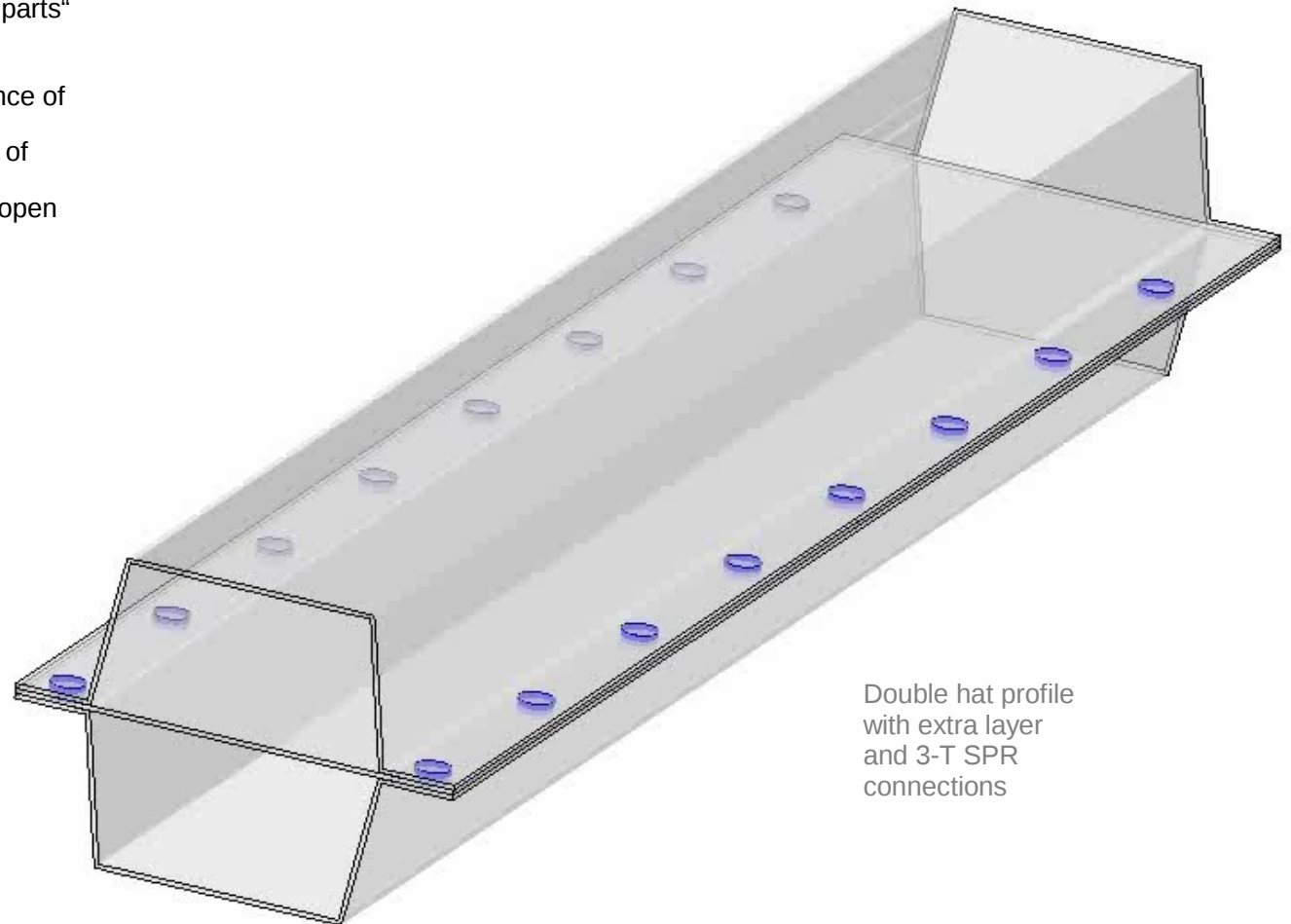
```
101
```

```
Func101(d1, d2, d3)=1.0-d1
```



*CONSTRAINED_SPR2

- Multi-sheet connection for self-piercing rivets
- Before: only 2 parts (master and slave)
- Now: up to 4 additional “extra parts”
- Question about interdependence of connections and reproduction of experimental results remains open
- Ongoing development ...



Double hat profile
with extra layer
and 3-T SPR
connections

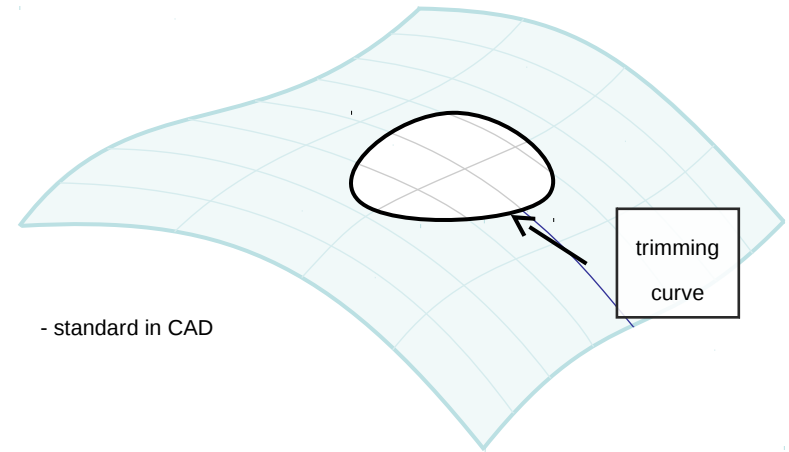
*CONTACT_AUTOMATIC_..._TIEBREAK_USER

- User-defined interface for tiebreak contact
- Alternative models to Dycoss and others can be implemented
- Available for SMP and MPP

```
subroutine utb101(sig_n,sig_t,disp_n,disp_t,vel_n,vel_t,cn,ct,  
  . uparm,uhis,idcon,idsn,idms,areasn,areams,time,dt2,ncycle,crv,  
  . nnpcrv,temp,ifail,ioffset)  
  
c  
c   User subroutine for tiebreak contact: OPTION=101  
c  
c   Purpose: To define normal and tangential stresses and possible failure  
c             in a contact with tiebreak connection  
c  
c   Variables:  
c  
c   sig_n,sig_t   = normal and tangential stress (output)  
c   disp_n,disp_t = normal and tangential displacement (input)  
c   vel_n,vel_t   = normal and tangential relative velocity (input)  
c   cn,ct         = normal and tangential stiffness (input)  
c   uparm        = user defined tiebreak parameters (input)  
c   uhis         = user defined tiebreak history variables (input/output)  
c   ...
```

*ELEMENT_SHELL_NURBS_PATCH

- Added „trimmed-NURBS“ capability
- Before: only „standard-NURBS“
- Unlimited number of trimming loops (NL)
- supported by LSPP
- Ongoing development ...



*ELEMENT_SHELL_NURBS_PATCH

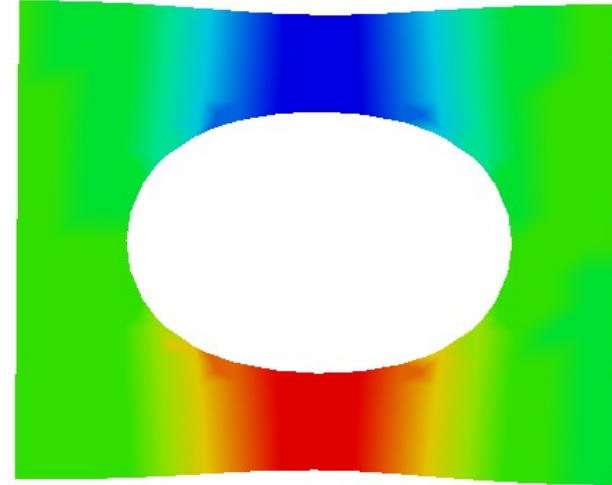
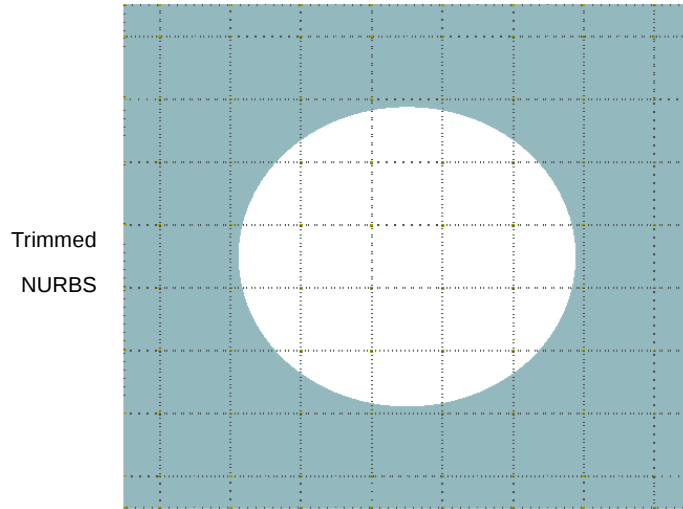
	1	2	3	4	5	6	7	8		
Card 1	NPEID	PID	NPR	PR	NPS	PS				
Card 2	WFL	FORM	INT	NISR	NISS	IMASS	NL			
...										
Card X	NEL									
Card Y	NEL:	E1	number of edges for trimming loop	E2	E3	E4	E5	E6	E7	E8

one trimming loop {

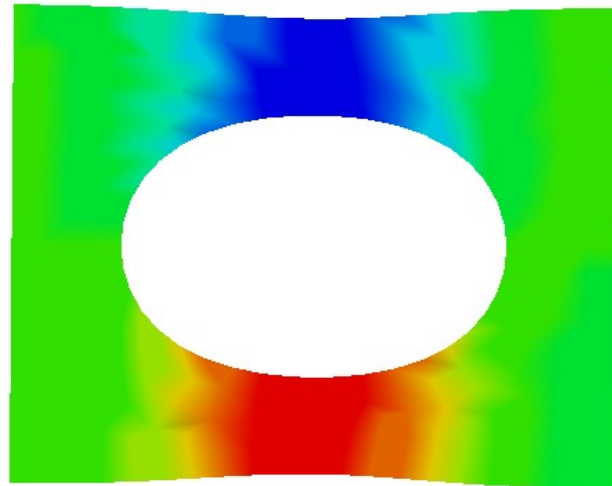
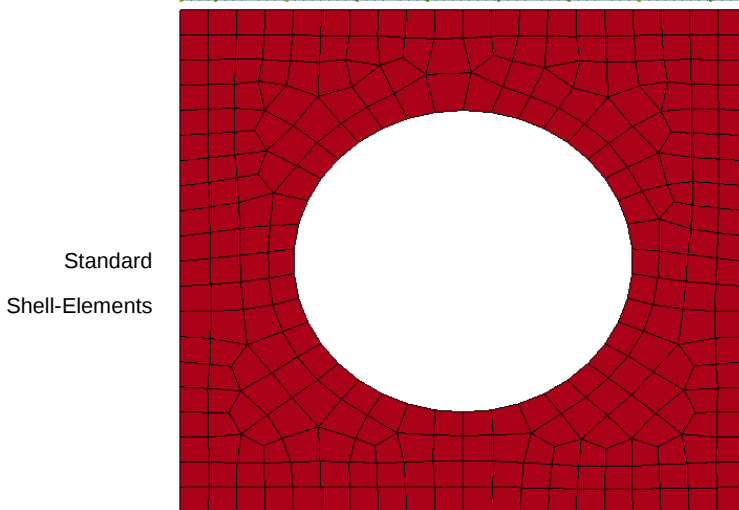
E_i : Edge (Curve) ID defining this edge - use *DEFINE_CURVE with DATTYP=6

*ELEMENT_SHELL_NURBS_PATCH

- „trimmed-NURBS“ capability



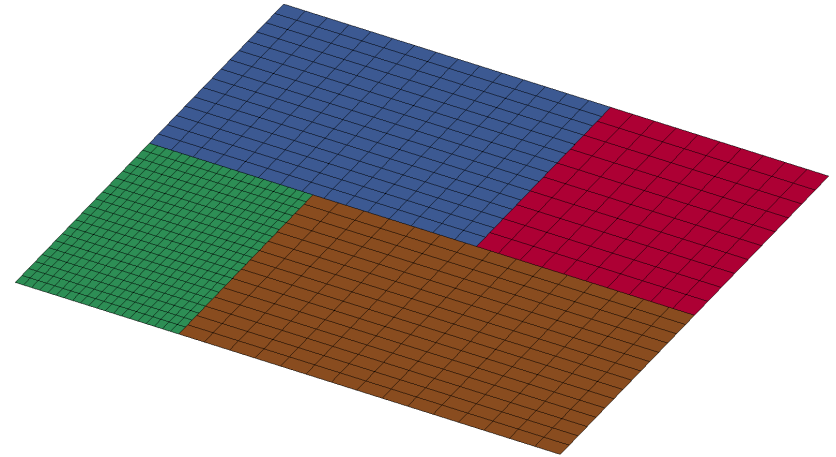
displacement



displacement

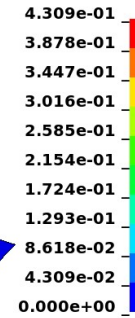
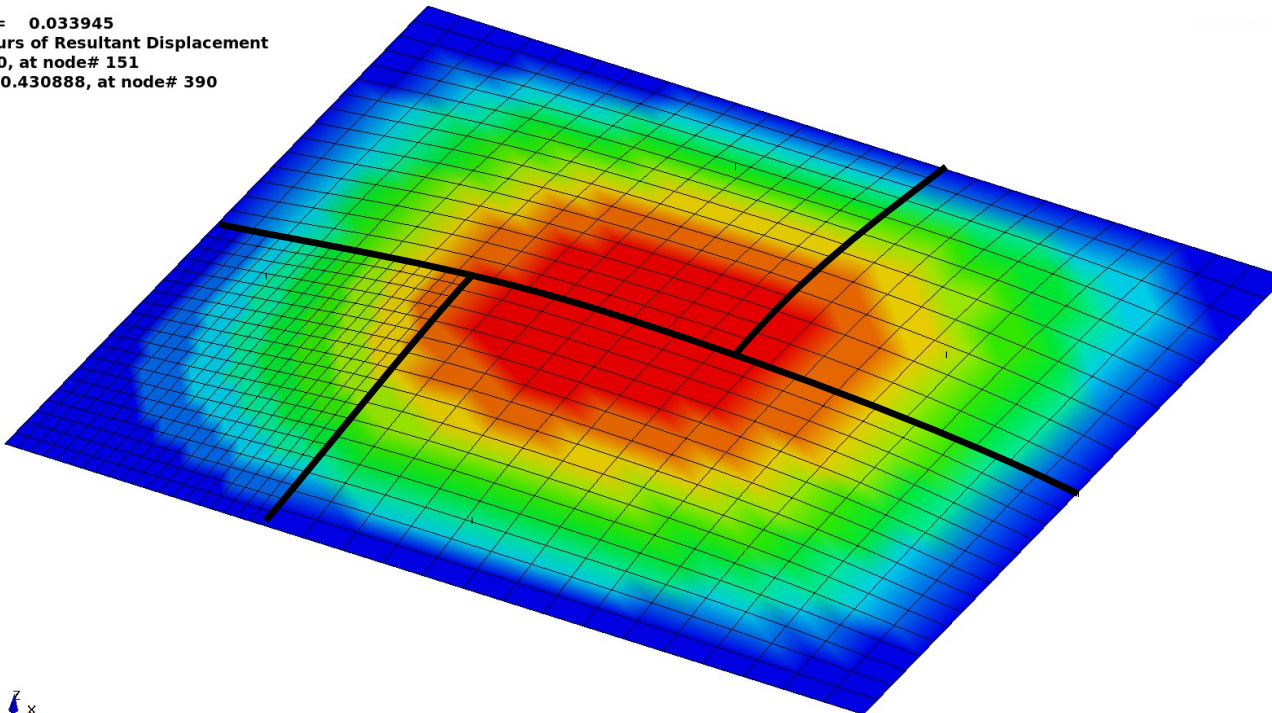
*ELEMENT_SHELL_NURBS_PATCH

- Tying of „Standard-NURBS“
- Constrained- & Penalty-Formulation
- Ongoing development



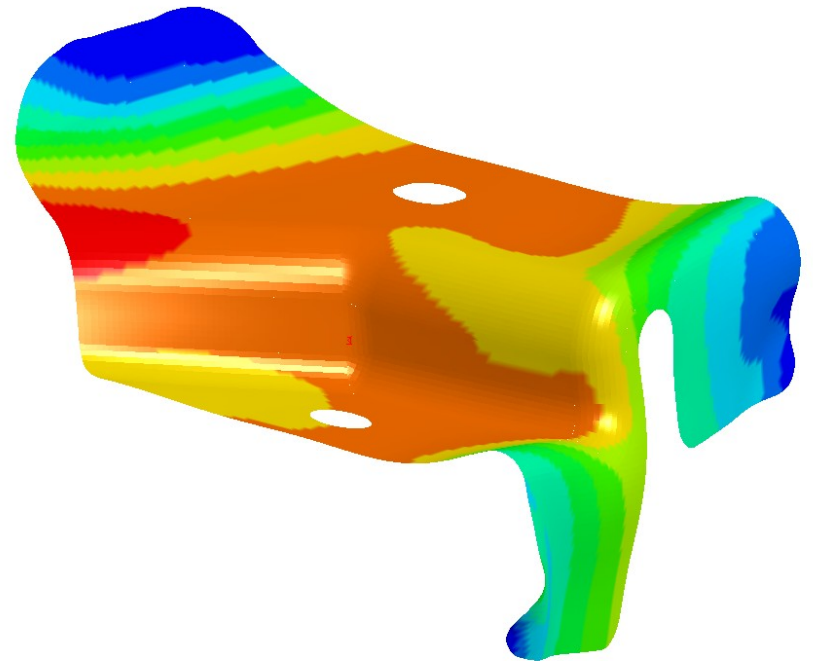
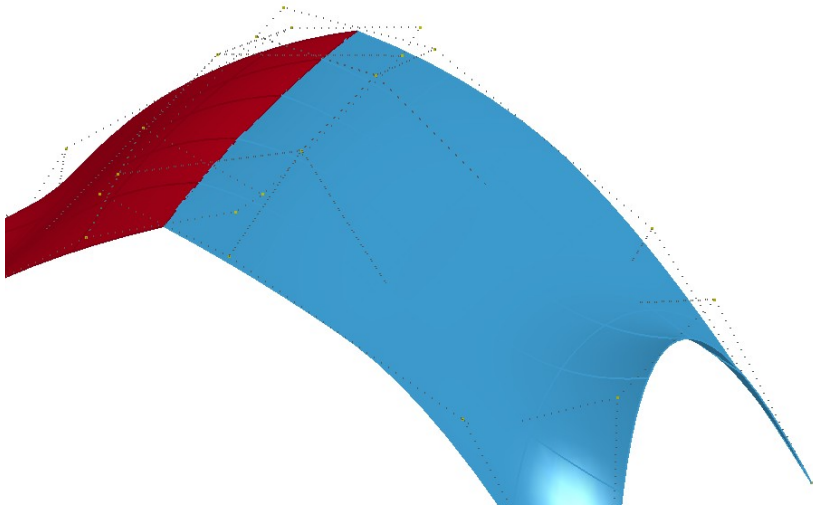
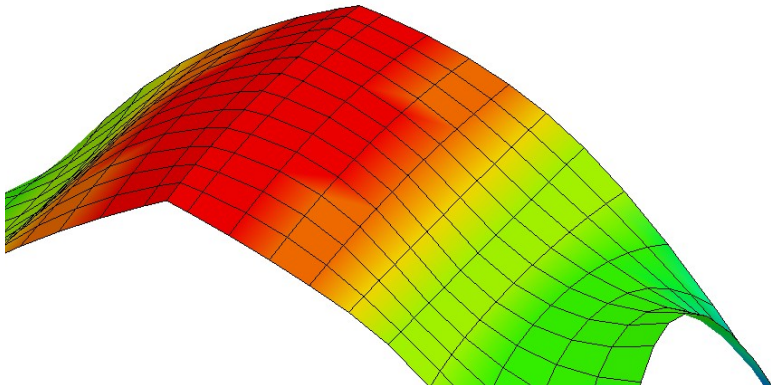
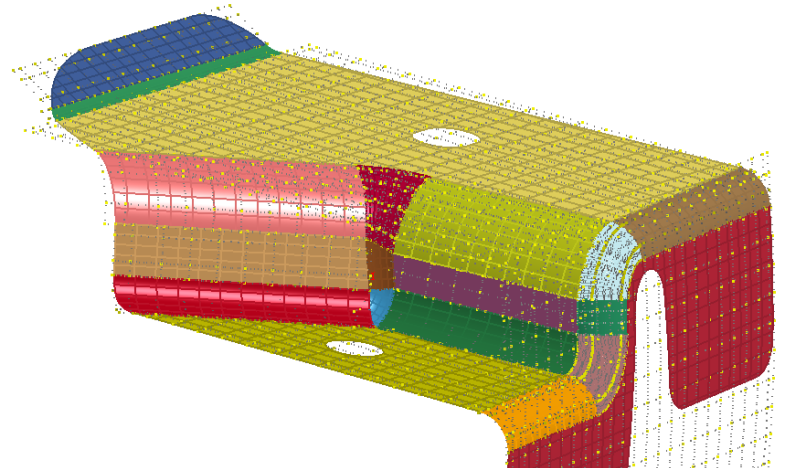
Time = 0.033945
Contours of Resultant Displacement
min=0, at node# 151
max=0.430888, at node# 390

Post



*ELEMENT_SHELL_NURBS_PATCH

- Tying of „trimmed-NURBS“
- Constrained-Formulation (Mortar)
- under development ...



together with D.J. Benson(UCSD)

Particle Methods



Jason Wang

Jingxiao Xu

Hailong Teng

Solid Formulation 24

- Accurate for large deformation, severe distortion
- Non-uniform row summation mass lumping
- Selective reduced integration to alleviate volumetric locking
- No hourglass stabilization needed
- Excellent behavior in bending, one element is used over plate thickness
- Supports both implicit & explicit

```
*SECTION_SOLID
$-----1-----2-----3-----4
$#  SECID  ELFORM  AET
      1      24
```

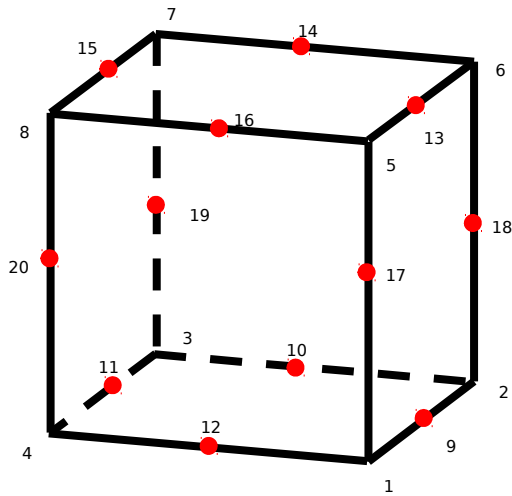
- Elform .eq. 24 27-node solid formulation

Element Connectivity

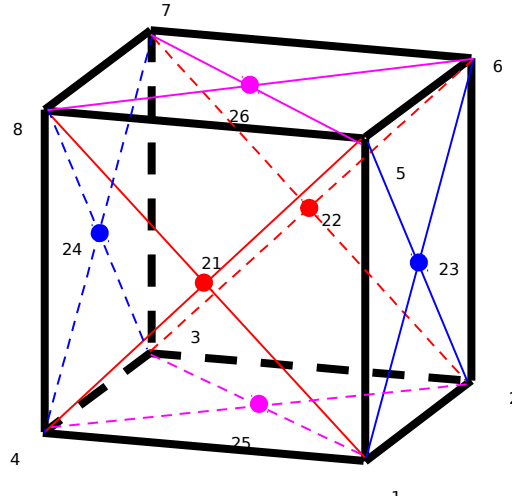
*ELEMENT_SOLID_H27

```

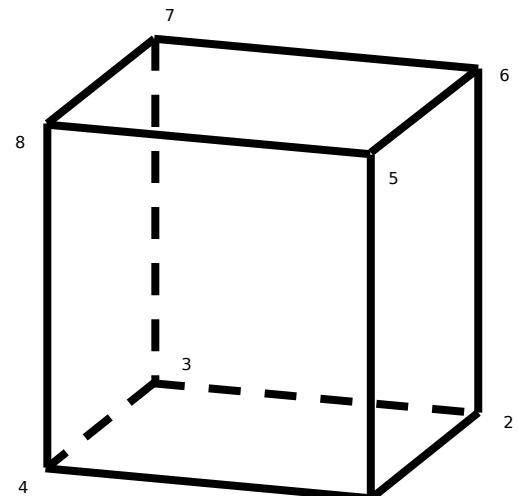
$#  eid  pid
      1   1
$#  n1   n2   n3   n4   n5   n6   n7   n8   n9   n10
      1   2   3   4   5   6   7   8   9   10
$#  n11  n12  n13  n14  n15  n16  n17  n18  n19  n20
      11  12  13  14  15  16  17  18  19  20
$#  n21  n22  n23  n24  n25  n26  n27
      21  22  23  24  25  26  27
    
```



Corner and edge nodes



Corner and face center nodes



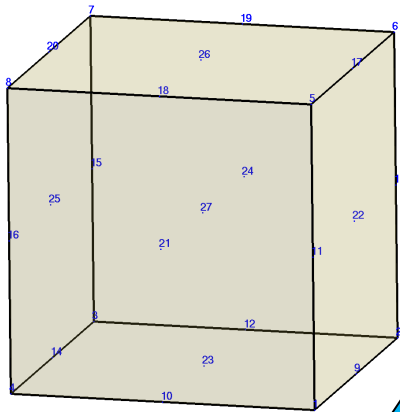
*ELEMENT_SOLID_H8TOH27

```

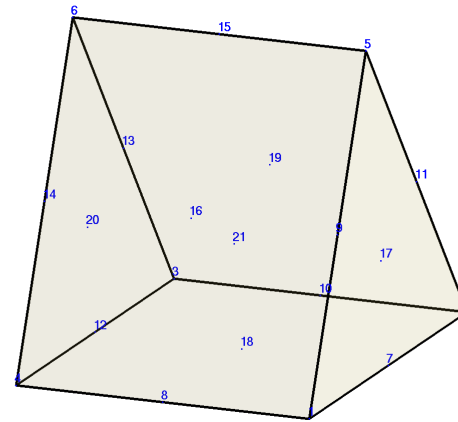
$#  eid  pid  n1  n2  n3  n4  n5  n6  n7  n8
      1   1   1   2   3   4   5   6   7   8
    
```

27-node Element and Degenerated Element

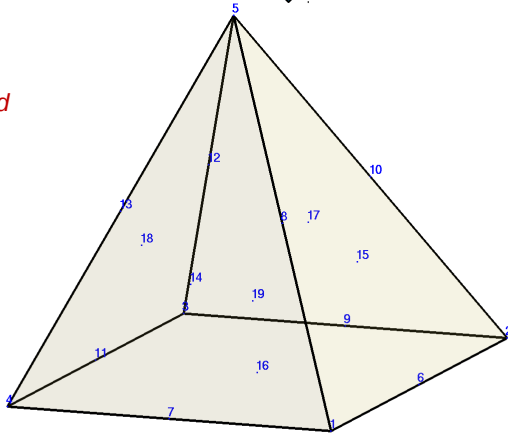
27-node Hexahedron



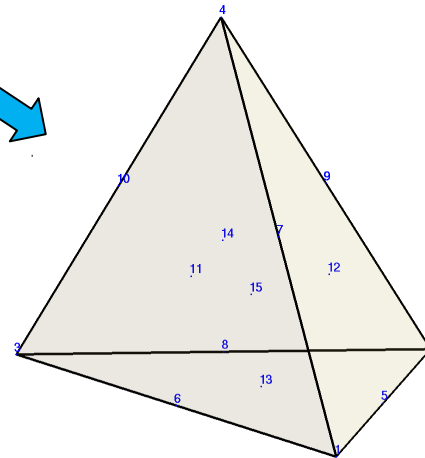
21-node Pentahedron



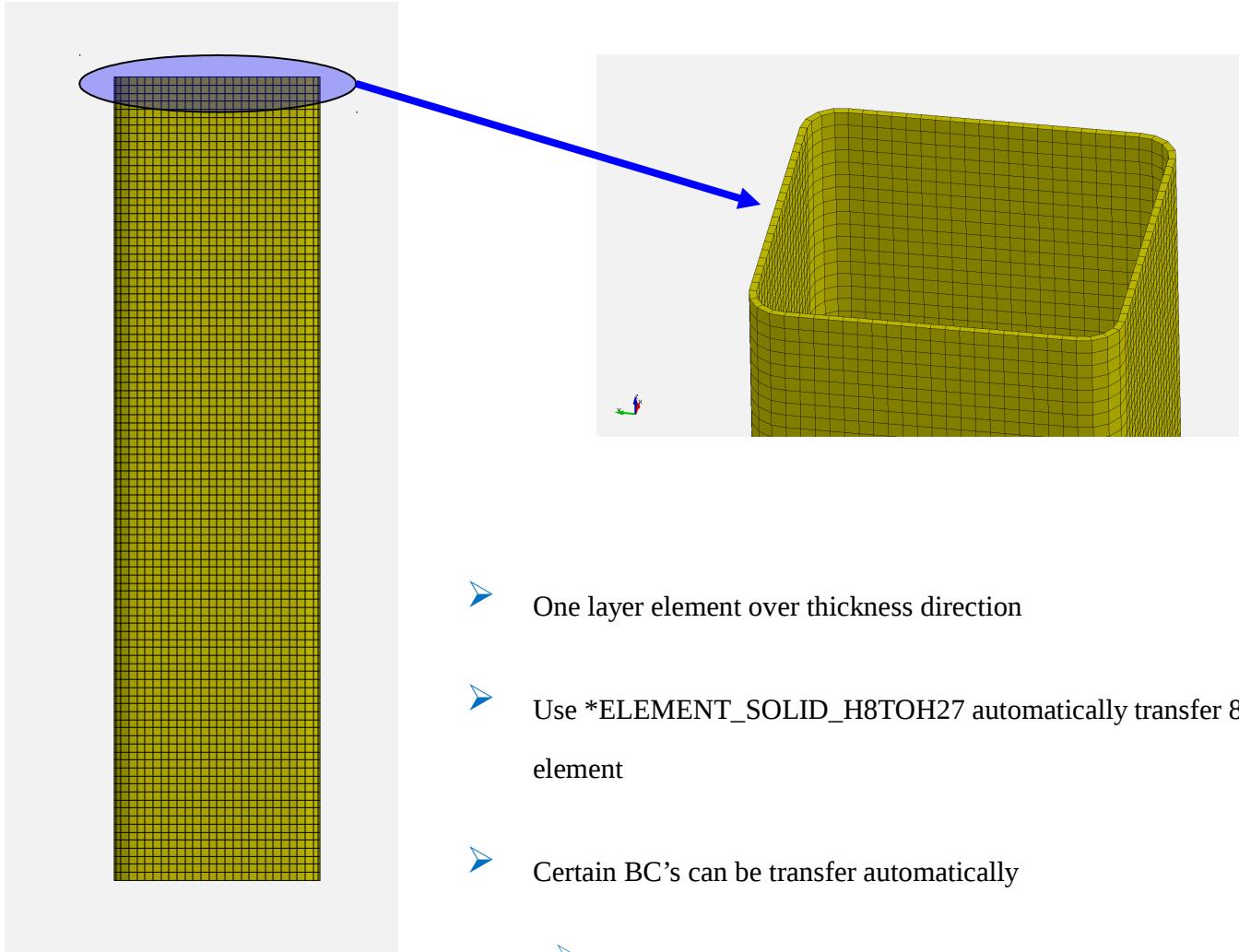
19-node Pyramid



15-node Tetrahedral

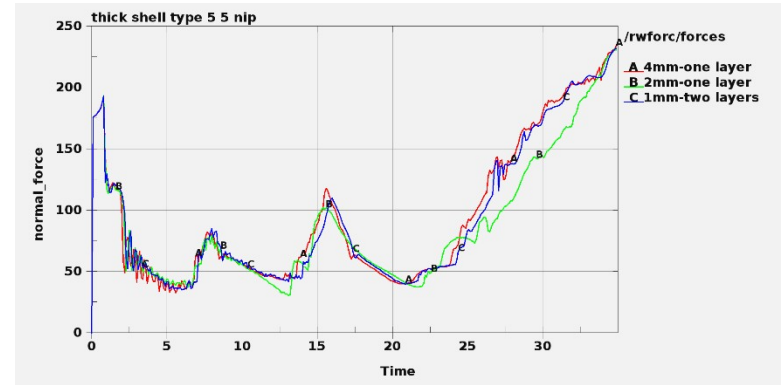
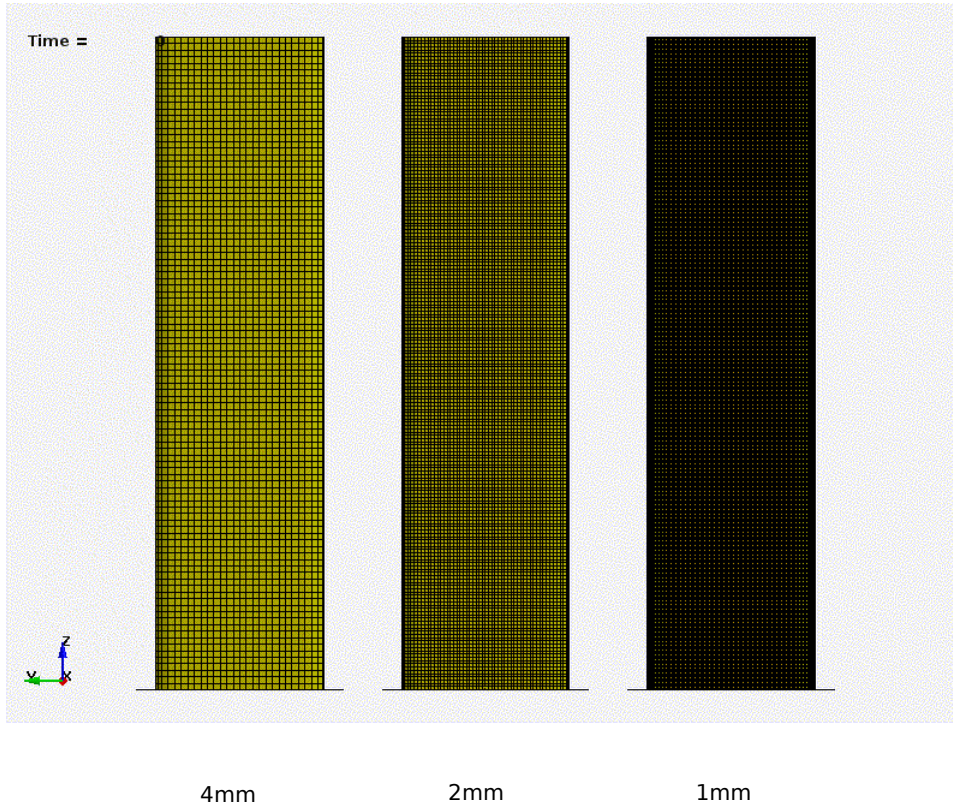


Solid 24

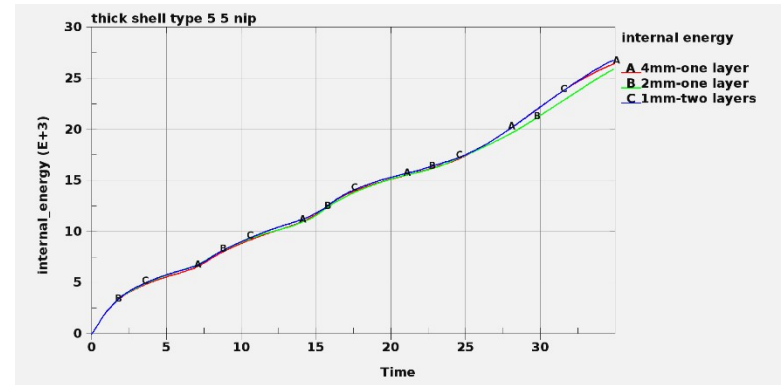


- One layer element over thickness direction
- Use `*ELEMENT_SOLID_H8TOH27` automatically transfer 8-node element to 27-node element
- Certain BC's can be transfer automatically
 - `*NODE`
 - `*SET_NODE_LIST`

Solid 24



Contact Force



Internal energy

Relative coarse mesh can get converged results

Elform2 fine	27 node coarse	27 node fine
1	1.35	28

SPH Enhancements

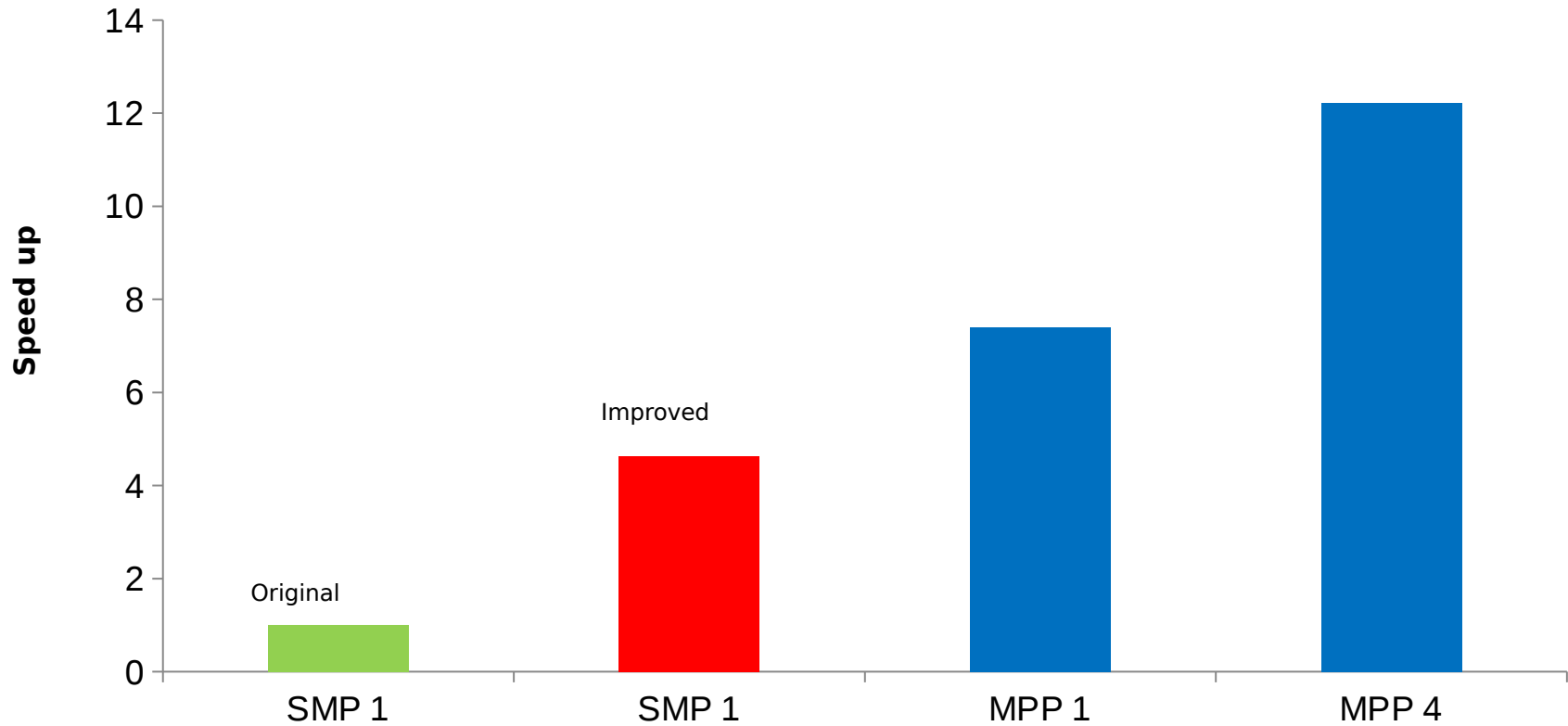
- Support 2D and 3D
- *CONTACT to couple with FEM/DEM
- *CONTACT to couple with different SPH parts
- SPH/Thermal explicit coupling
- More fluid capabilities

- Applications
 - Multiple injection planes
 - High explosive - SPH/DEM coupling
 - Brid strike
 - Tank Sloshing
 - Multiphase,etc

*CONTACT_2D_NODE_TO_SOLID_OPTION

- MPP enabled of SPH 2d contact
- Enhancing performance for SMP and MPP with improved algorithm.

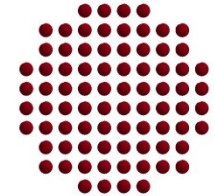
2D extrusion with 1600 SPH particles



*DEFINE_SPH_INJECTION

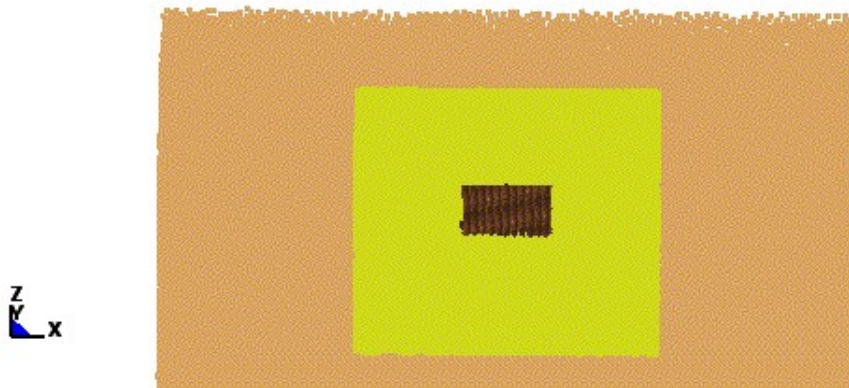
- Multiple injection planes
- Injects SPH flows from user defined grid points and material model

Time = 0



*DEFINE_SPH_DE_COUPLING

Particle Blast
Time = 0



Penalty based interaction between various particle method

- SPH and SPH particles defined by different parts
- SPH and DEM particles

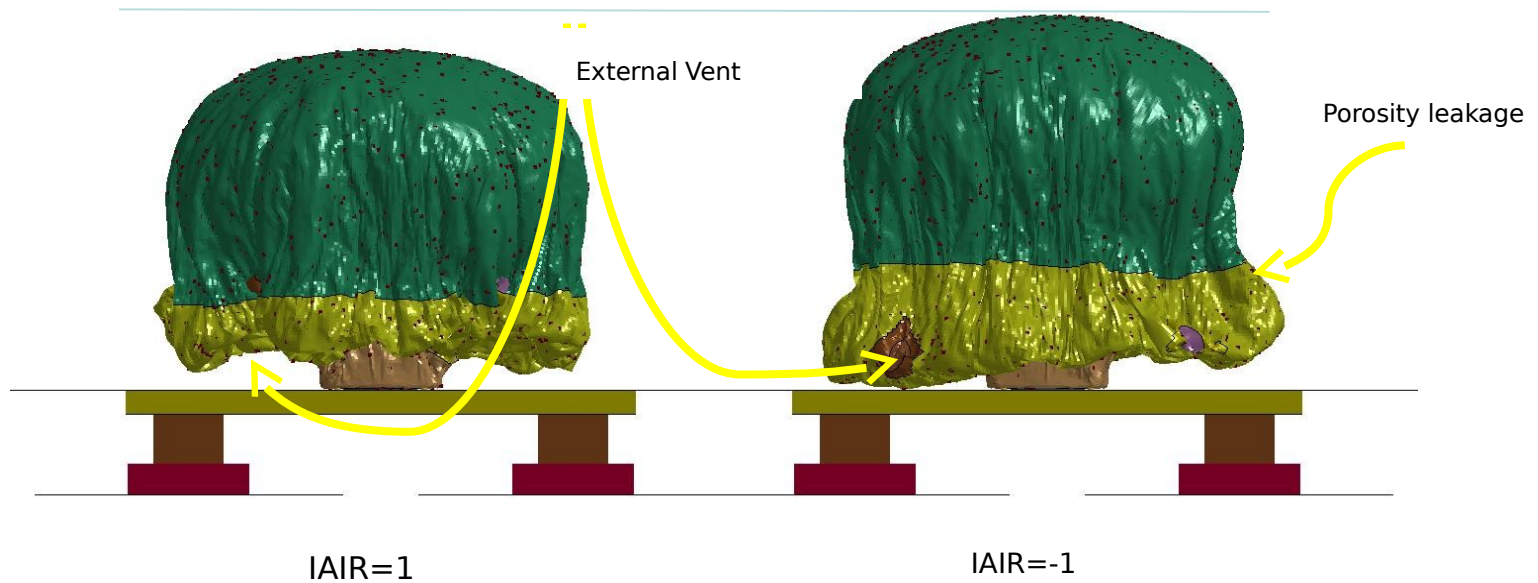
CPM (Ideal Gas Particle)

- Based on Kinetic Molecular Theory (KMT)
- Follow Maxwell-Boltzmann velocity distribution
- Correct describe pressure variation in airbag

- Applications
 - OOP analysis for driver, passenger, curtain, etc bags
 - Multi-chamber analysis
 - CPM and UP interaction
 - Switching from CPM to traditional UP

*AIRBAG_PARTICLE/IAIR=-1

- At the beginning of the bag inflation, the bag pressure may drop below ambient pressure due to jetting. When IAIR=-1, it will allow external vents to draw in outside air
- The feature has been extended for porosity leakage
- Works also after CPM switch to UP airbag

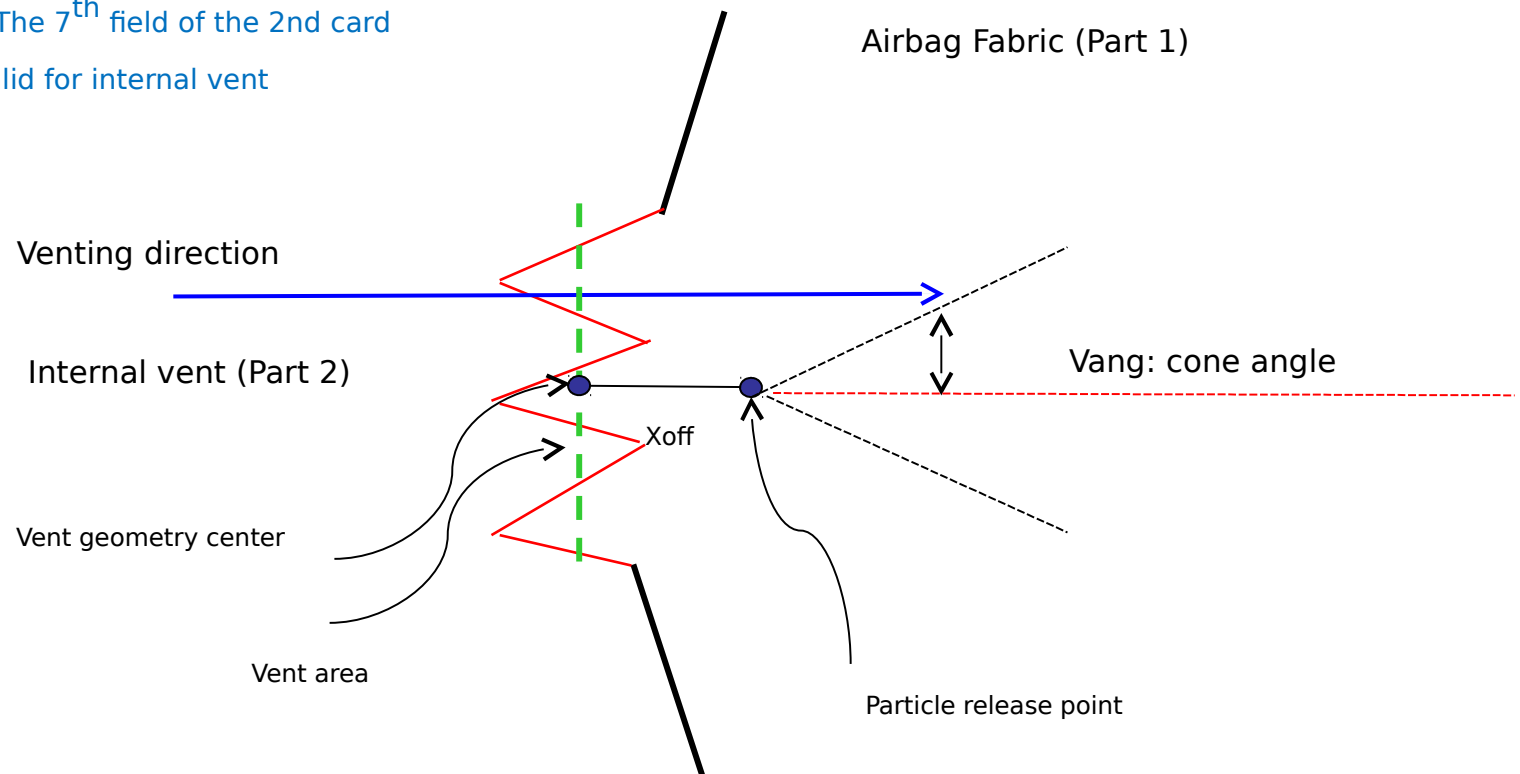


*DEFINE_CPM_VENT

Internal vent with uni-direction/cone angle

*DEFINE_CPM_VENT

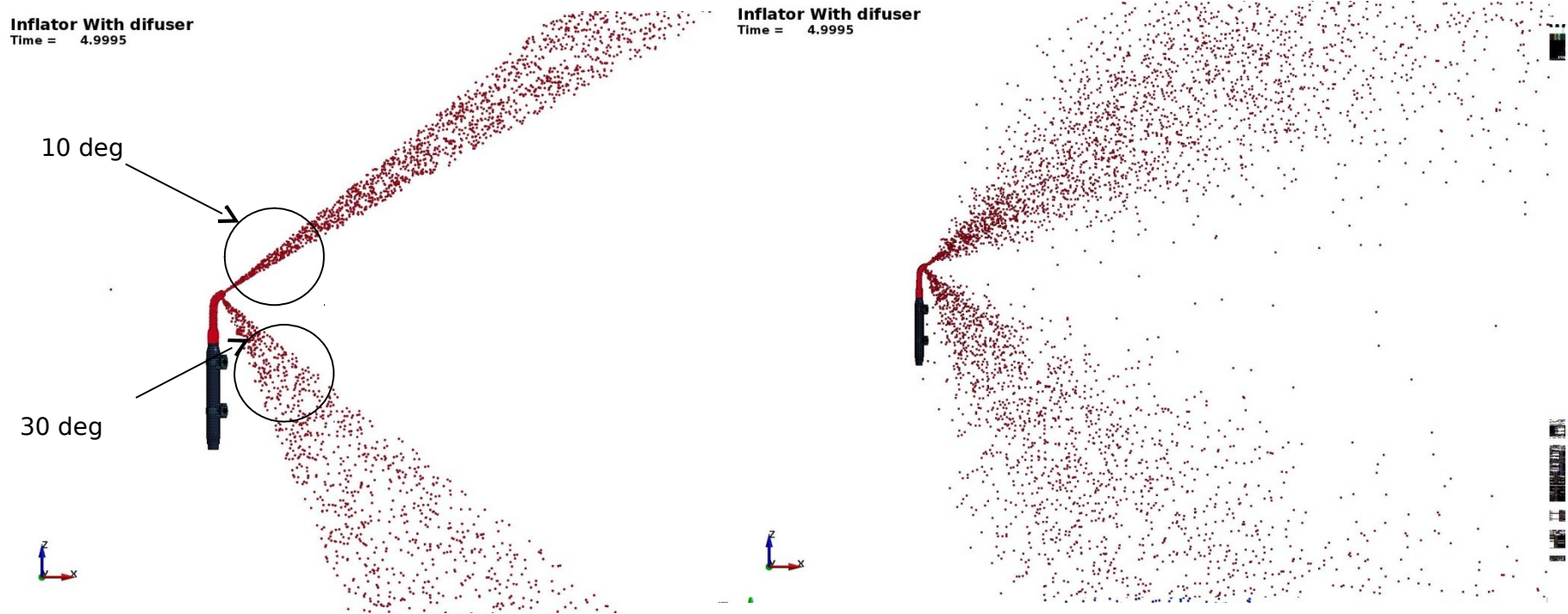
- VANG: The 7th field of the 2nd card
- Only valid for internal vent



- Vent area needs to be greater than 0
- $0 < \text{Vang} < 270$ degrees or $\text{Vang} < 0$ (uni-direction)
- $\text{Xoff} = 5.0\text{e-}4 \times \text{characteristic length}$ (This offset tries to avoid vent to the wrong side.)

*DEFINE_CPM_VENT

Internal vent with uni-direction/cone angle

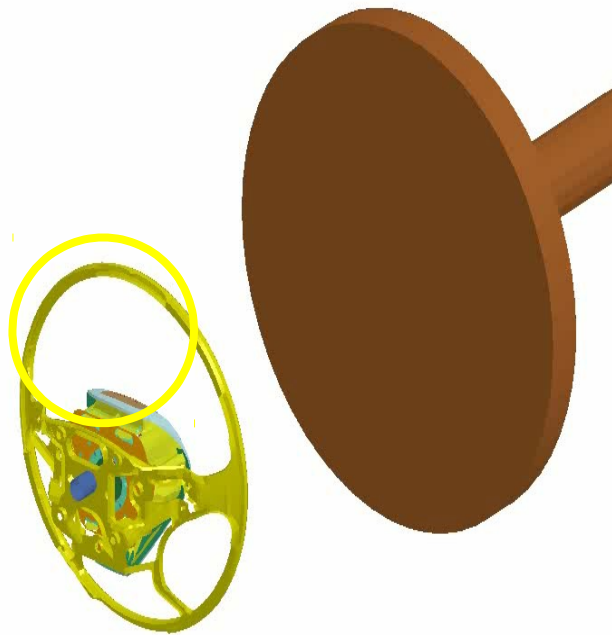


disable/enable p2p contact to validate the cone angle

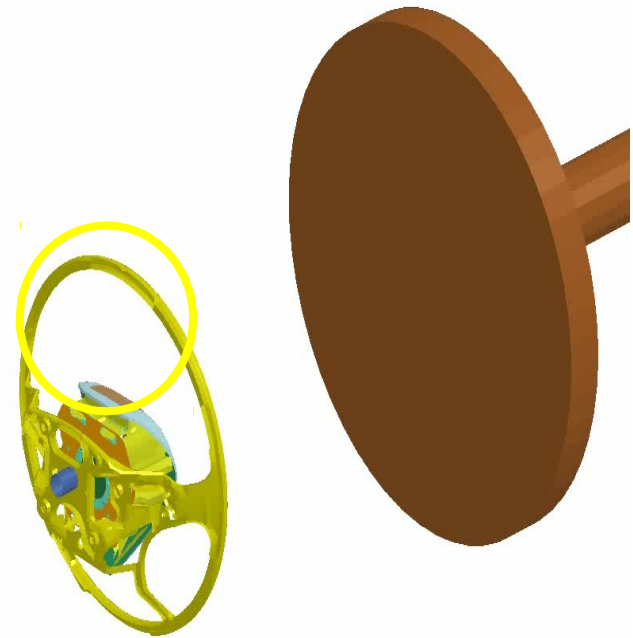
*DEFINE_CPM_VENT

Push out vent

Time = 0



Time = 0



37.27 frame/sec



35.00 frame/sec

MPP Decomposition

**CONTROL_MPP_DECOMPOSITION_ARRANGE_PARTS*

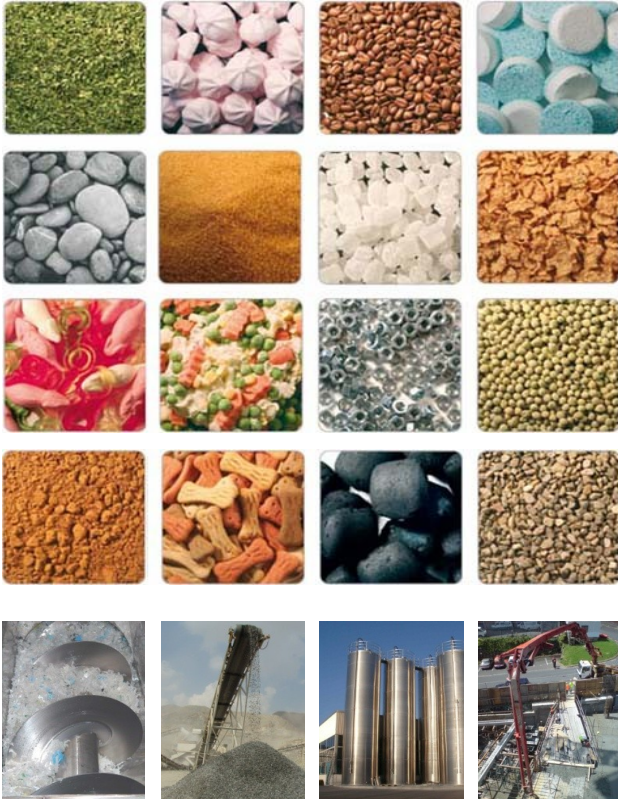
Part/Part Set ID, TYPE, NPROC, FRSTP

- Part/Part Set ID
- TYPE: 0 Part ID to be distributed to all processors
 - 1 Part Set ID to be distributed to all processors
 - 10 Part ID to be lumped into one processor
 - 11 Part Set ID to be lumped into one processor
- NPROC: Evenly distributed elements in above Part/Part Set to number of NPROC processors
- FRSTP: Starting MPP rank

These options only work with element distribution

Discrete Element Method

■ Granular Media



Numerical Simulations Help to Design

Storage

Silos, Piles

Transportation

Conveyor belts, screws, Pumps

Processing

Sorting, Mixing, Segregation

Filling

Hopper/ funnel flow

Characteristics of Granular Media

Solid behavior when compacted

Fluid-like behavior when in motion

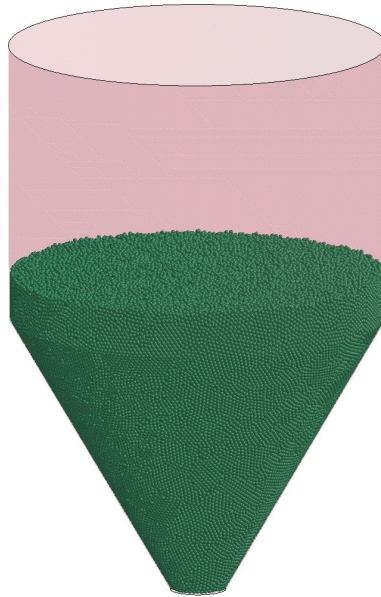
Discrete Element Method (DEM) - Performance

Benchmark Model

www.cfdem.com/media/DEM/benchmarks/LIGGGHTS_Benchmark.pdf

Bin flow, Model 1

Bin Flow, Model 1
Time = 0

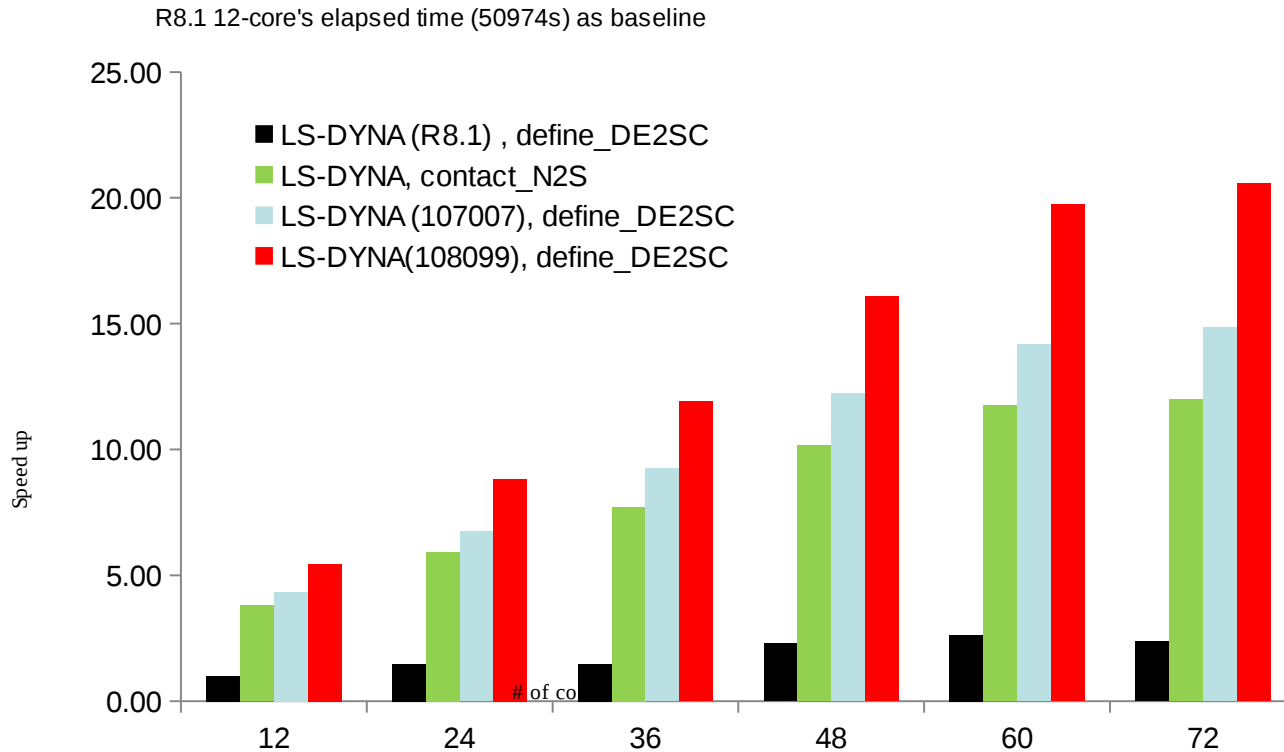


Initial # of particles	300000
Particle diameter (m)	0.003
Particle density (kg/m ³)	1000
Poisson ratio	0.25
Young's modulus (MPa)	25
Normal damping coeff.	0.6
Static friction coefficient	0.2
Rolling friction coefficient	0
Timestep (sec)	1.00E-05
Flow time (sec)	3



DEM MPP Performance

Parallel Scaling



- Use DE2SC instead of N2S. It is developed for DEM and has DEM special features
- A more efficient MPP algorithm is implemented to get ~25% improvement (current development)

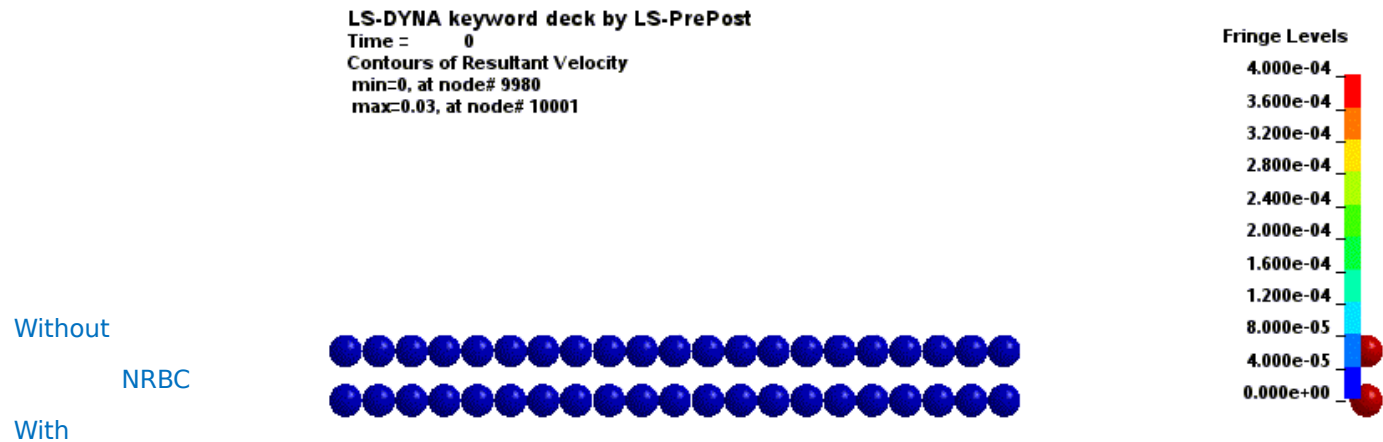
Discrete Element Method

Non_reflecting BC's for DEM

```
*BOUNDARY_DE_NON_REFLECTING
$-----1-----2-----3-----4-----5-----6-----7-----8
$#   NSID
      22
```

- NSID: Node set ID

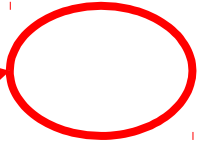
Non-reflecting boundaries are used on the exterior boundaries of an analysis model of an infinite domain, such as a half-space to prevent artificial stress wave reflections generated at the model boundaries from reentering the model and contaminating the results



Discrete Element Method (DEM)

Wear prediction

```
*DEFINE_DE_TO_SURFACE_COUPLING
$#  SLAVE  MASTER  STYPE  MTYPE
    300    1      0      1
$#  FricS  FricD   DAMP   BSORT   LCVx   LCVy   LCVz   WEARC
    0.5    0.01   0.2    100    0      0      0
$#    W1     W2     W3     W4     W5     W6     W7     W8
    1.0E7
```



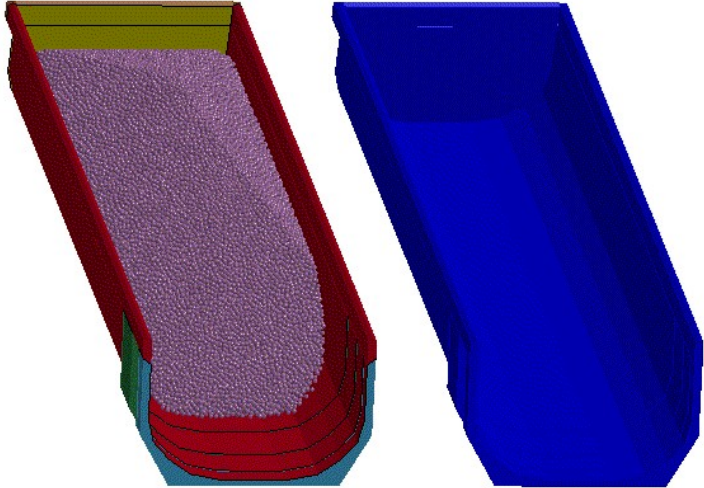
LS-DYNA keyword deck by LS-PrePost
Time = 0
Contours of wear depth
min=0, at elem# 1
max=0, at elem# 1

WEARC

GT. 0 : Archard's wear law

EQ.-1 : Finnie wear law

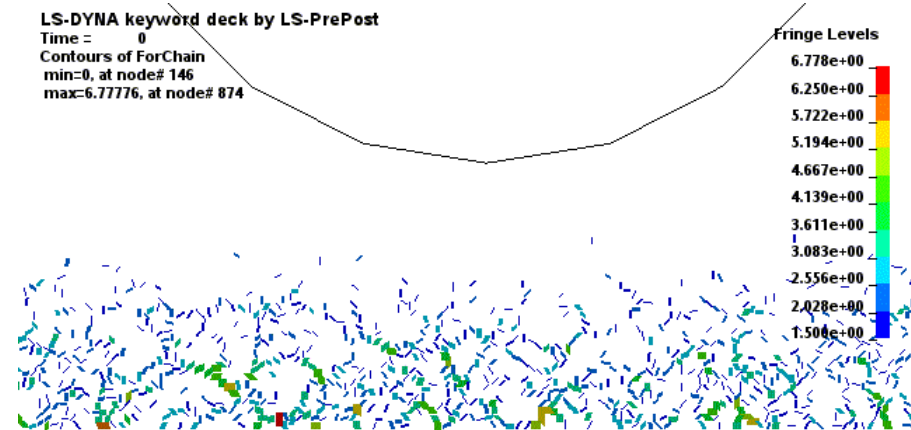
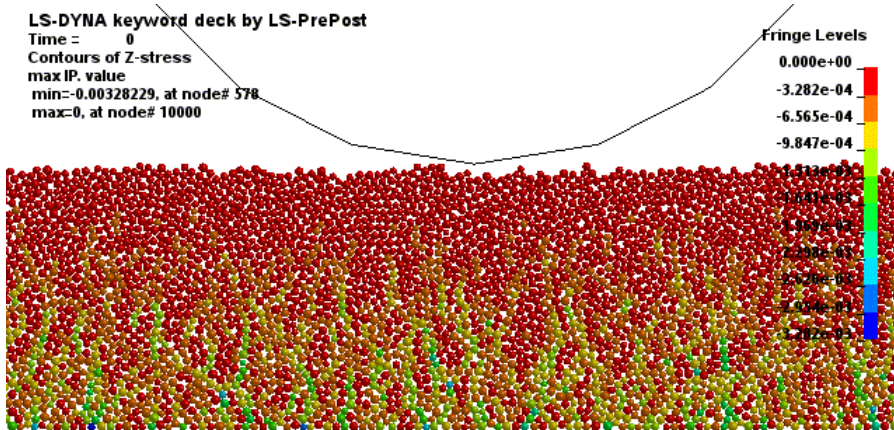
EQ.-100 : User defined routine



Discrete Element Method (DEM)

Force Chain Plot

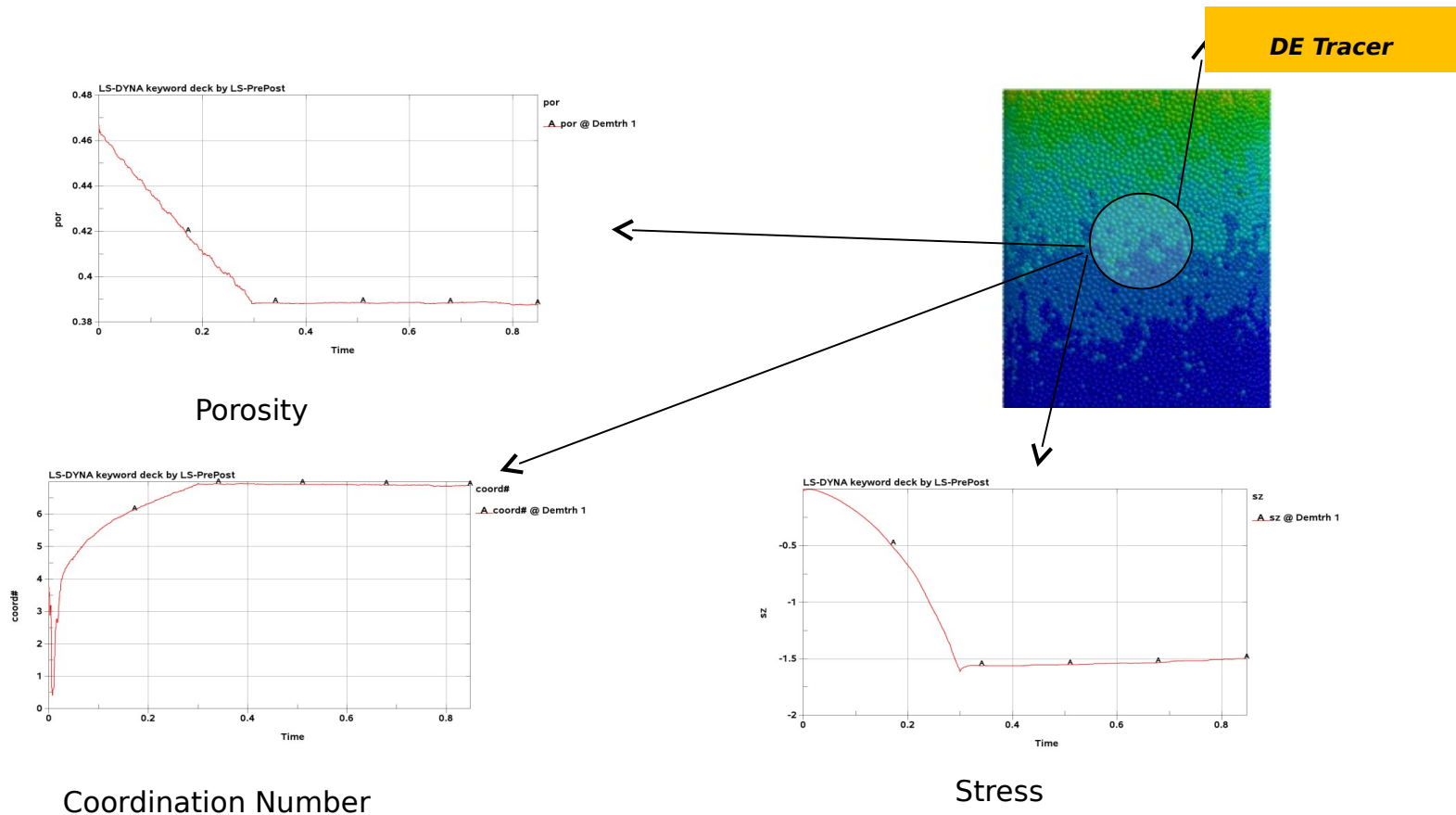
A force chain consists of a set of particles within a compressed granular material that are held together and jammed into place by a network of mutual compressive forces---- From Wikipedia



Discrete Element Method (DEM)

*DATABASE_TRACER_DE

- Porosity, void ratio and coordination number are very important parameters in granular media.
- The corresponding value are evaluated for representative elementary volume (REV) defined by DE tracer.

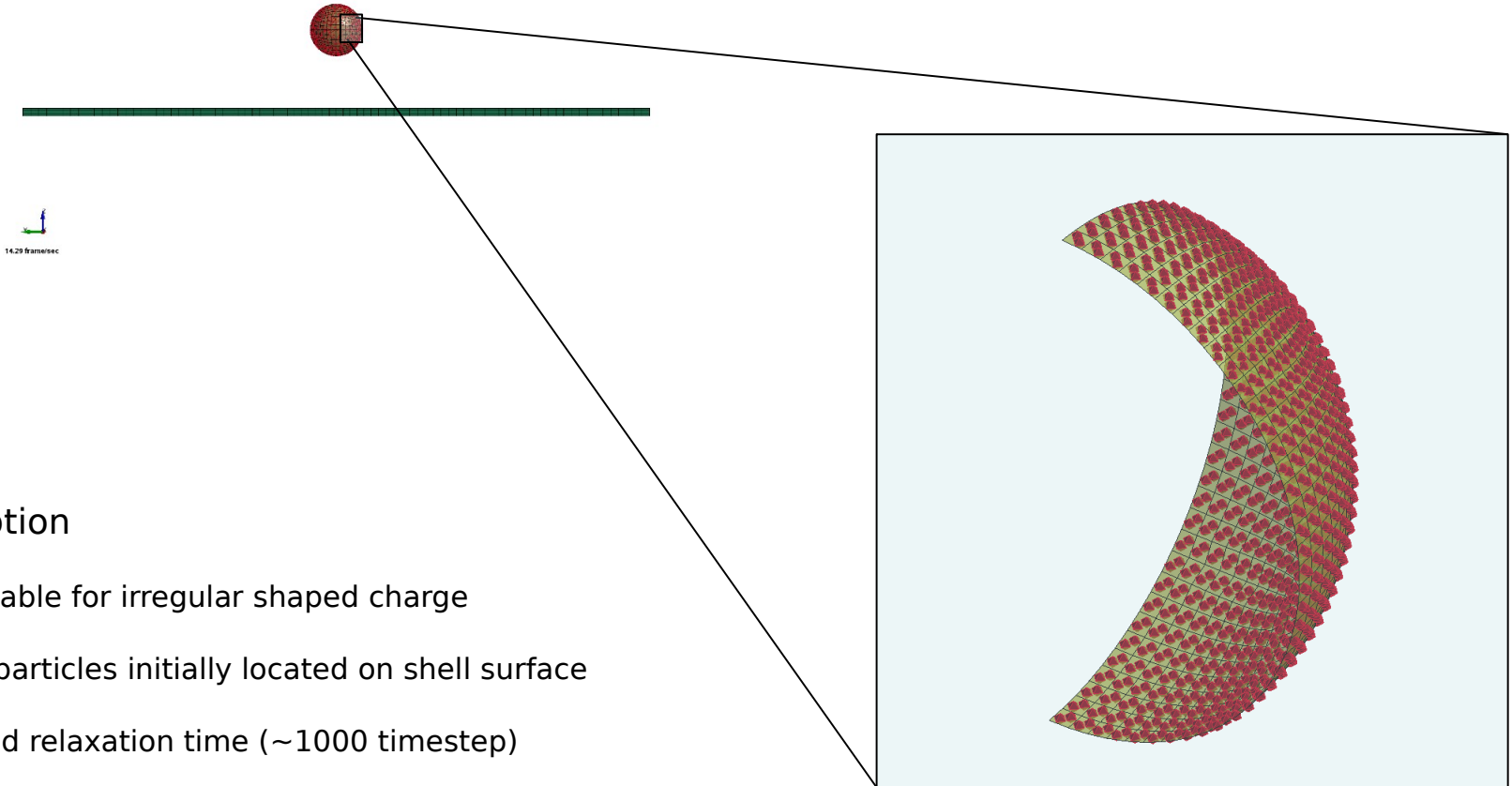


*PARTICLE_BLAST

- HE and Air using CPM
- Sand/Dirt using DEM
- Fast converge
- Easy setup

*PARTICLE_BLAST

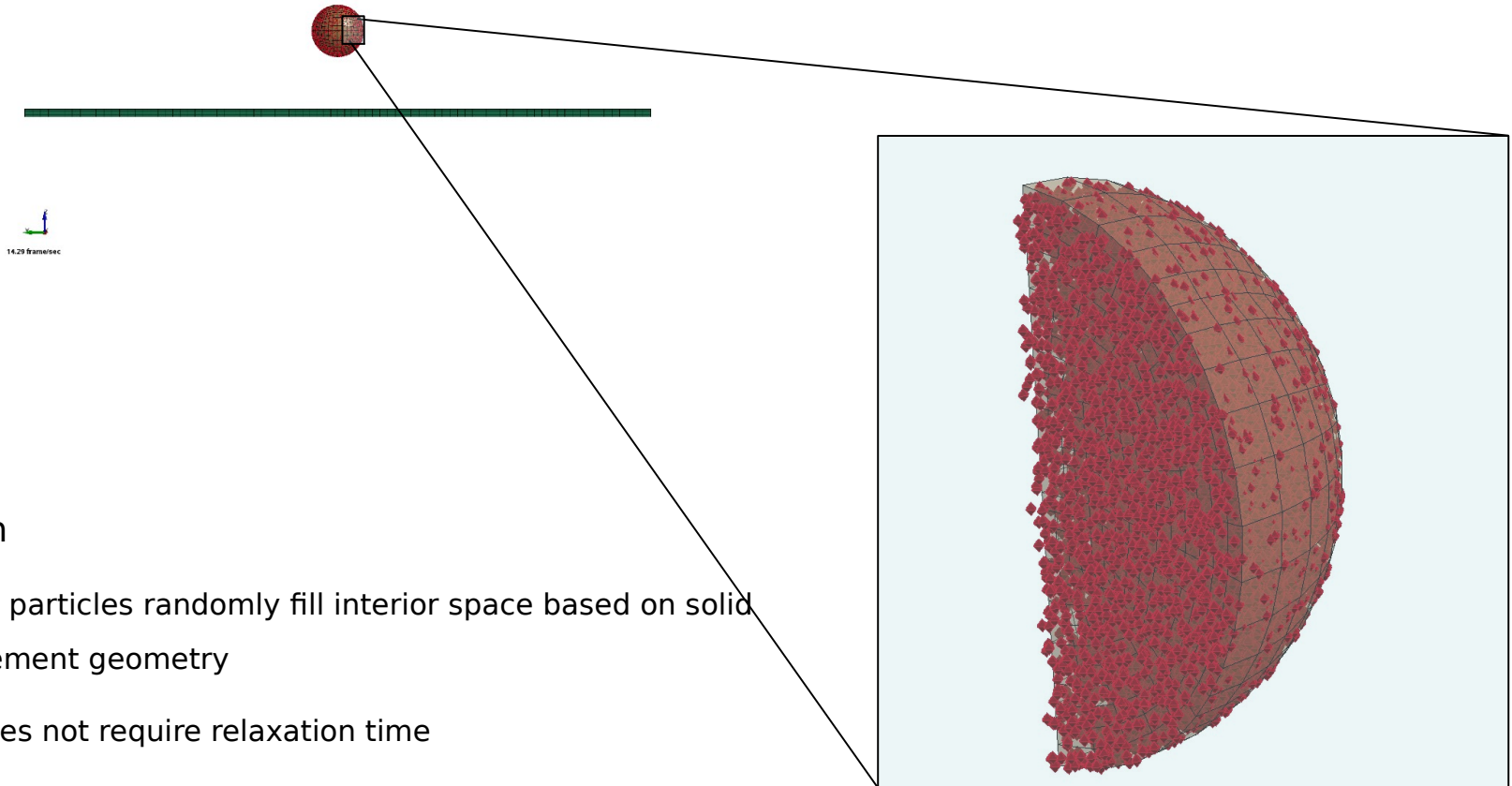
Shell option for HECTYPE=0/1(Old)



- Shell option
 - Suitable for irregular shaped charge
 - HE particles initially located on shell surface
 - Need relaxation time (~1000 timestep)
 - Not convenient, waste CPU time

*PARTICLE_BLAST

Solid option for HECTYPE=0/1(New)



Solid option

- HE particles randomly fill interior space based on solid element geometry
- Does not require relaxation time
- Support Tet and Hex element

*PARTICLE_BLAST

Ground Blast with Cylindrical Shaped Charge

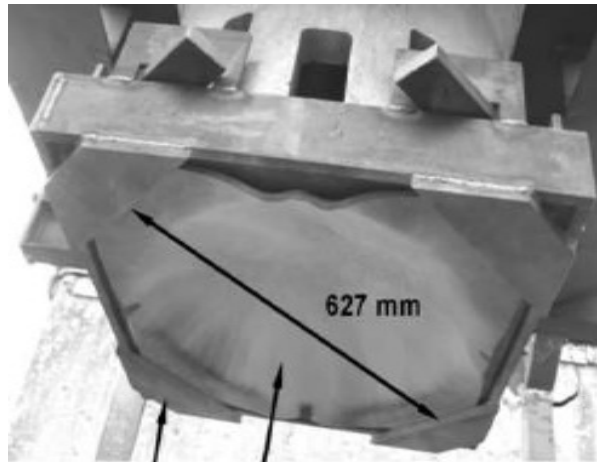


Plate holder

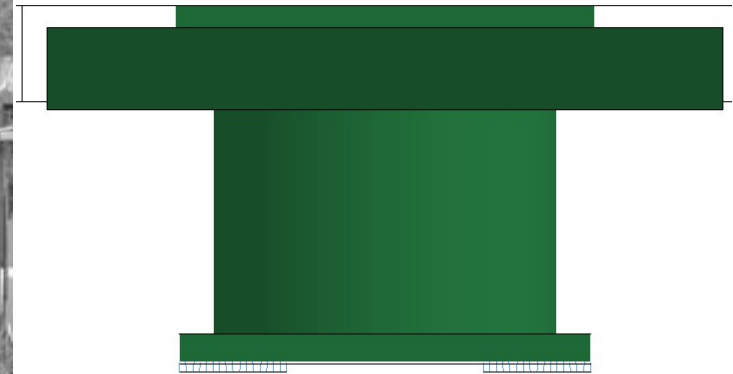
Target plate

Position sensor

Crush gauge

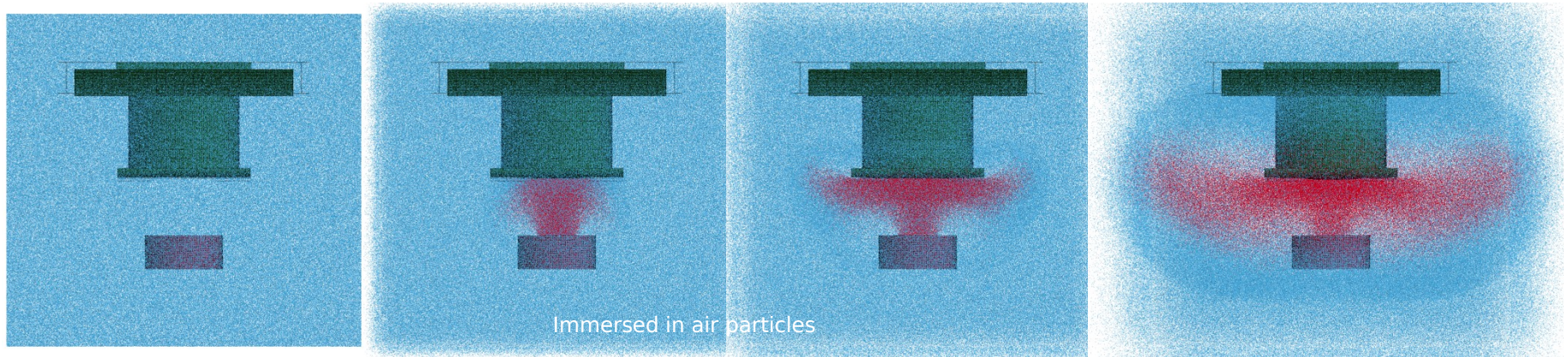
Test module

Steel pot

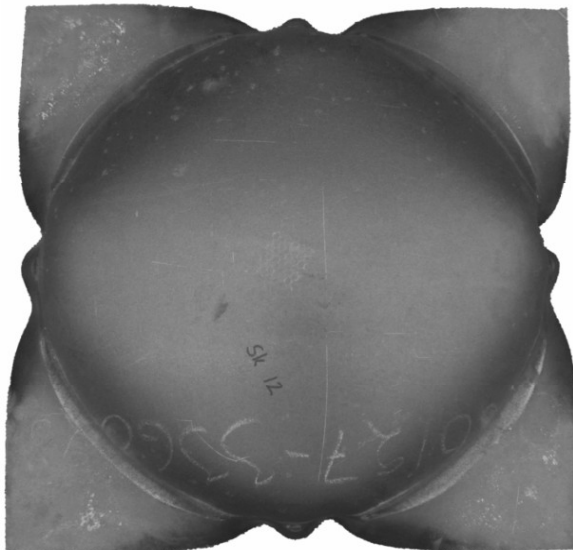


*PARTICLE_BLAST

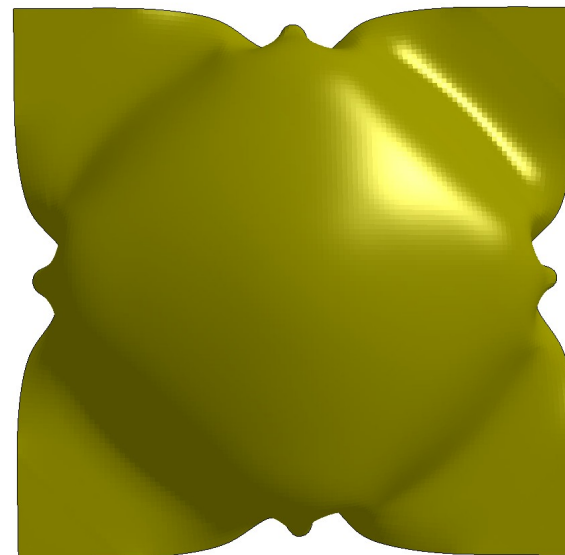
Ground Blast with Cylindrical Shaped Charge



The residual deformation of the target viewed from inside the rig



Test

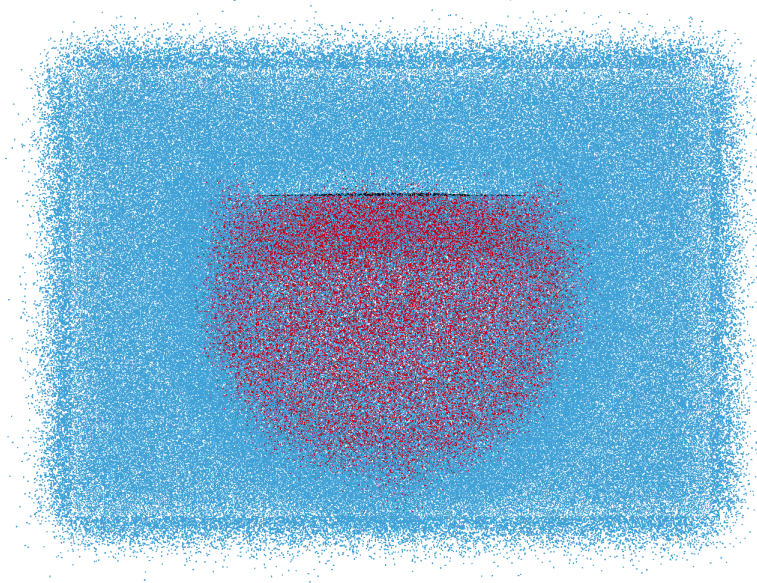


Simulation

*PARTICLE_BLAST

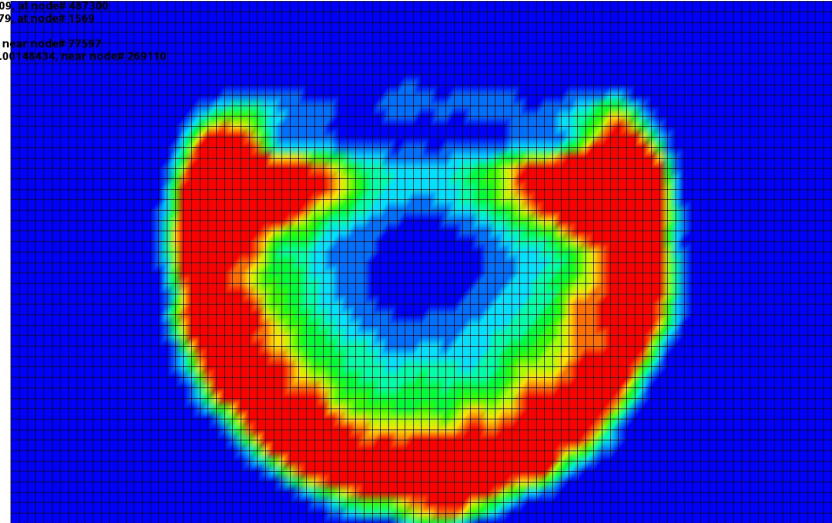
Pressure fringe supported by LS-Prepost

word deck by LS-PrePost



LS-DYNA keyword deck by LS-PrePost

Time = 0.0999
Contours of pressure
min = 1.49534e-09, near node# 437300
max = 0.00254679, at node# 1518
section min = 0, near node# 77587
section max = 0.00148434, near node# 269110

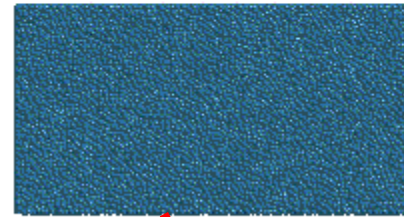
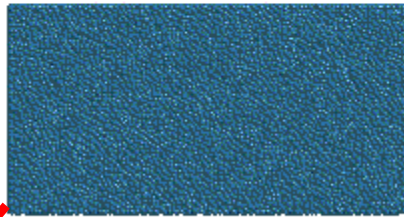
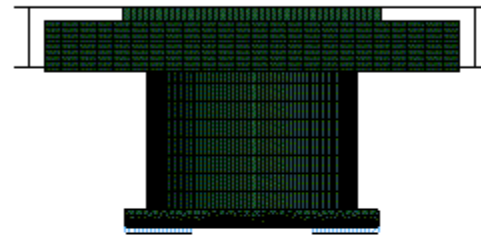
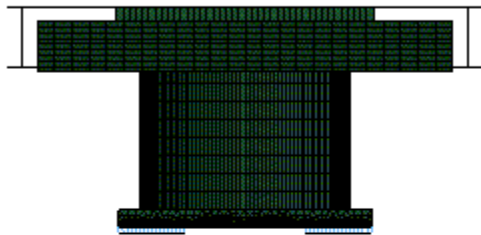


pressure
2.547e-03
2.292e-03
2.037e-03
1.783e-03
1.528e-03
1.273e-03
1.019e-03
7.640e-04
5.094e-04
2.547e-04
1.496e-09

0.00 frame/sec

*PARTICLE_BLAST

Non reflecting B.C.



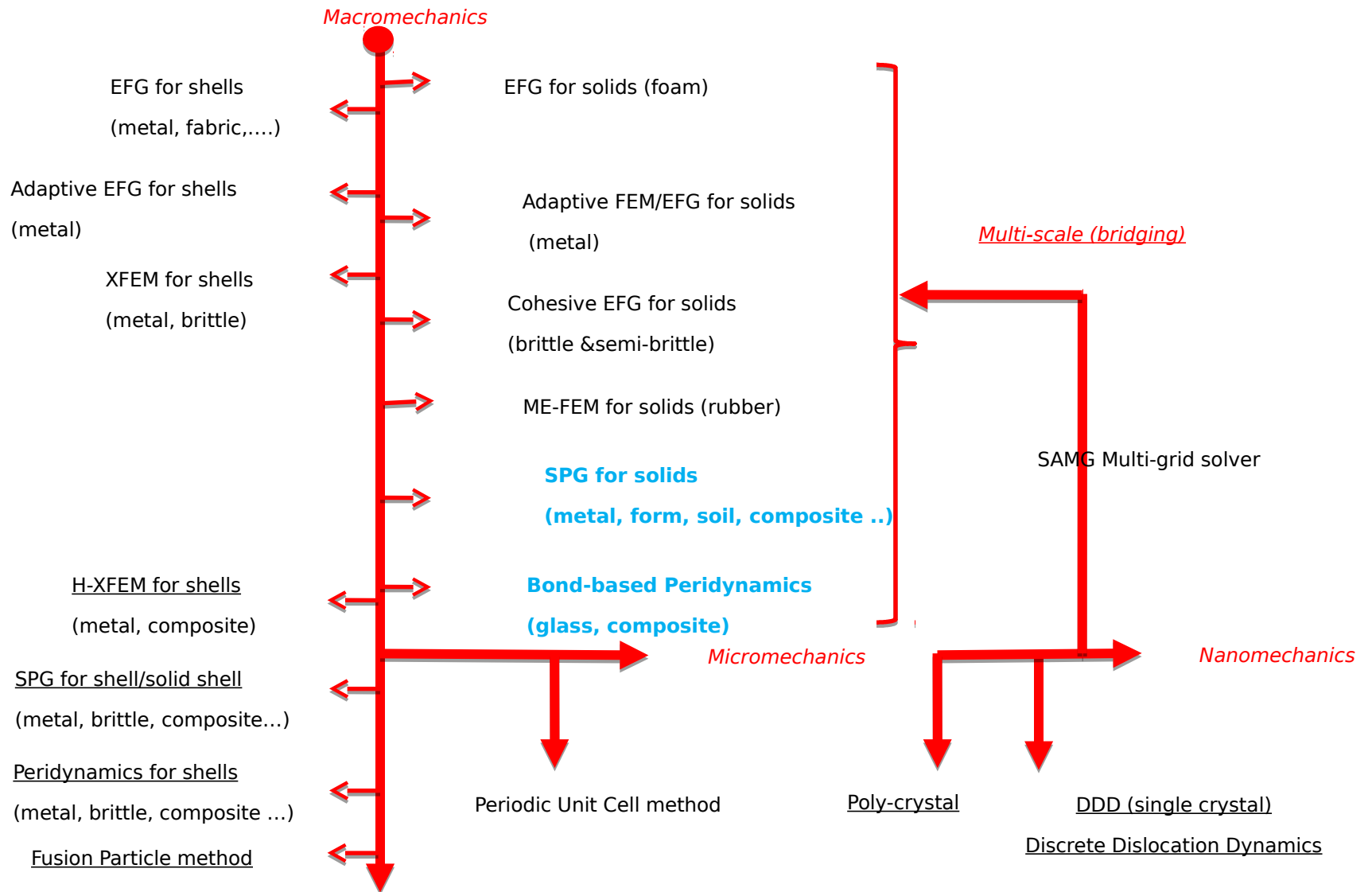
Fixed boundary conditions

Non_Reflecting boundary conditions

Advanced FEM and Meshfree Methods

Cheng-Tang (C.T.) Wu

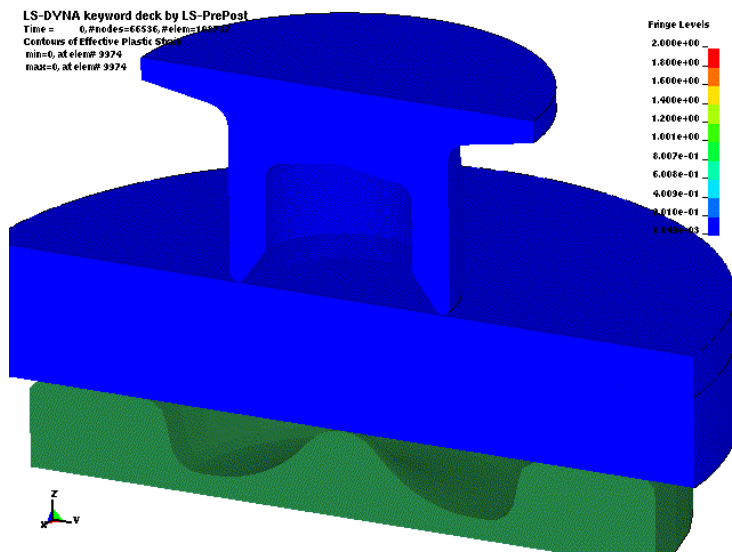
Advanced FEM/Meshfree methods in LS-DYNA[®] for Solids and Structures Analysis



SPR Analysis by Adaptive EFG Method

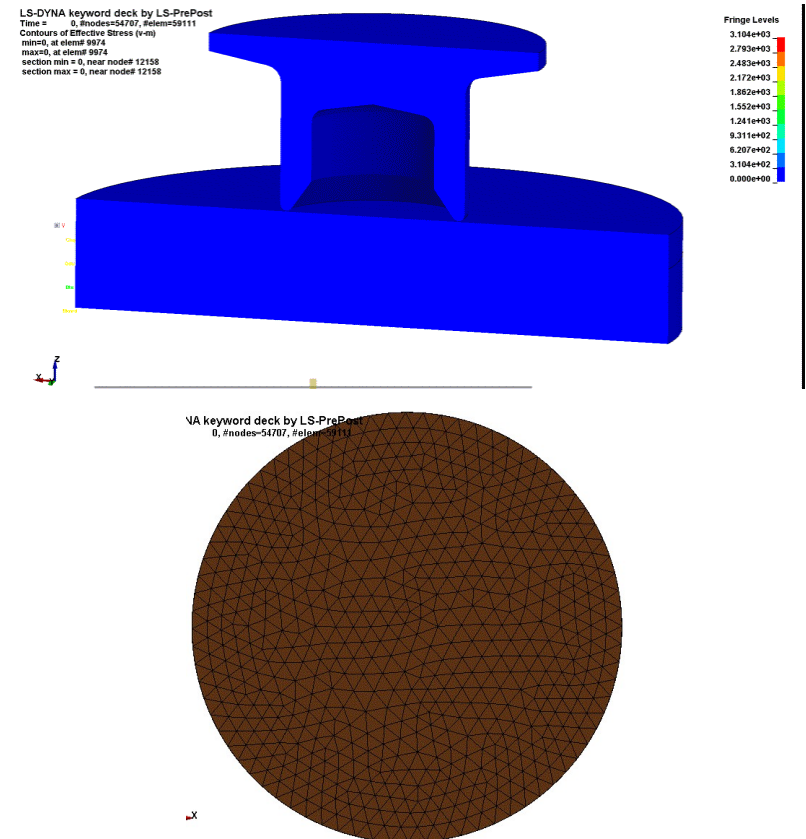
- ❑ Adaptive FEM/EFG method is available for implicit thermo-mechanical coupled analysis.
- ❑ Allows local refinement and has high accuracy.
- ❑ Is suitable for **forging and extrusion simulations** with spring-back analysis.
- ❑ Nevertheless, it is inconvenient to simulate certain manufacturing and fastening operations such as metal cutting, FDS, SPRprocesses.

Manually erode a thin layer of elements



Stop adaptivity of top sheet after erosion

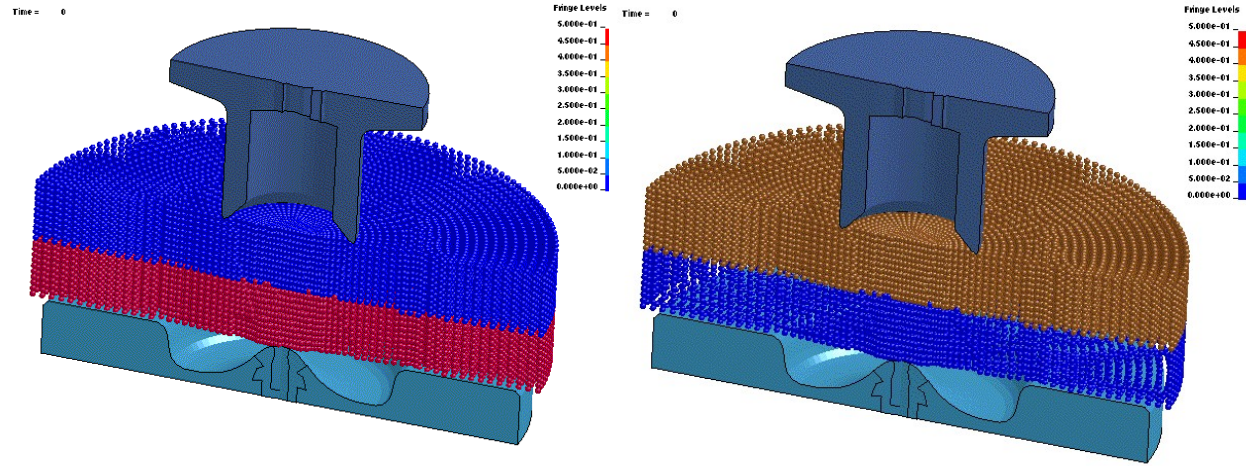
Manually cut the mesh using Hypermesh



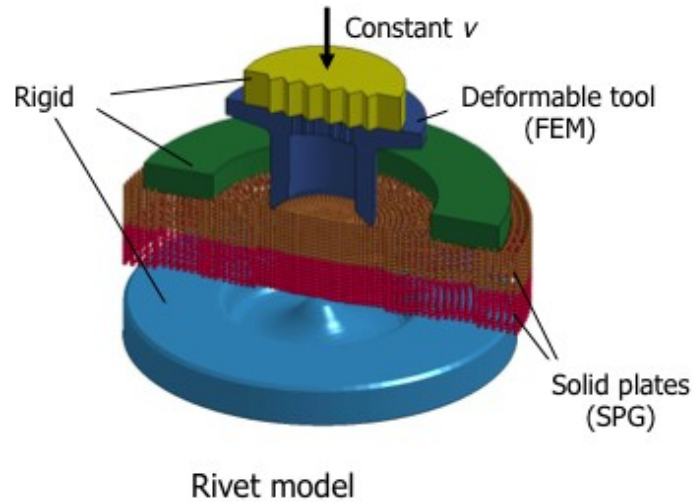
Adaptivity of top sheet continues on

SPR Analysis by SPG Method

- A pure meshfree method.
- Using existing FEM mesh.
- No element erosion or manual cut of the model.
- Strain-based failure criteria.
- A continuous-discontinuous displacement approach.

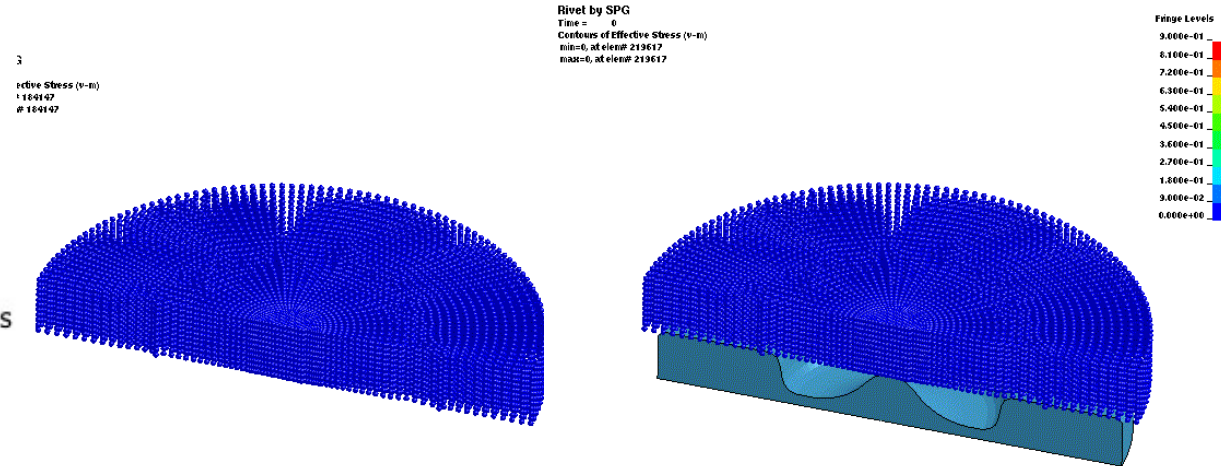


Effective Plastic Strain contour



Upper plate model

Lower plate model



Von Mises stress contour

Smoothed Particle Galerkin (SPG) Method

Developed for manufacturing simulation involving ductile material failure.

Only available in LS-DYNA.

- Was developed at LSTC in 2014.
- Currently implemented in explicit version.
- Currently implemented in integral form.
- Is a pure nodal integration method without integration cell.
- Improves the low-energy modes due to rank deficiency in nodal integration method.
- Is related to residual-based Galerkin meshfree method.
- Without stabilization control parameters.
- Stability analysis via Variational Multi-scale analysis.
- First-order convergence in energy norm.

- Penalized Galerkin Weak Form-Explicit Dynamics

$$\bar{\Pi} = \arg \min_{\mathbf{v} \in H^1(\Omega)} \left[\Pi(\mathbf{v}) + \frac{1}{2} \int_{\Omega} (\bar{\Theta}_h \boldsymbol{\varepsilon}(\mathbf{v}) - \boldsymbol{\varepsilon}(\mathbf{v})) : \mathbf{C} : (\bar{\Theta}_h \boldsymbol{\varepsilon}(\mathbf{v}) - \boldsymbol{\varepsilon}(\mathbf{v})) d\Omega \right]$$

Minimization



Finding $\hat{\mathbf{u}} \in \mathbf{V}^h$, such that $l^h(\hat{\mathbf{u}}, \delta \hat{\mathbf{u}}) = l(\delta \hat{\mathbf{u}}) \quad \forall \delta \hat{\mathbf{u}} \in \mathbf{V}^h$

$$a^h(\hat{\mathbf{u}}, \delta \hat{\mathbf{u}}) = \int_{\Omega} \delta(\nabla^s \hat{\mathbf{u}}) : \mathbf{C} : (\nabla^s \hat{\mathbf{u}}) d\Omega + \int_{\Omega} \delta(\bar{\nabla}^{(2)} \hat{\mathbf{u}}) : \mathbf{C} : (\bar{\nabla}^{(2)} \hat{\mathbf{u}}) d\Omega$$

$$= a_{stan}^h(\hat{\mathbf{u}}, \delta \hat{\mathbf{u}}) + a_{stab}^h(\hat{\mathbf{u}}, \delta \hat{\mathbf{u}})$$

$$l(\delta \hat{\mathbf{u}}) = \int_{\Omega} \delta \hat{\mathbf{u}} \times \mathbf{f} d\Omega + \int_{\Gamma_N} \delta \hat{\mathbf{u}} \times \mathbf{t} d\Gamma$$

$$a_{stab}^h(\hat{\mathbf{u}}, \delta \hat{\mathbf{u}}) = \int_{\Omega} \delta(\bar{\Theta}_h \boldsymbol{\varepsilon}(\hat{\mathbf{u}}) - \boldsymbol{\varepsilon}(\hat{\mathbf{u}})) : \mathbf{C} : (\bar{\Theta}_h \boldsymbol{\varepsilon}(\hat{\mathbf{u}}) - \boldsymbol{\varepsilon}(\hat{\mathbf{u}})) d\Omega$$

$$= \int_{\Omega} \delta(\bar{\nabla}^{(2)} \hat{\mathbf{u}}) : \mathbf{C} : (\bar{\nabla}^{(2)} \hat{\mathbf{u}}) d\Omega \quad O(h^2)$$

Not Laplace operator !

or



Flow Drill Screw (FDS) Analysis Using SPG

Head with internal or external drive system

stage 1

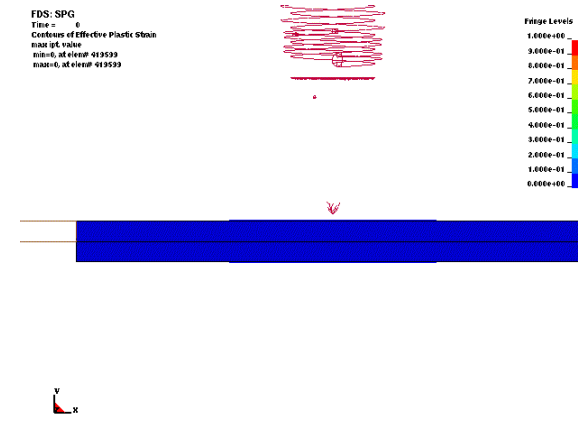
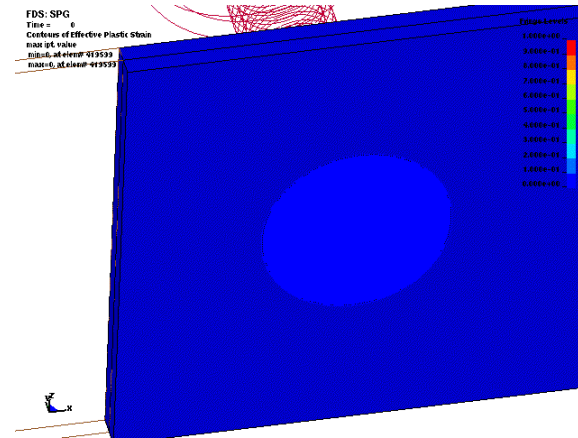
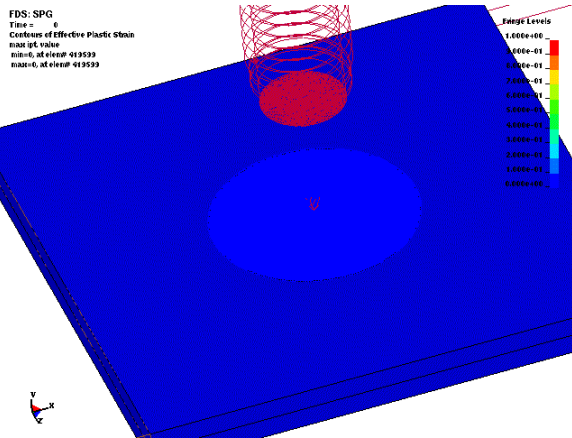
Thread forming zone

Flow drilling zone

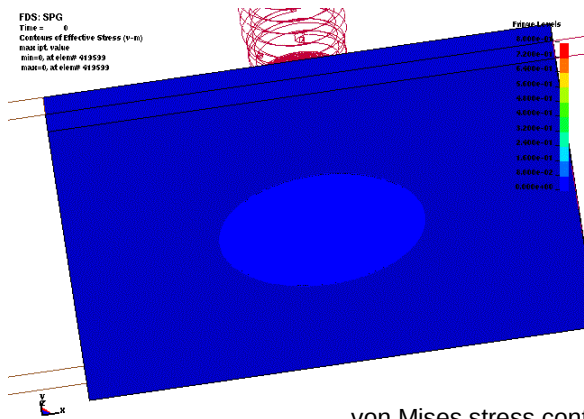
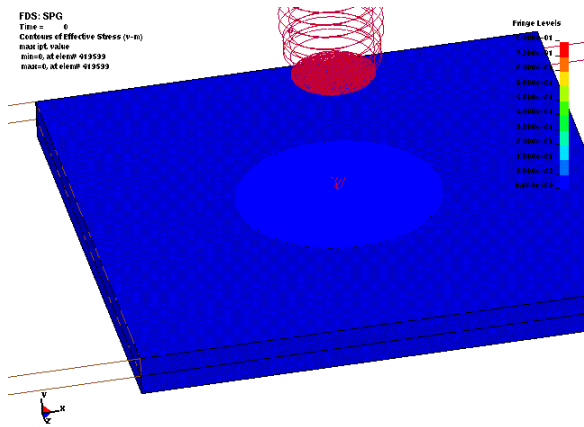
stage 2

EPS contour

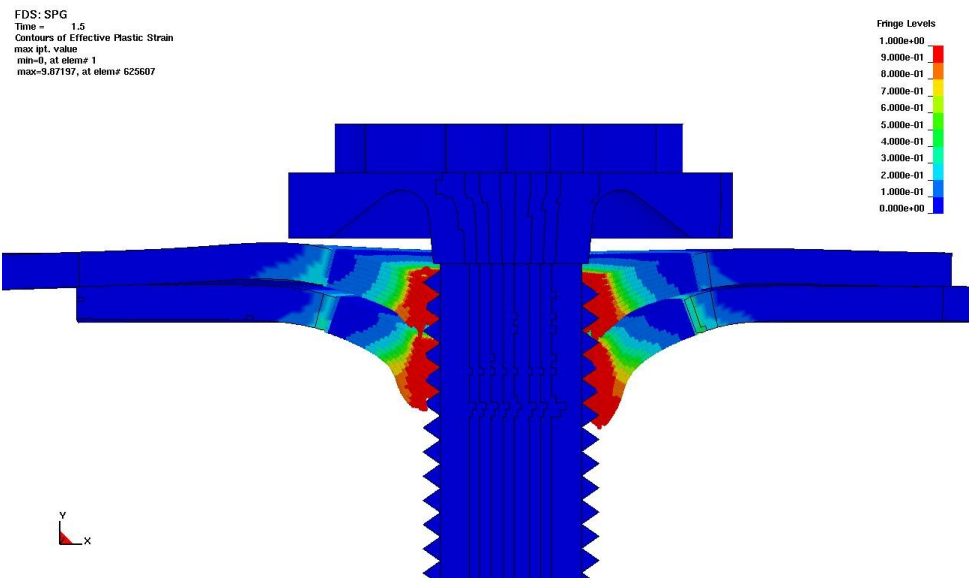
stage 1



stage 1



von Mises stress contour

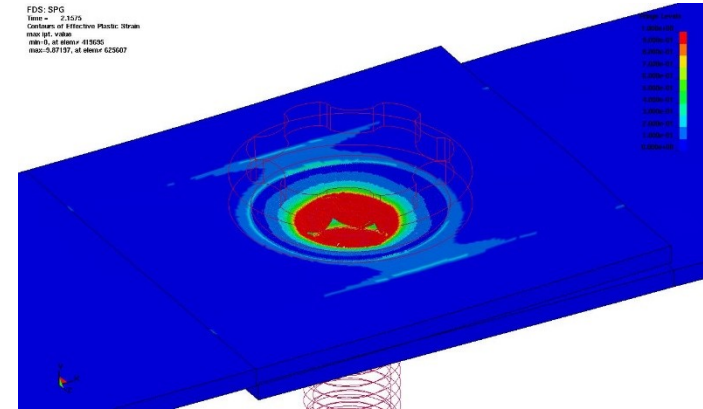
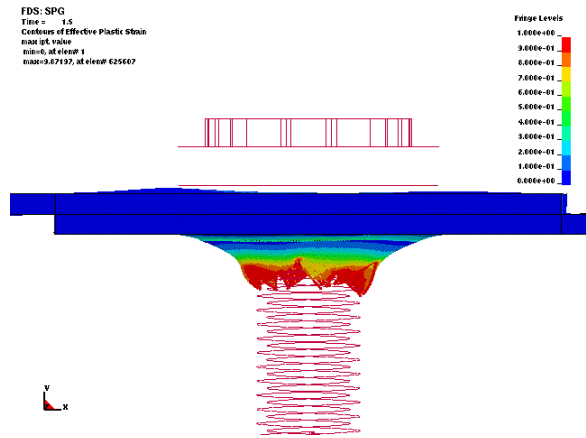
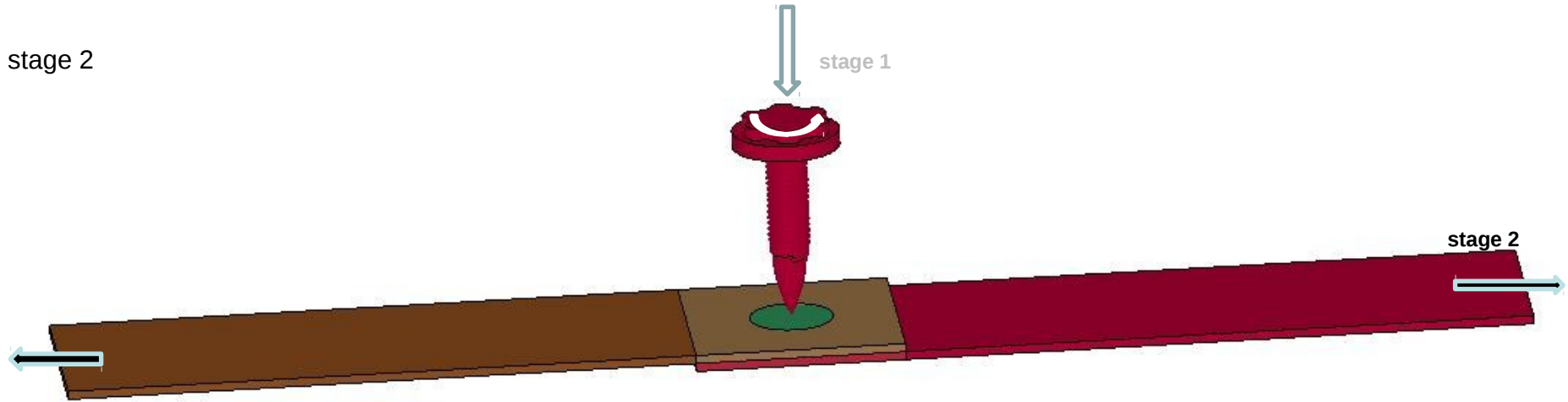


Cross-section in EPS contour

stage 2

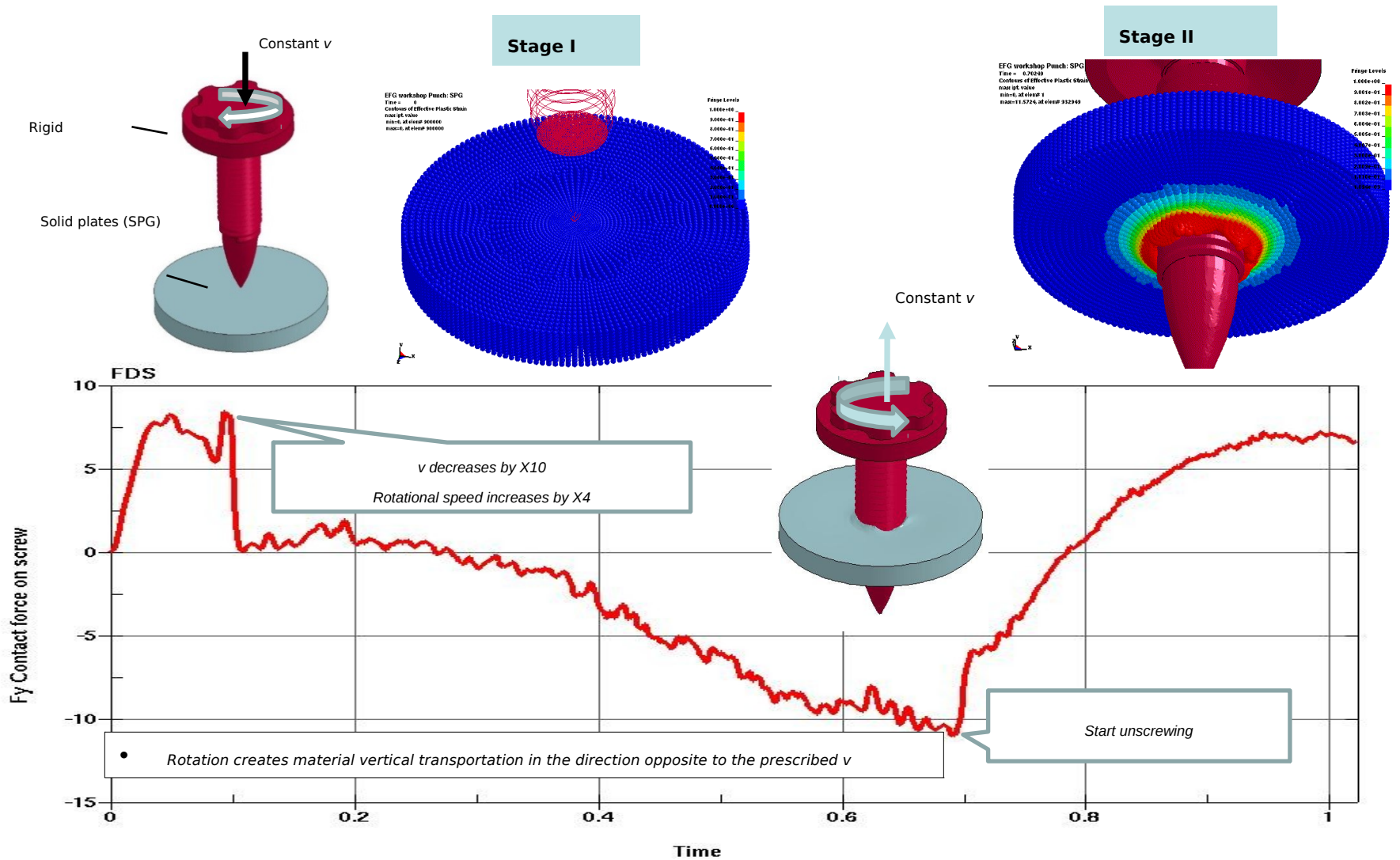
stage 1

stage 2



EPS contour

Pull Out Test Using SPG

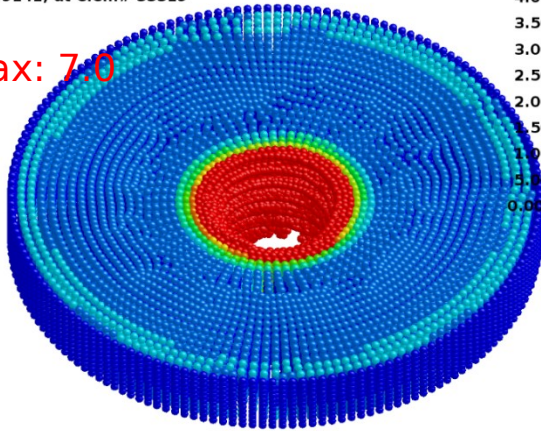
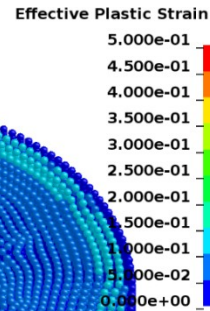


SPG with Thermal Effect

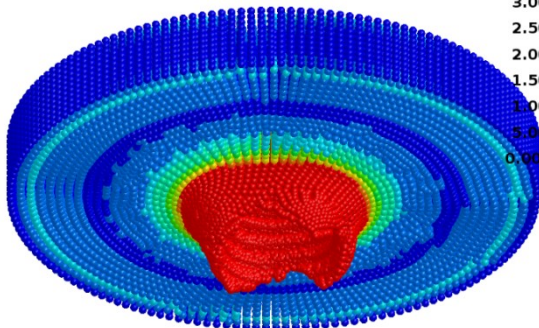
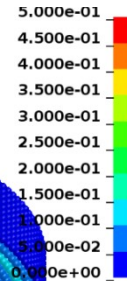
With thermal

Time = 1.295
Contours of Effective Plastic Strain
max IP. value
min=0, at elem# 14953
max=6.99141, at elem# 33319

Max: 7.0



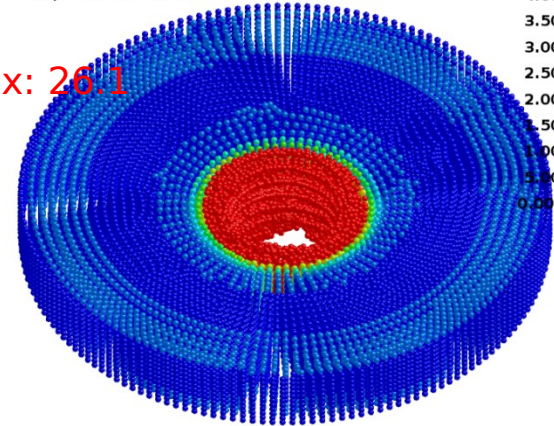
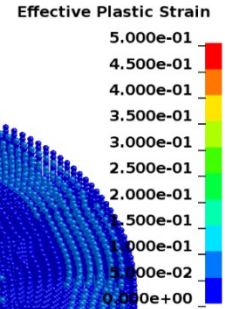
Contours of Effective Plastic Strain
max IP. value
min=0, at elem# 14953
max=6.99141, at elem# 33319



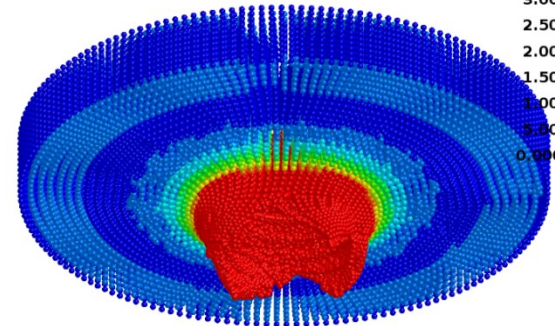
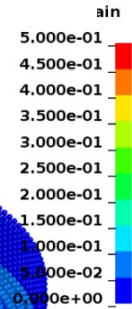
Without thermal

Time = 1.295
Contours of Effective Plastic Strain
max IP. value
min=0, at elem# 14953
max=26.1368, at elem# 32919

Max: 26.1

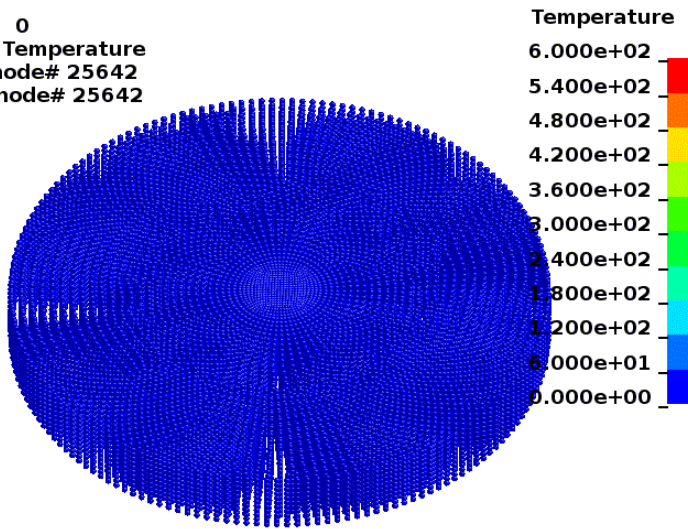


Contours of Effective Plastic Strain
max IP. value
min=0, at elem# 14953
max=26.1368, at elem# 32919

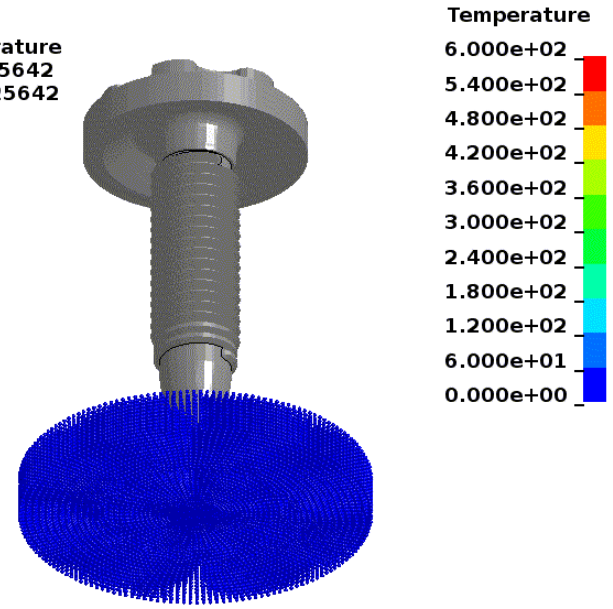


Evolution of temperature field

Time = 0
Contours of Temperature
min=0, at node# 25642
max=0, at node# 25642



Time = 0
Contours of Temperature
min=0, at node# 25642
max=0, at node# 25642



Peridynamics Method

Developed for brittle fracture analysis.

Only available in LS-DYNA.

- Was developed by Dr. Steward Silling at Sandia Nat. Lab. in early 2000.
- Is a discontinuous Galerkin (DG) FEM approach with bond-based peridynamics theory.
- Accommodates for non-uniform mesh and allow the direct enforcement of boundary conditions and constraints.
- Failure is based on critical energy released rate. No element deletion is needed to advance the cracks.
- Branching of the cracks is an outcome of the DG approach. Self-contact between cracks is possible but CPU time consuming.
- Was released in late 2015 for LS-DYNA SMP/MPP version.
- In crashworthiness simulation, it is useful for windshield or plastic panels damage analysis.

- Discontinuous Galerkin Weak Form-Explicit Dynamics

If $\Omega \in R^n$ is the domain of $\mathbf{u} \in U$ with boundary $\partial\Omega$, the solution of a dynamic system is located in a subspace of Banach space :

$$S(\Omega) = \{\mathbf{u}(\mathbf{X}) \in L^2(\Omega) | \mathbf{u}(\mathbf{X}_g) = g(\mathbf{X}_g) \quad \forall \mathbf{X}_g \in S_u\}$$

Let $\mathbf{v}(\mathbf{X})$ denote a test function located at

$$S'(\Omega) = \{\mathbf{v}(\mathbf{X}) \in L^2(\Omega) | \mathbf{v}(\mathbf{X}_g) = 0 \quad \forall \mathbf{X}_g \in S_u\}$$

The weak form of the governing equation:

$$\int_{\Omega} \rho \ddot{\mathbf{u}}(\mathbf{X}) \cdot \mathbf{v}(\mathbf{X}) dV_{\mathbf{X}} \quad \forall \mathbf{u}(\mathbf{X}) \in S(\Omega), \quad \mathbf{v}(\mathbf{X}) \in S'(\Omega)$$

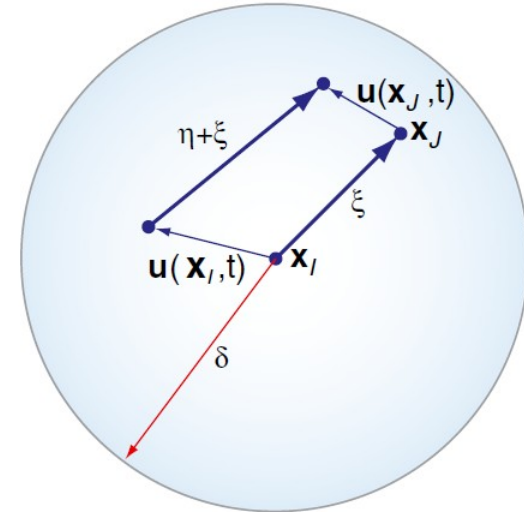
$$= \int_{\Omega} \int_{H_{\mathbf{v}}} \mathbf{f}(\eta, \xi) dV_{\mathbf{X}'} \cdot \mathbf{v}(\mathbf{X}) dV_{\mathbf{X}} + \int_{\Omega} \mathbf{b}(\mathbf{X}) \cdot \mathbf{v}(\mathbf{X}) dV_{\mathbf{X}}$$

$$\mathbf{f} = c s \frac{\eta + \xi}{|\eta + \xi|}, \quad s = \frac{|\xi + \eta| - |\xi|}{|\xi|}, \quad c = \frac{18K}{\pi \delta^4}$$

Here s is the bond stretch with micro modulus c . A bond will break permanently when its bond stretch over a critical value:

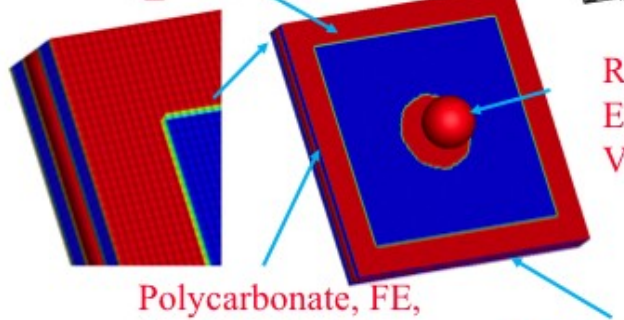
$$s \geq s_c = \sqrt{\frac{10G_c}{\pi c \delta^5}}$$

G_c Strain energy released rate



Fracture in Glass-PC-Glass Composite

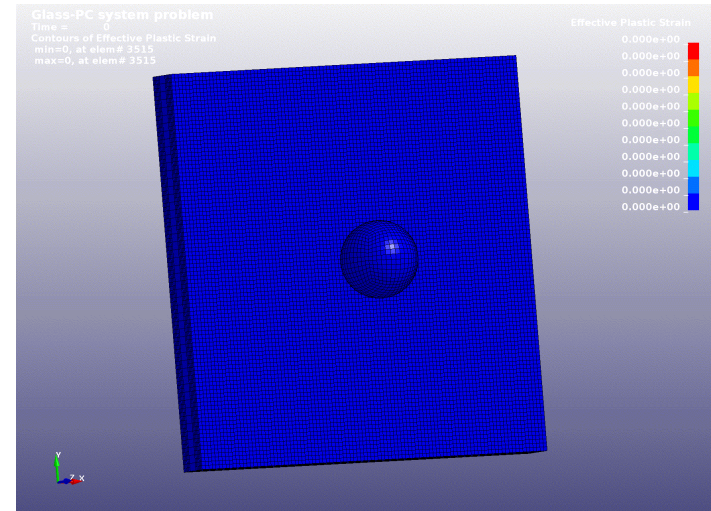
Essential boundary
 $V_z=0.0$ m/s



Polycarbonate, FE,
Elastic material
E: 2G pa, $\nu:0.25$

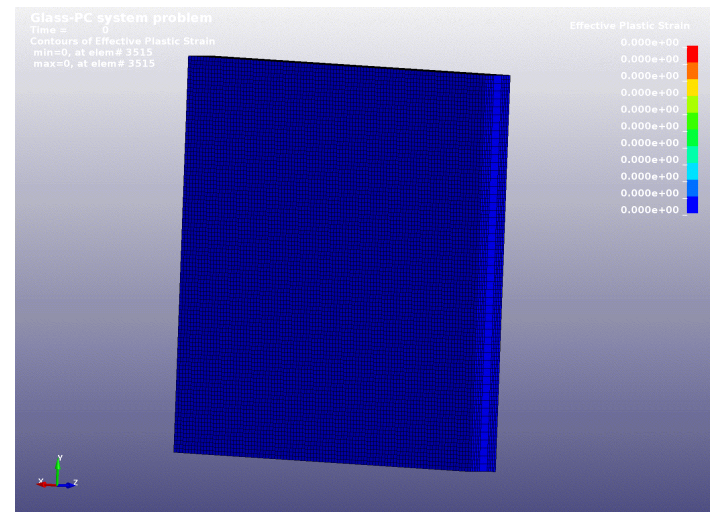
Soda-Lime glass,
Peridynamic model
E: 72G pa, $G:8$ J/m²

Rigid body, FE
E: 211G pa, $\rho: 2$ g
V=30 m/s



Top View

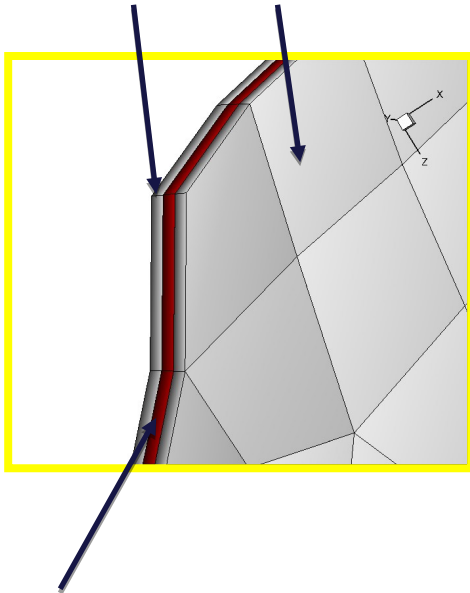
Evolution of damage field (0~1)



Rear View

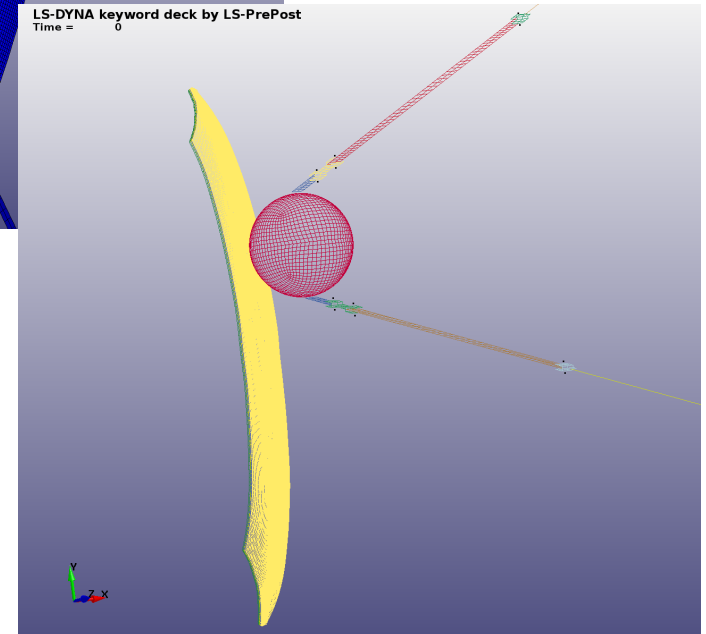
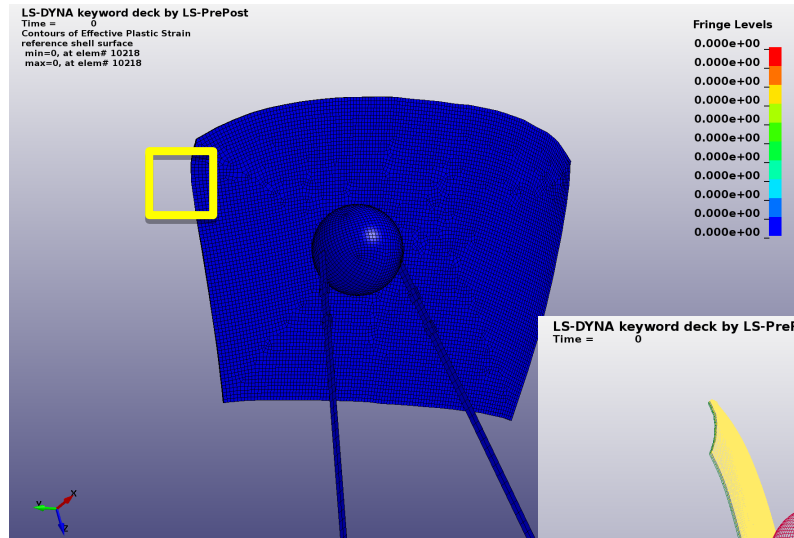
Windshield failure analysis by Peridynamics

Glass layers, Peridynamic Model, MAT_ELASTIC_PERI

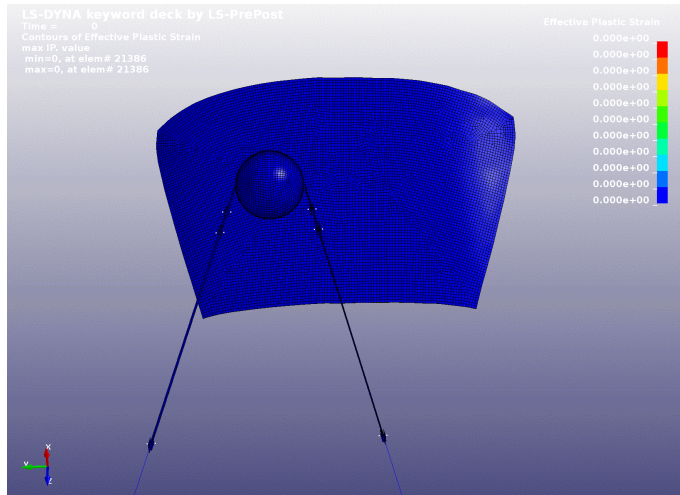


vinyl layer, FEM Model,
MAT_PIECEWISE_LINEAR_PLASTICITY

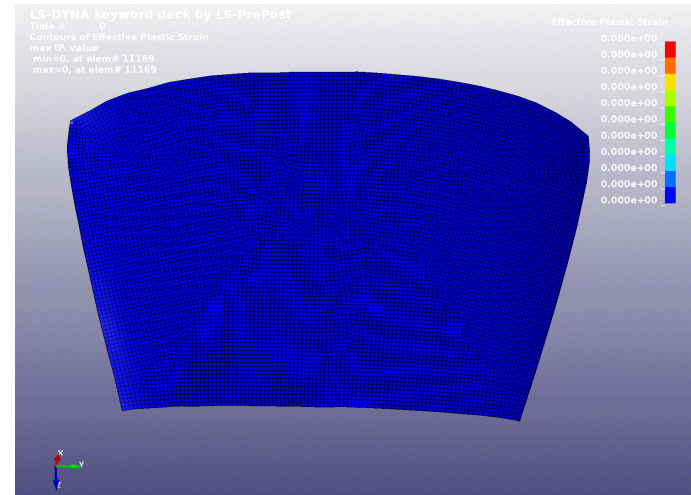
Interface of Vinyl and glasses:
CONTACT_TIED_SURFACE_TO_SURFACE_OFFSET



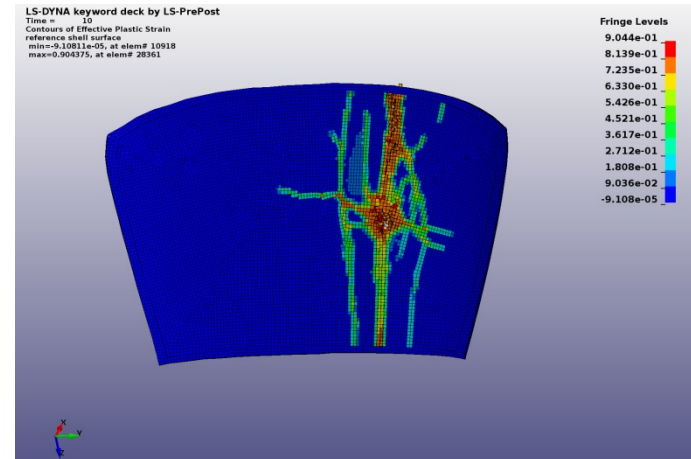
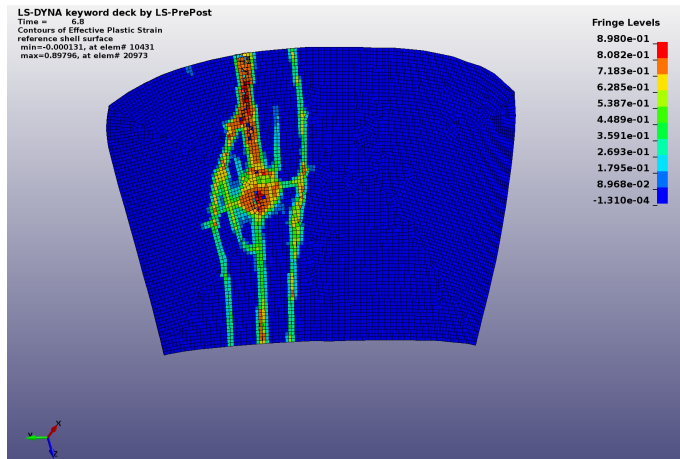
Evolution of damage field (0~1)



top view

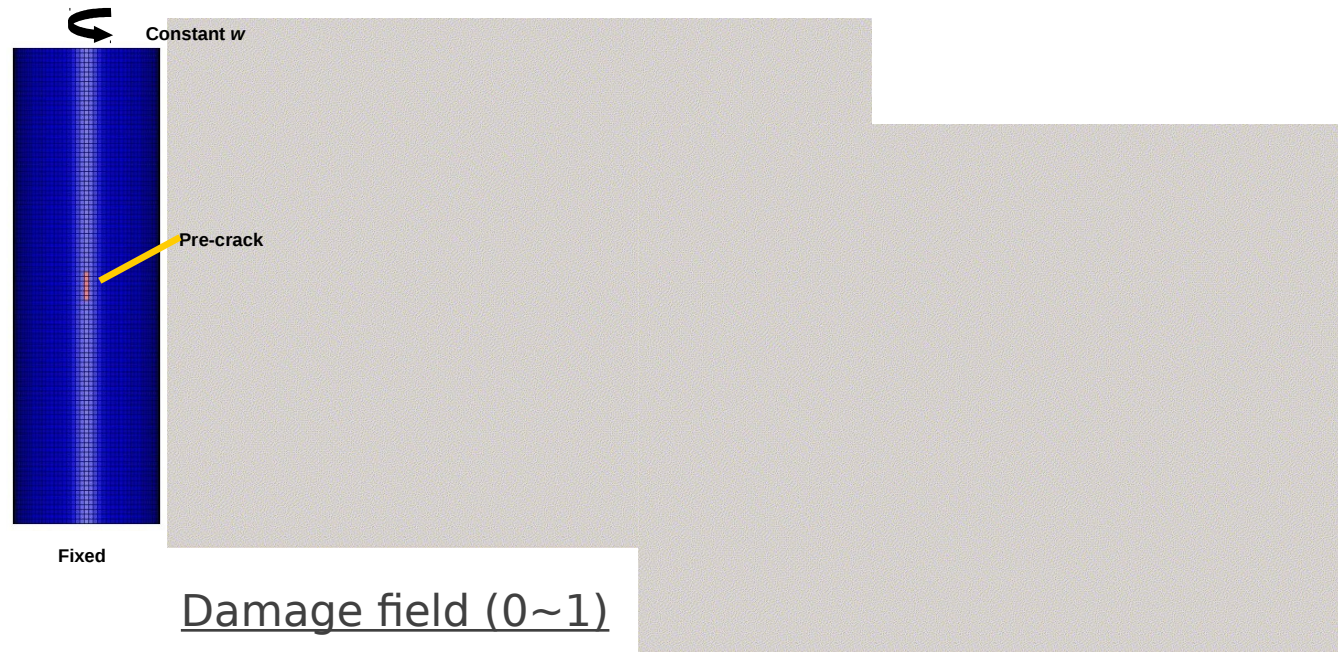
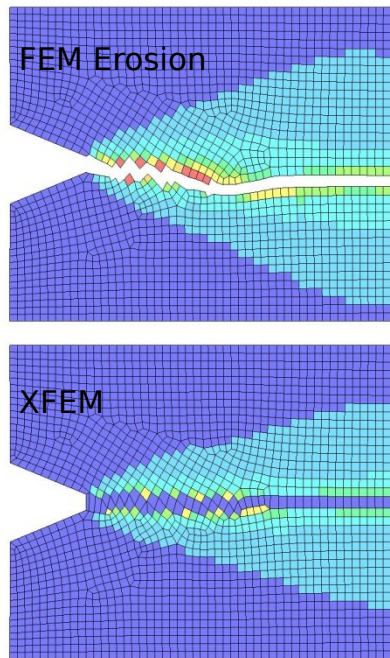


rear view



Extended Finite Element Method (XFEM) for Shell

Ductile fracture analysis in shell structures



- Is based on the phantom node approach.
- Works for FEM shell #2 and #16.
- Various failure criteria have been implemented.
- Recently strain regularization/meshfree visibility have been introduced to yield better convergence for ductile material failure simulation.

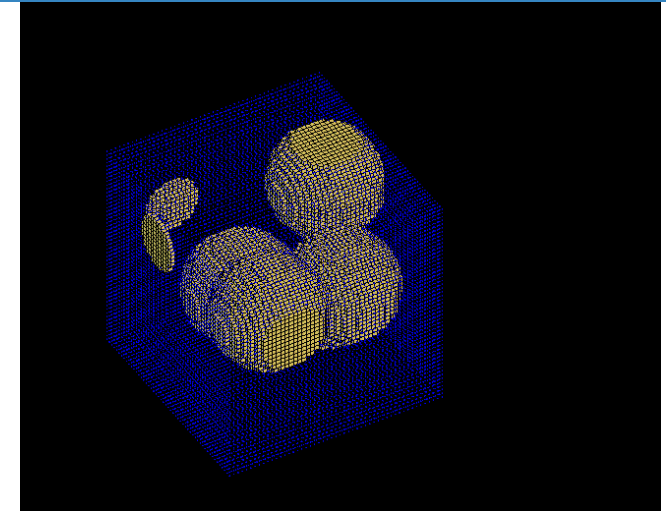
EPS

Meshfree-enriched Finite Element Method (MEFEM)

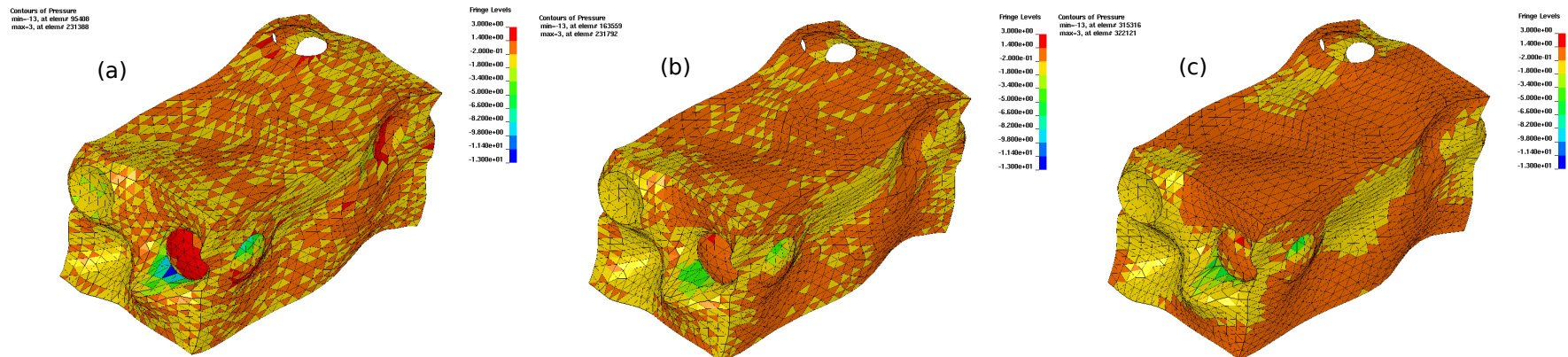
Developed for near-incompressible analysis.

Only available in LS-DYNA.

- Available for explicit and implicit analyses.
- Is a 5-noded finite element method.
- Requires LS-Pre/Post mesh generator.
- Is inf-sup stable.

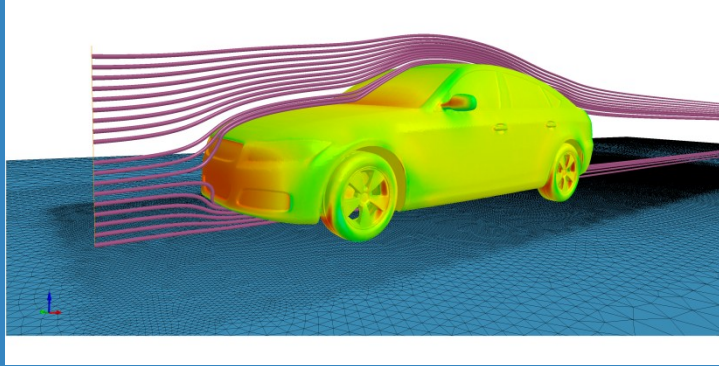


Unit Cell approach for Composite Analysis



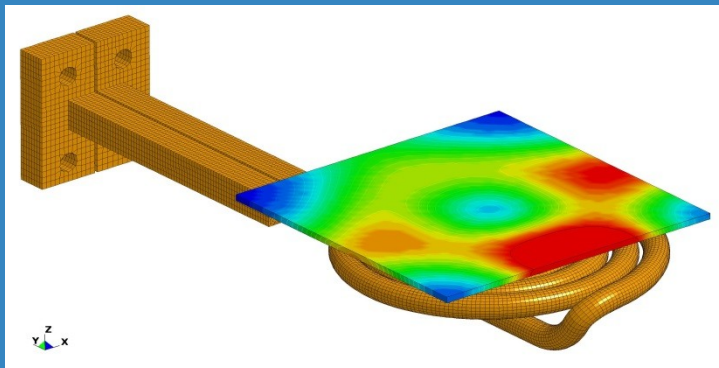
Comparison of pressure contours: (a) displacement-based meshfree Galerkin method (b) displacement-based meshfree Galerkin method with pressure smoothing and (c) presented method.

Computational fluid dynamics (CFD)



Electromagnetics

Iñaki Çaldichoury



ICFD Solver

It is a module for simulating incompressible flows. It supports multiple turbulence models as well as free surface flows. It is coupled with the structural mechanics solver for fluid-structure interaction, the thermal solver for conjugate heat transfer and the discrete element method. As a stand alone CFD solver it provides accurate results for drag and lift.

Multi-Physics :

Coupling with structure (FSI)

Coupling with thermal (Conjugate heat transfer)

Coupling with DEM :

New coupling of ICFD with Discrete Element Method for the simulation of mud or snow deposition on ground vehicles.

Classic CFD :

Turbulence models :

New RANS models: Realizable K-epsilon, K-Omega, K-Omega SST, Spalart-Almaras.

New tools for boundary layer mesh control.

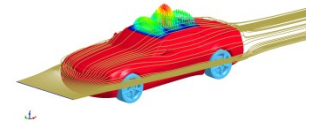
Free surface problems :

New Wave Generator

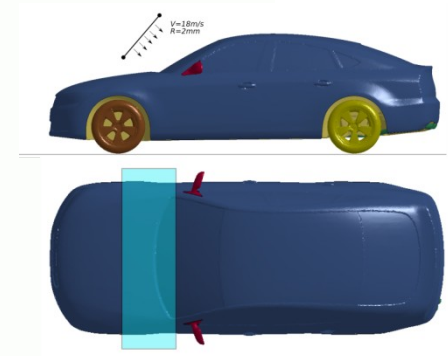
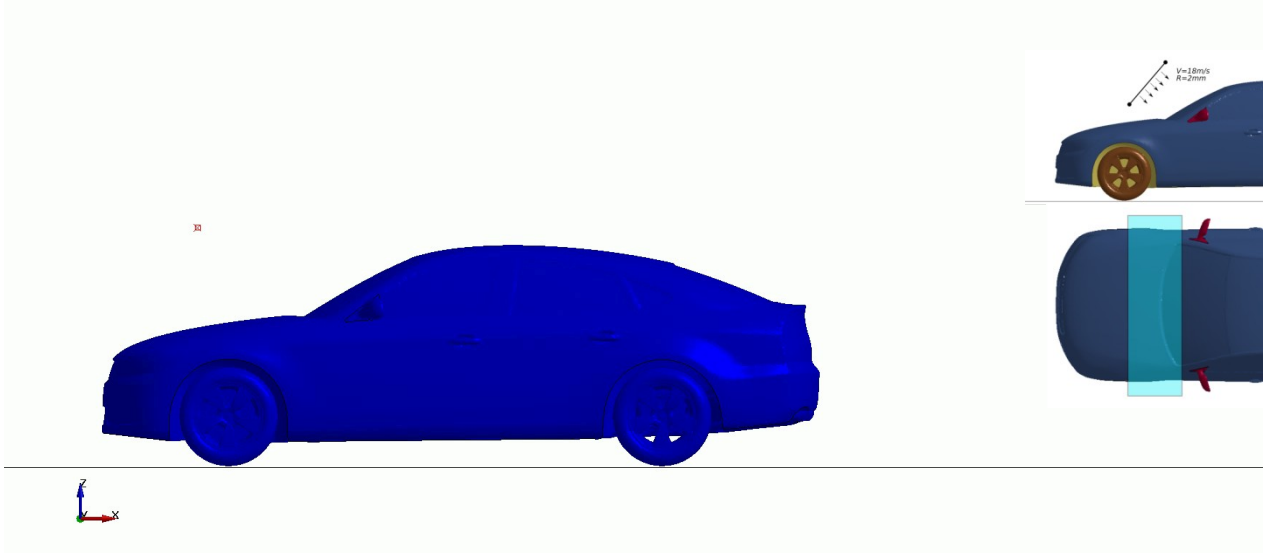
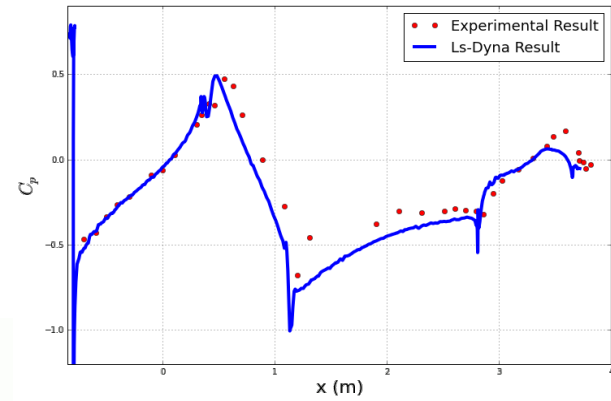
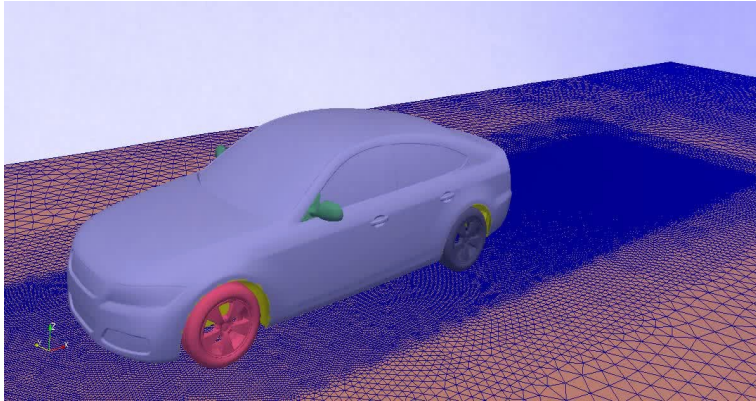
Non-Newtonian fluids and Porous media :

New Models :Power-Law, Carreau and Cross. Advances in Resin Transfer Molding Simulation. Temperature variable viscosity laws.

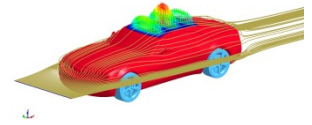
DEM coupling



Mud and Snow Deposition. Potential applications include drug delivery, erosion of river bed and FSI using particle bonding capabilities

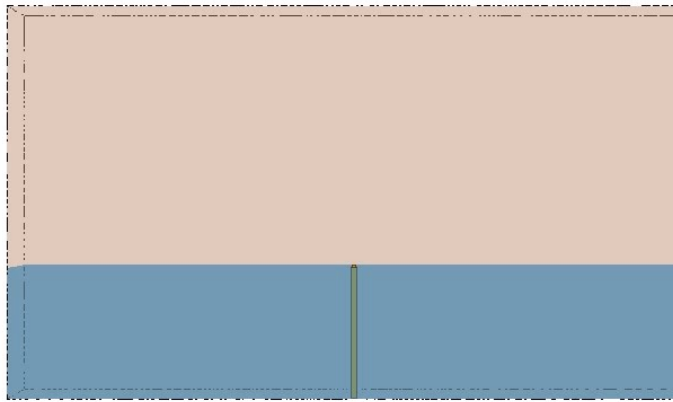


Sloshing and slamming with FSI

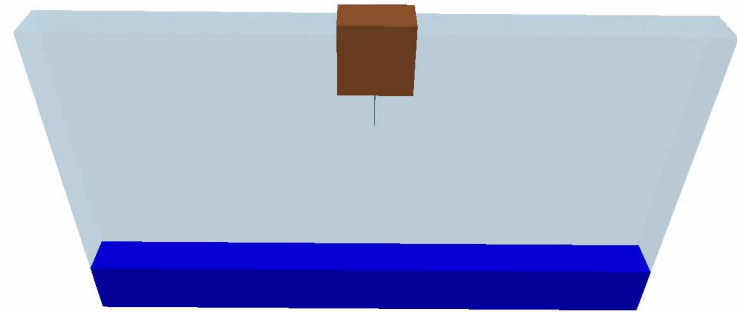


Time = 0, #nodes=2146228, #elem2d=274382, #elem3d=6403785

Time = 0

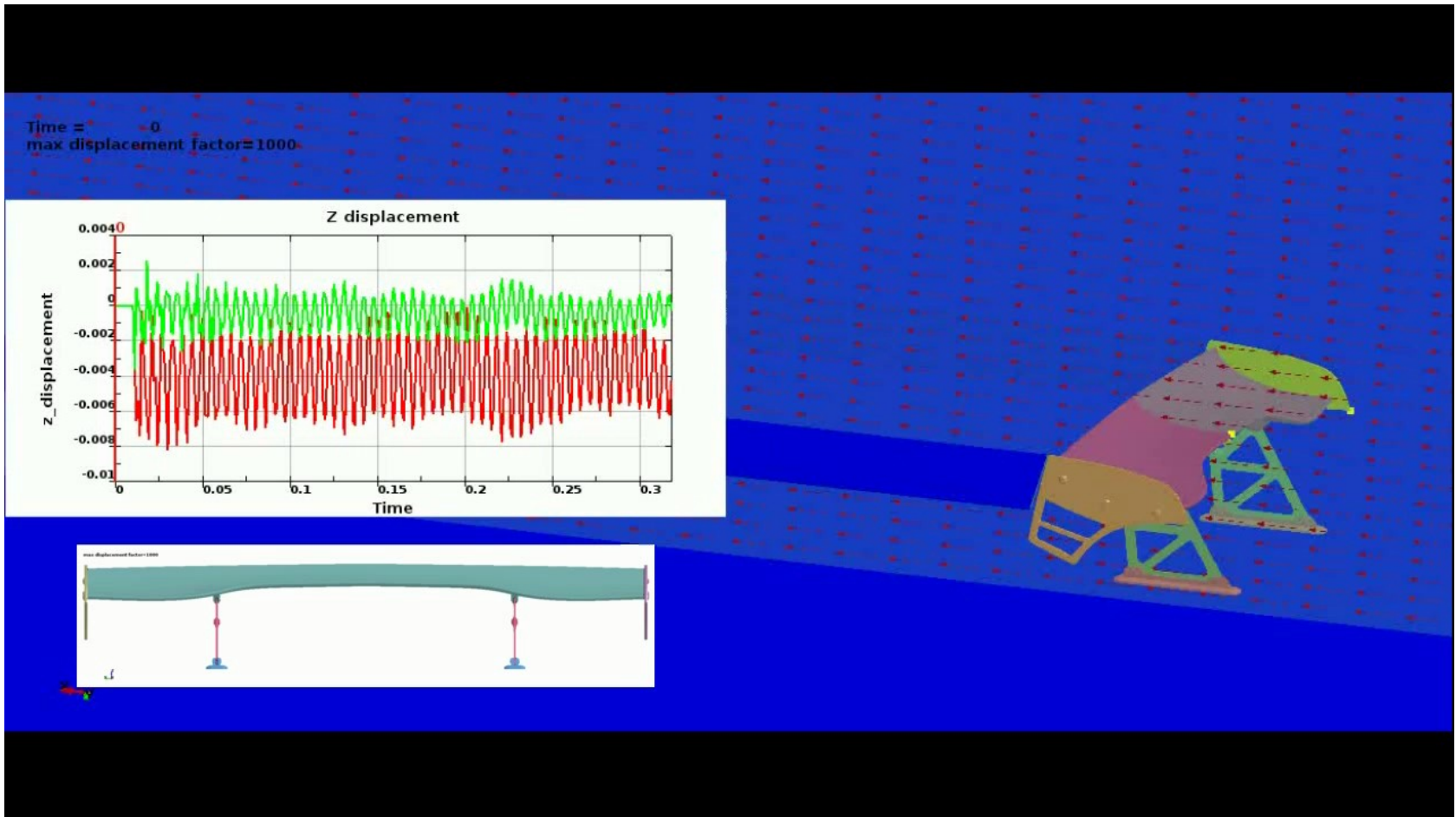
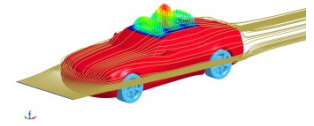


Fluid Elastic Body Interaction Problem

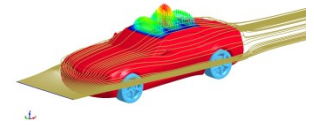


Tuned Liquid Damping Problem

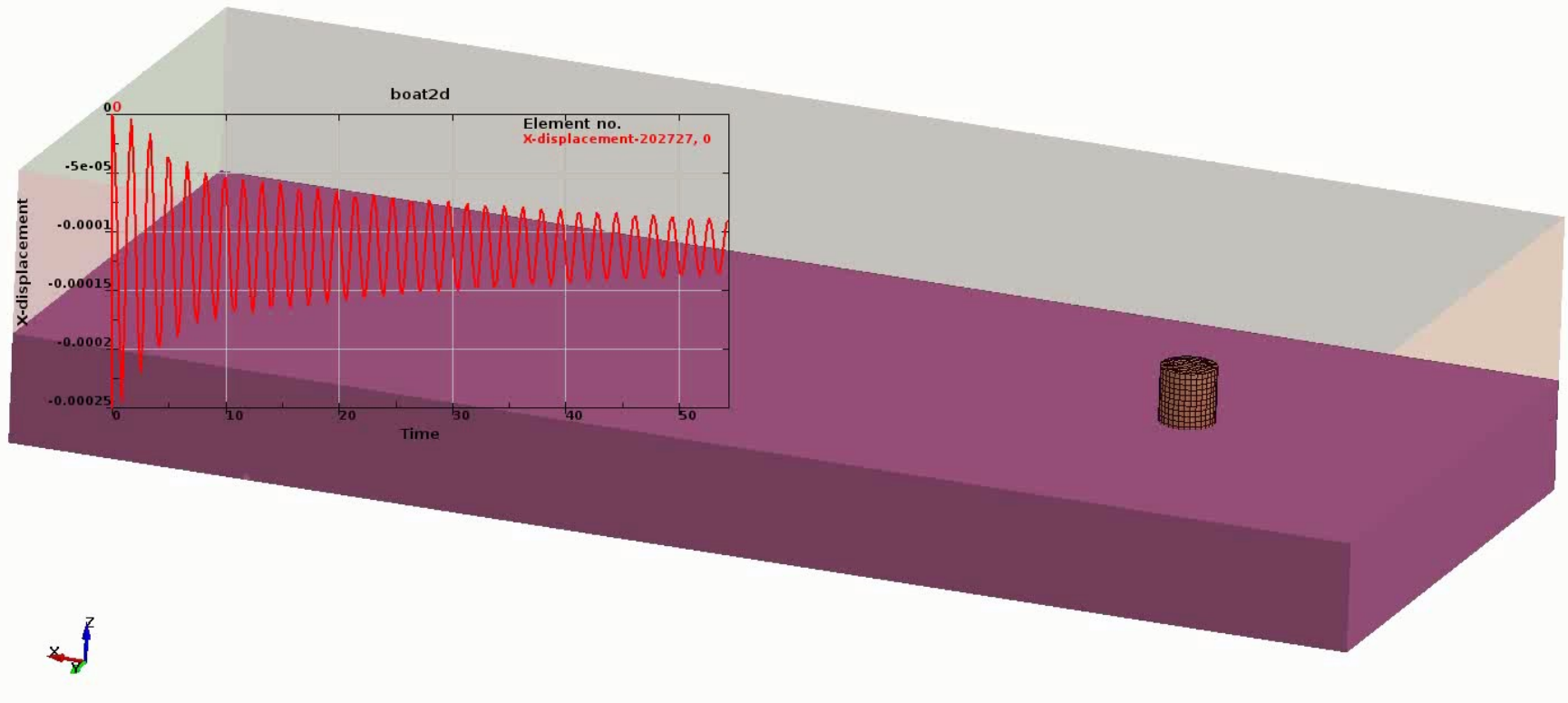
Vibration analysis



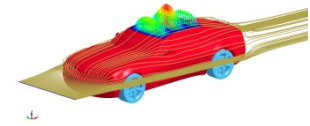
Wave generation



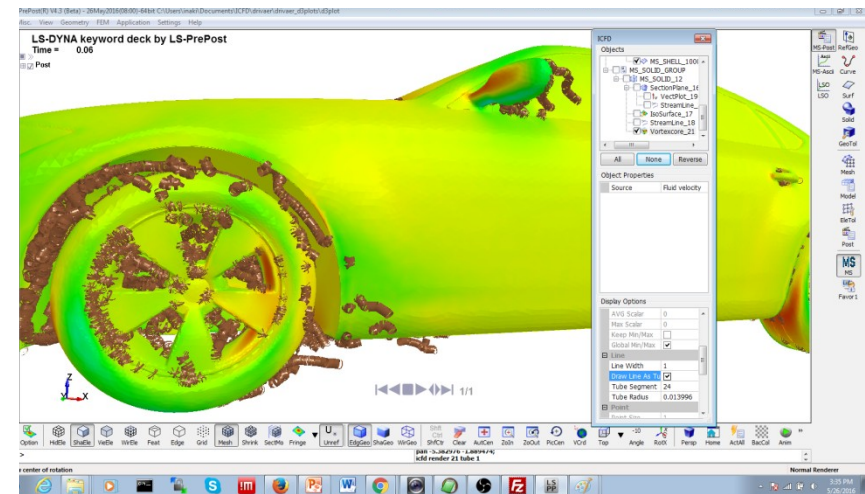
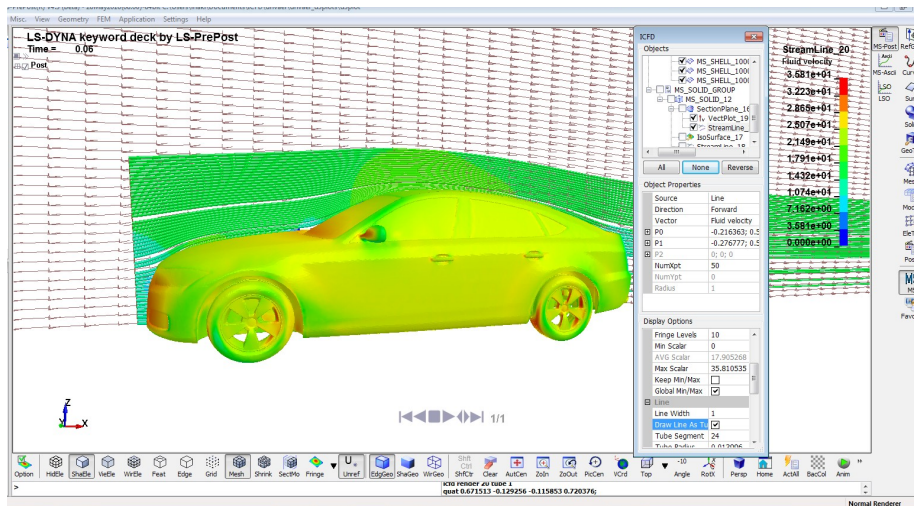
Time = 0



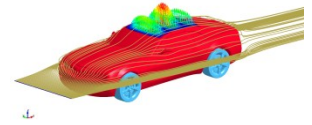
Pre and Post treatments.



A specific interface in order to post treat CFD results is under development (available in LSPP4.3). It follows a tree structure allowing for robust, flexible and powerful CFD oriented post treatments. The CFD Pre interface, available for beta testing aims at providing the CFD user with a friendly environment to define his problem and allowing him to easily check his models for error and inconsistencies between keywords.



In summary the ICFD solver:



Can provide accurate and scalable CFD results for a large range of industrial applications making it a good alternative to traditional commercial CFD solvers.



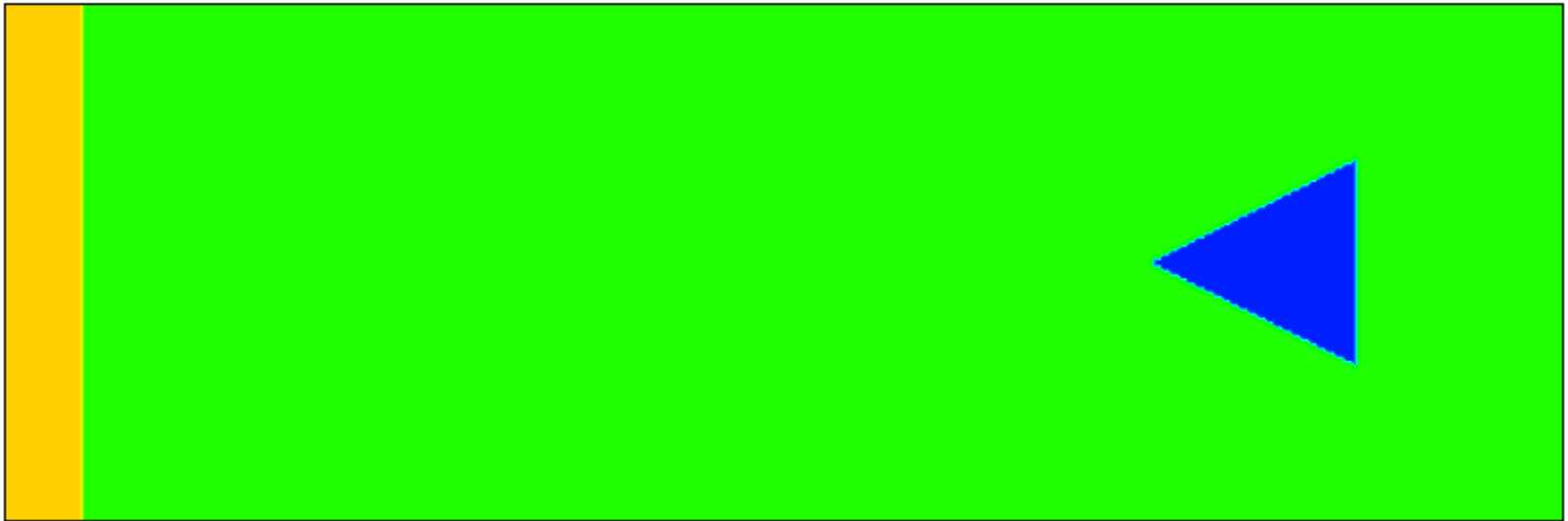
It is coupled to other modules in LS-DYNA which allow multi-physics/multi-scale simulations in the area of fluid-structure interaction, conjugate heat coupled to electromagnetism and discrete element methods.



Presents a steady growth of features mostly implemented as a request by users.

CESE Solver

It is a module for simulating compressible flows. It is based upon the Conservation Element/Solution Element (CESE) method. Its unified treatment of space and time through the introduction of Conservation Element (CE) and Solution Element (SE) assures excellent conservation of the solution which makes it a suitable candidate in applications involving shock waves (supersonic flows, blast waves).

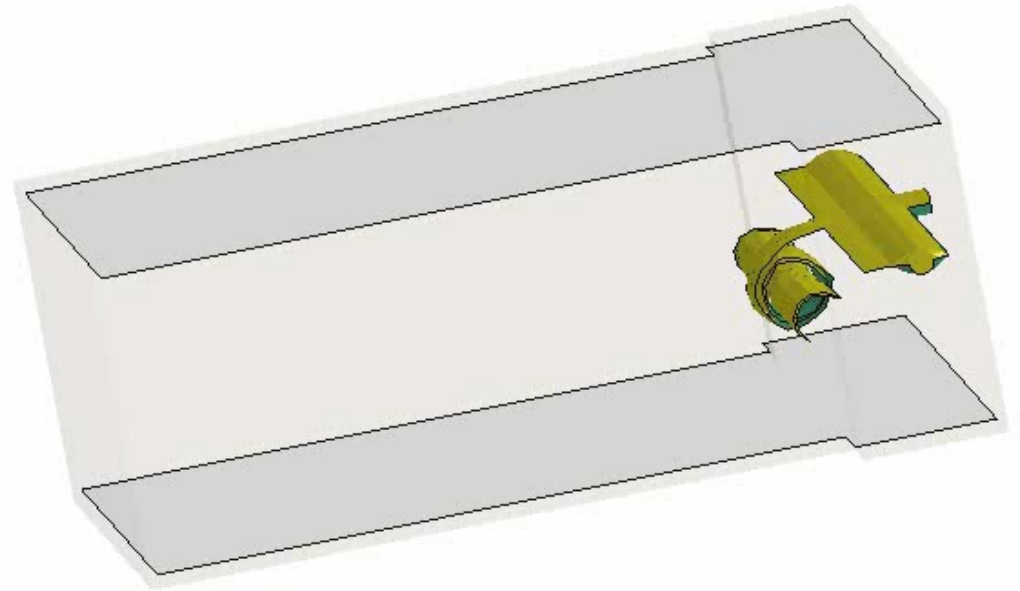


Airbag inflator

New EOS, ***CESE_EOS_INFLATOR2** allowing to define Cp and Cv thermodynamic expansions for an inflator gas mixture with two temperature ranges, one below 1000 Kelvins, one above 1000 Kelvins.

These Coefficient expansions for the specific heats are generated by the 0D inflator model solver. See ***CHEMISTRY_CONTROL_INFLATOR** and ***CHEMISTRY_INFLATOR_PROPERTIES**

rolled_bottom_bag_deployment
Time = 0.00225



Blast Waves

Support of *LOAD_BLAST_ENHANCED

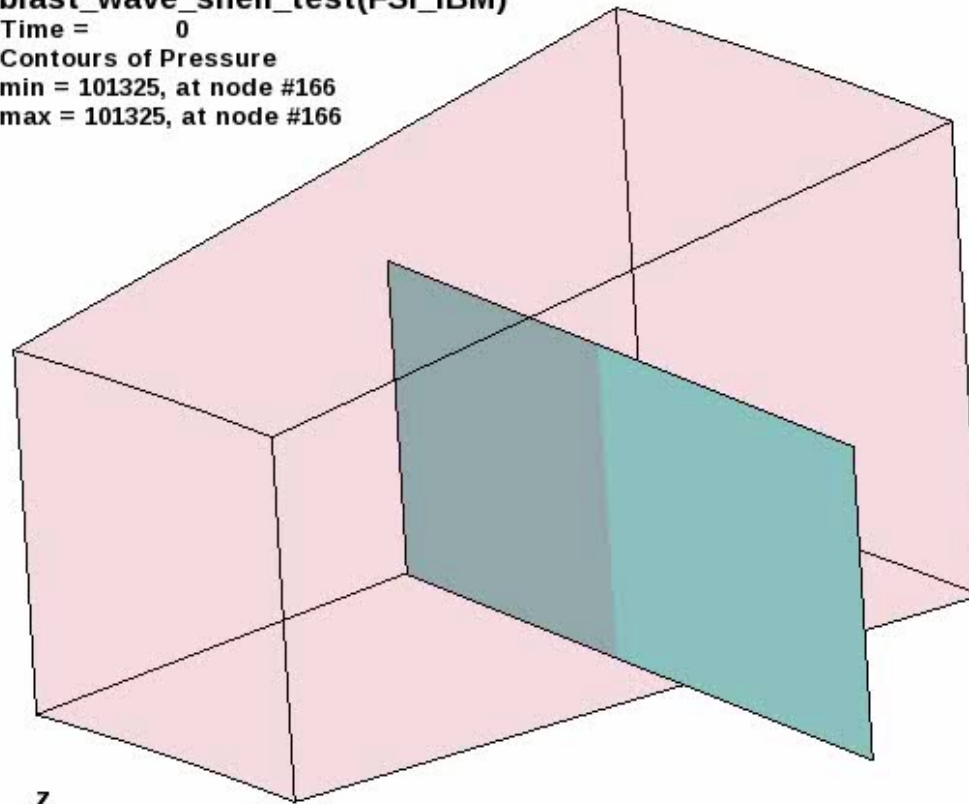
blast_wave_shell_test(FSI_IBM)

Time = 0

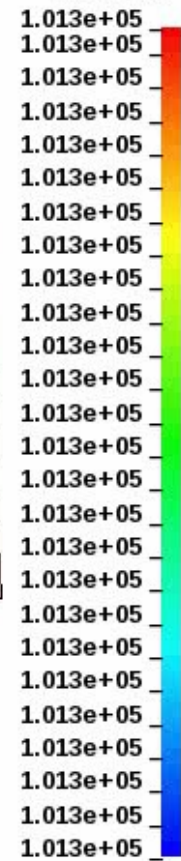
Contours of Pressure

min = 101325, at node #166

max = 101325, at node #166



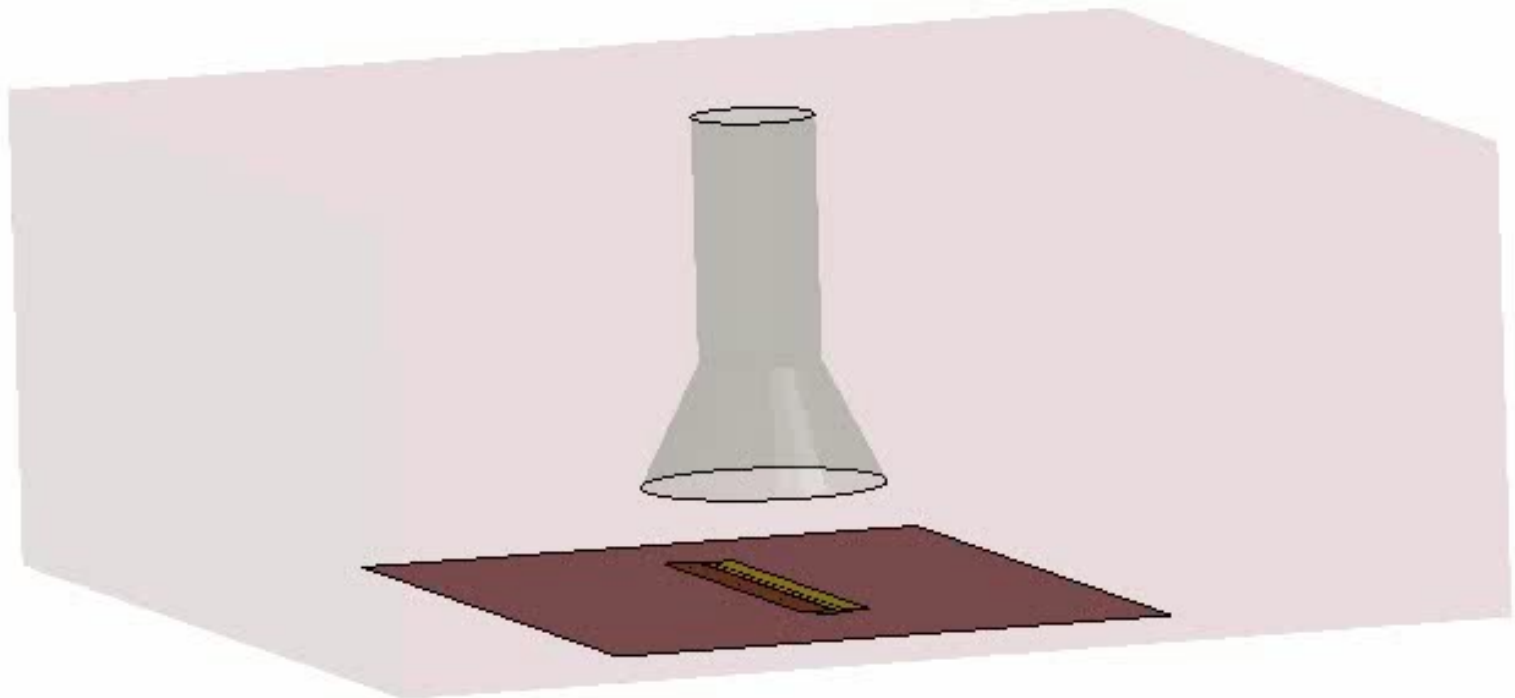
Pressure



And vacuum cleaners...

3_Flimsy_stack_up

Time = 0



LS-DYNA Electro-Magnetic Solver Applications

Current applications :

Magnetic Pulse Forming

Magnetic Pulse Welding

Induction welding

Induction heating

Resistive heating

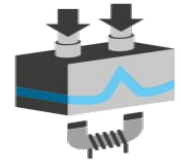
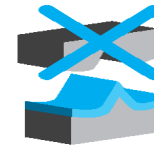
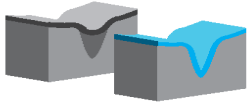
Electromagnetic spot welding

Coil design and optimization

Contact: rail gun, short circuits

Generation of ultra high magnetic fields

Magnetic Metal Forming



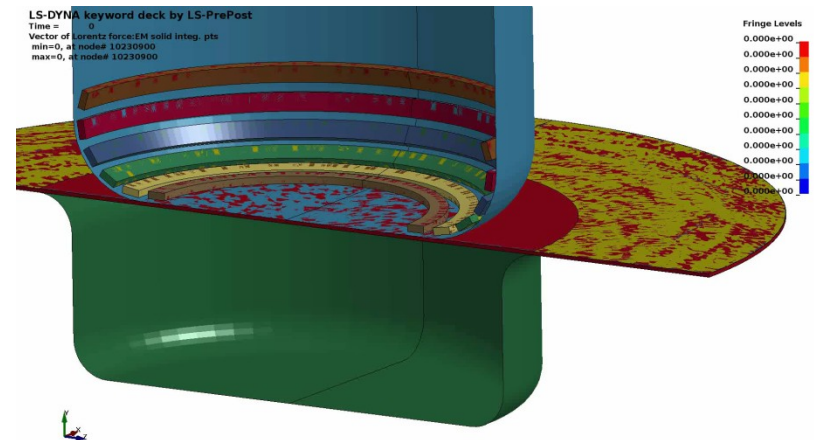
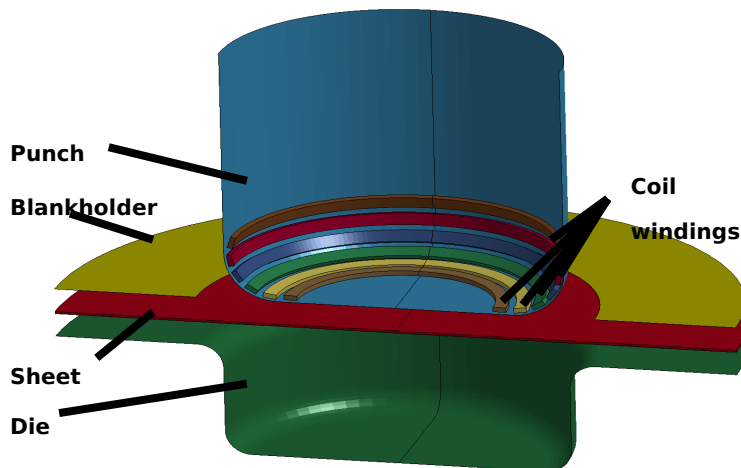
Achieve higher formability than traditional methods

Can produce Sharp corners and fine details

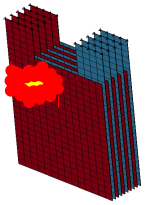
Greatly reduced springback and good stress distribution

Use one sided die (Optional - none metallic die)

Can be combined with any other forming technology

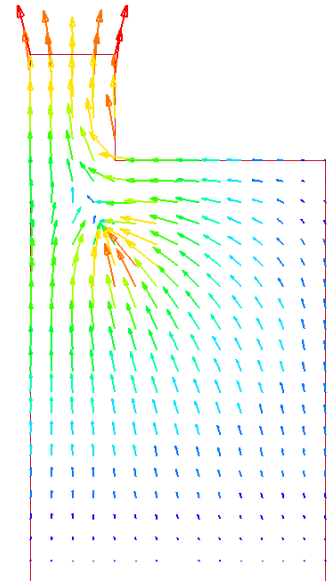
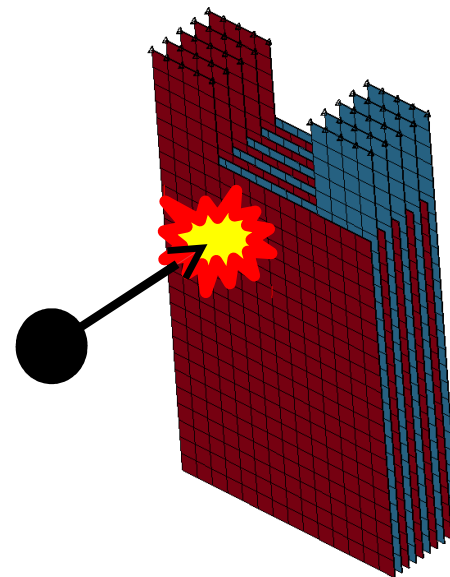
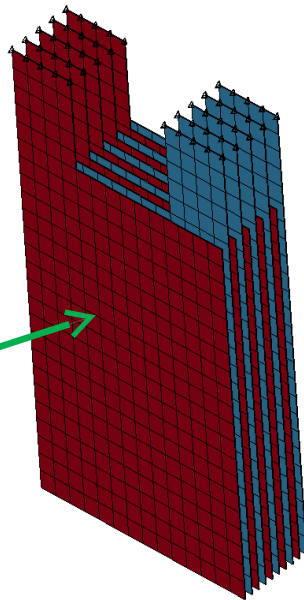


New battery module :



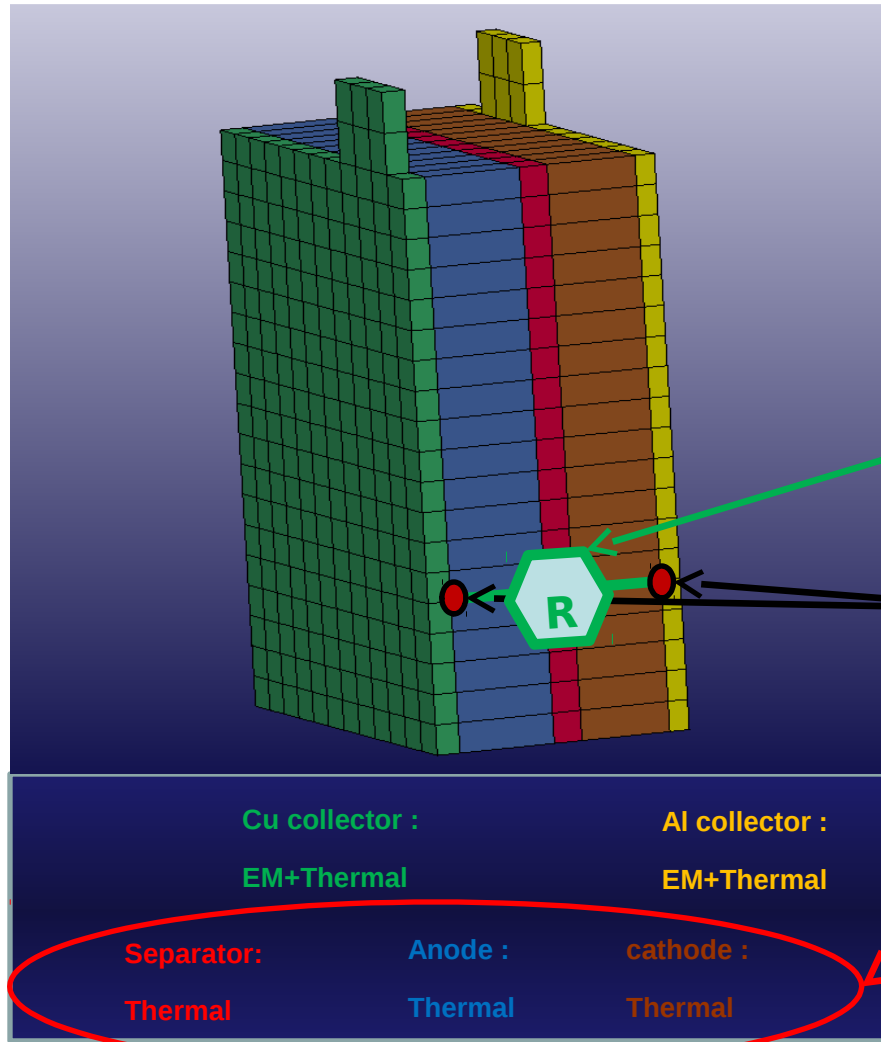
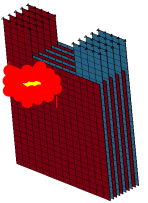
New capabilities are being developed within the EM module in order to simulate short circuits in batteries. The final objective is to be able to predict the combined structural, electrical, electrochemical, and thermal (EET) responses of automotive batteries to crash-induced crush and short circuit, overcharge, and thermal ramp, and validate it for conditions relevant to automotive crash.

Lithium-Ion cell

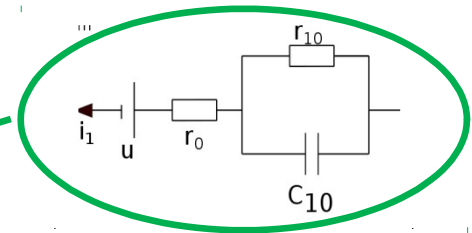


In collaboration with
J. Marcicki et al,
Ford Research and Innovation Center, Dearborn, MI

New battery module :



Battery charge effect simulated by introduction of a Randles circuit model

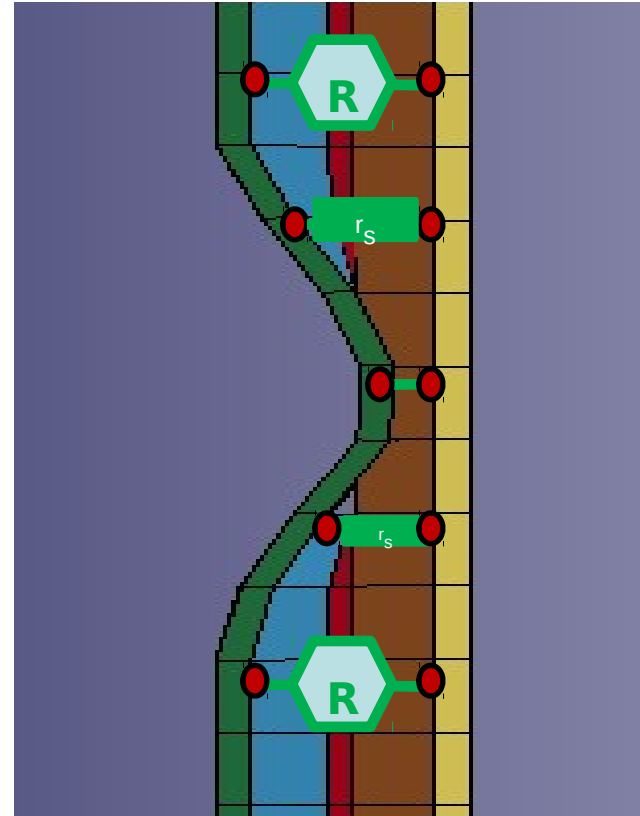
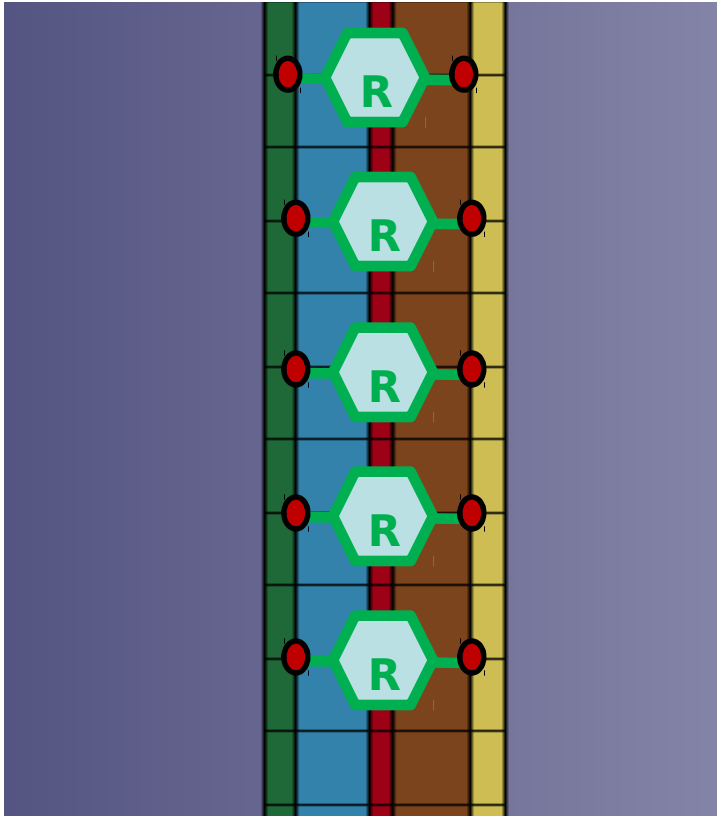
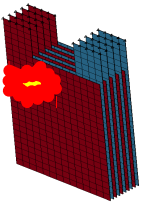


$r_0 * i^2$ added to thermal
 $ITdU/dT$ added to thermal

Allow correct material mass, heat capacity and thermal conductivity



Short-circuit simulation :



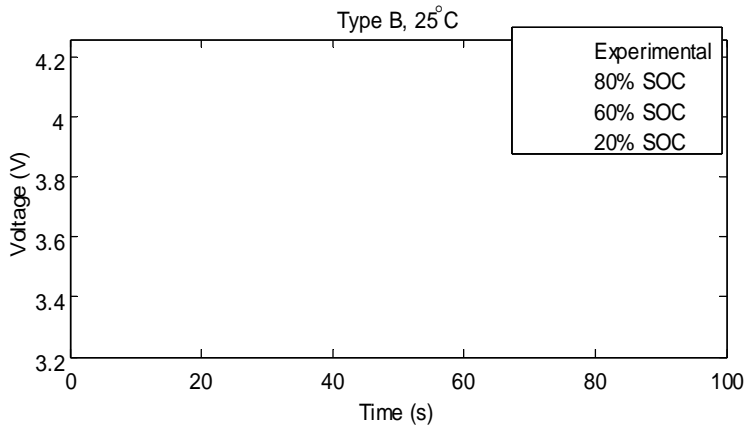
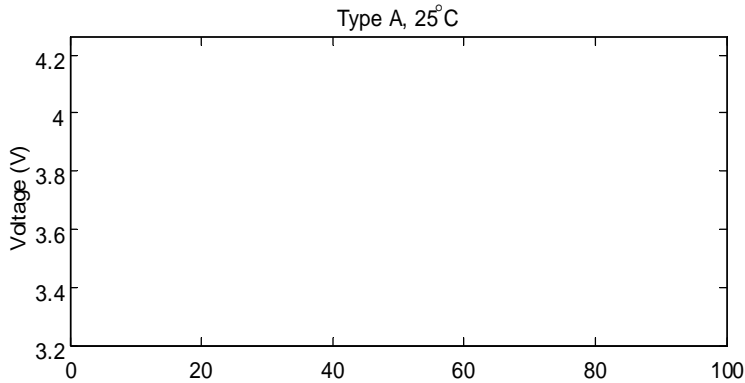
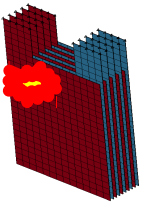
Replace Randle circuit by
resistance R_s

$R_s \times i^2$ added to thermal
added to thermal

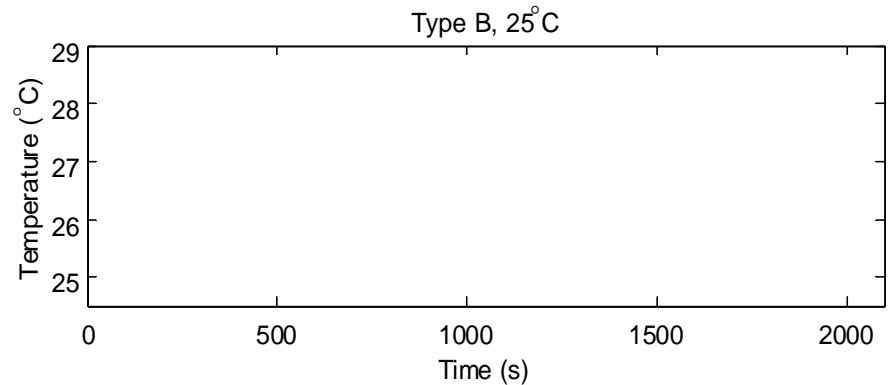
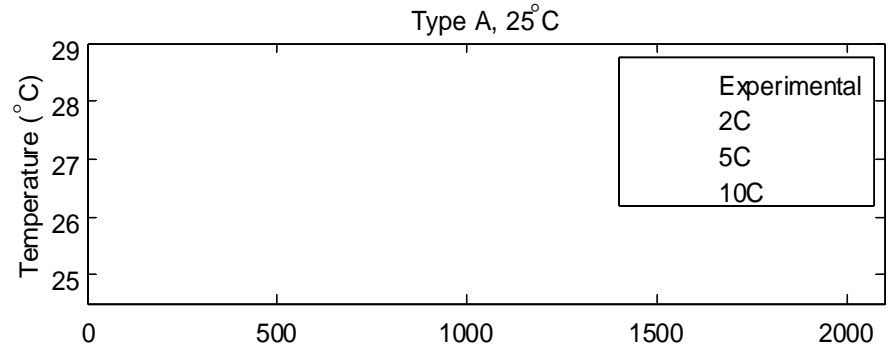


ONE FORD
ONE TEAM • ONE PLAN • ONE GOAL

Standard use validation :



Voltage vs time



Temperature vs time

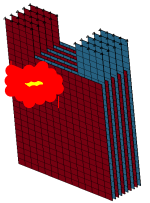
HPPC and multirate capacity benchmarks performed

by Ford research and Innovation center

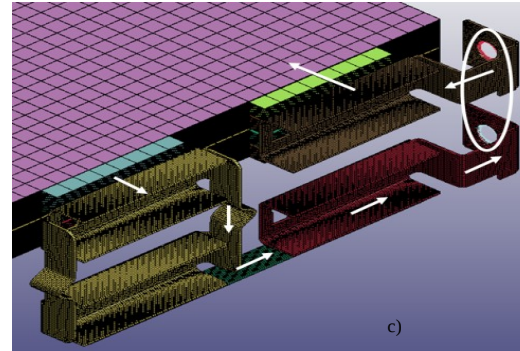
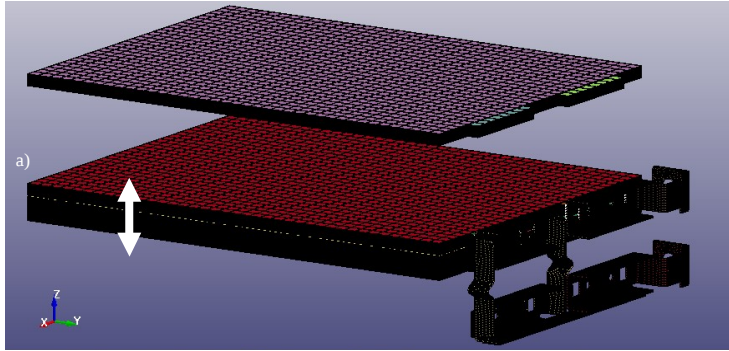


ONE FORD
ONE TEAM • ONE PLAN • ONE GOAL

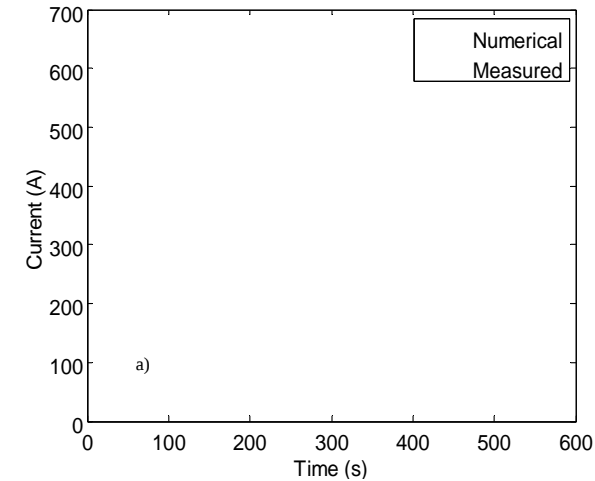
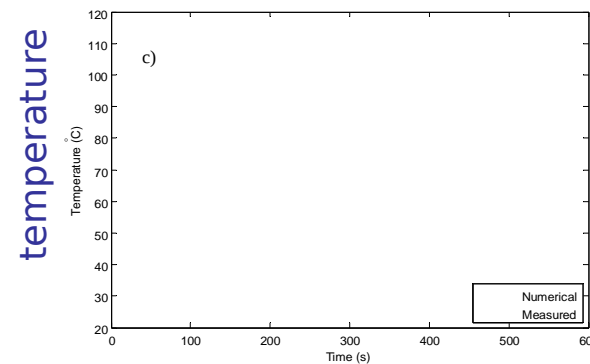
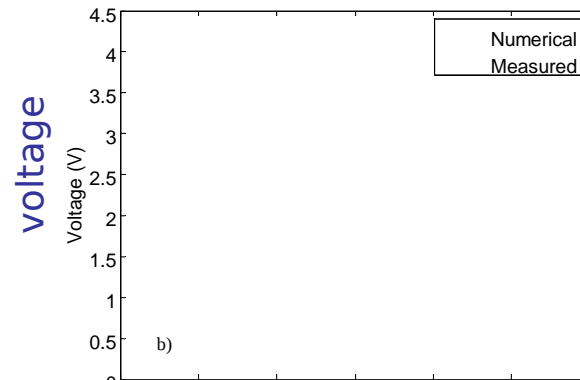
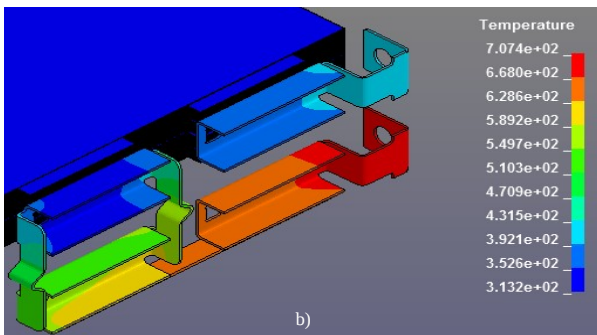
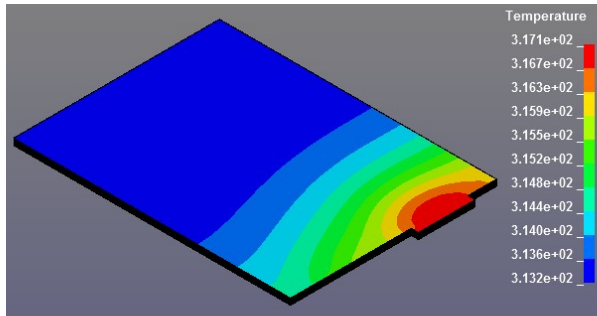
External short benchmark:



4 cells connected in parallel, 650k elements



+ and - connected
by experimental resistance

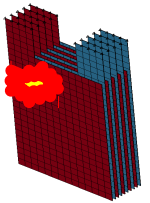


current

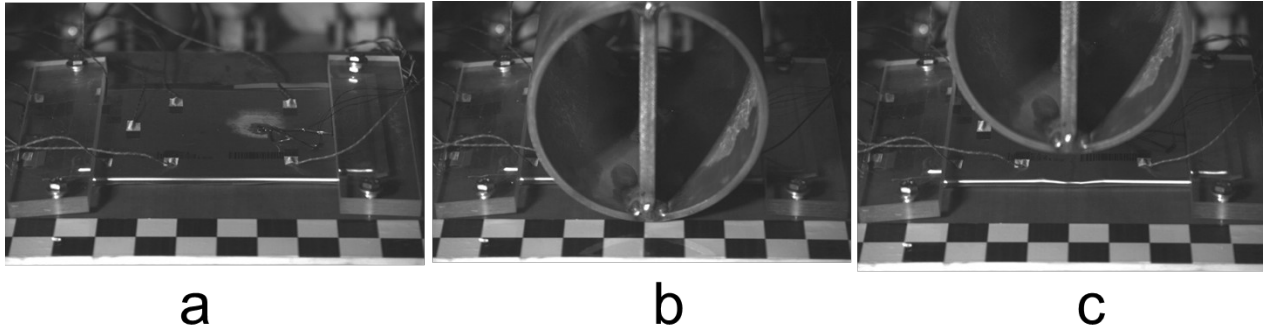


ONE FORD
ONE TEAM • ONE PLAN • ONE GOAL

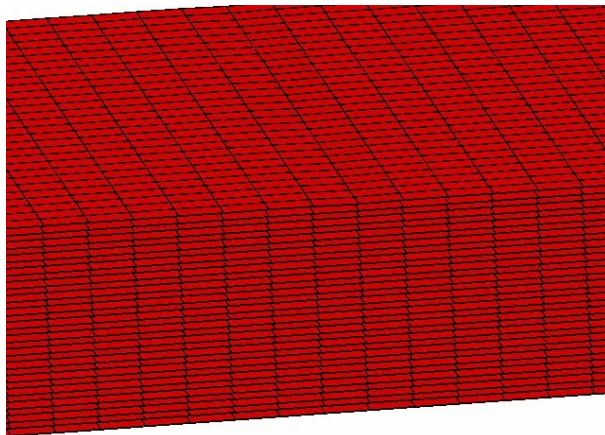
Internal short benchmark:



Impact of rod on a cell

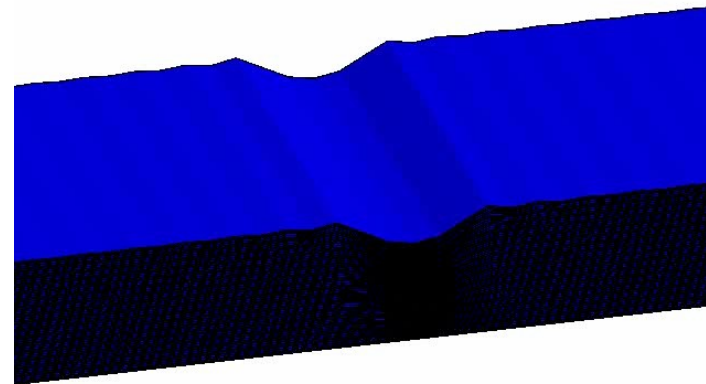


Whole short in the same simulation



25.00 frame/sec

Initial impact: $5\mu\text{s}$,
meca+EM



12.50 frame/sec

Further heating: 100s
EM+thermal

In summary the EM solver:



Is widely used electromagnetic metal forming/welding/bending applications because of its BEM method which removes the need to mesh the air and because of its robust and easy coupling with the thermal and structural thermal solvers in LS-DYNA.



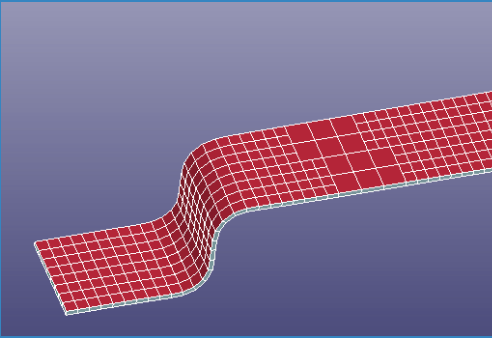
A simulation Framework for Battery Safety Modeling is under development in collaboration with Ford Motor Company and other partners (Oakridge National Lab, LS-DYNA Distributor DynaS).



Randles circuits are available in the development version and can be used with solid elements and thick shells. Future developments and studies will aim at improving shortcircuit models and the mechanical modeling of cells.

Metalforming

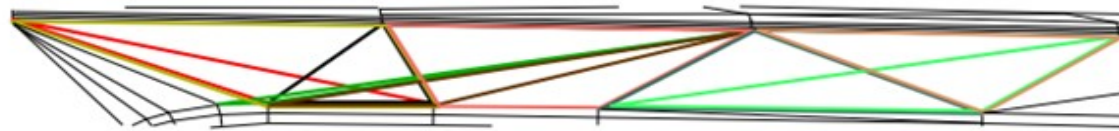
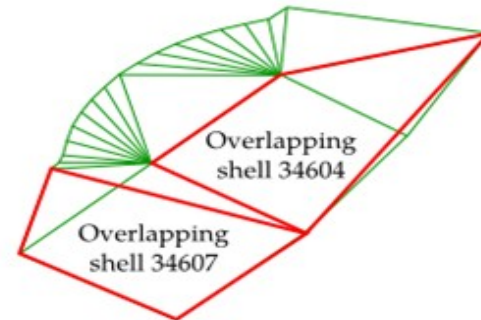
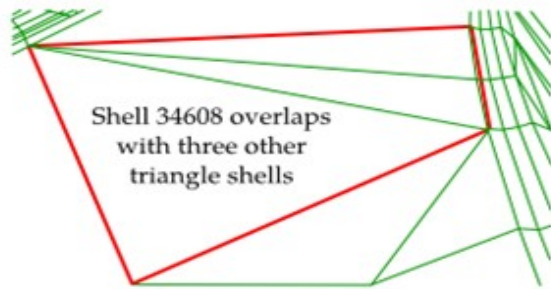
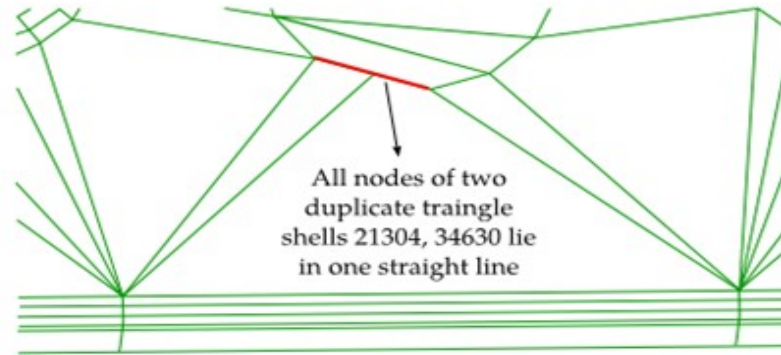
Xinhai Zhu



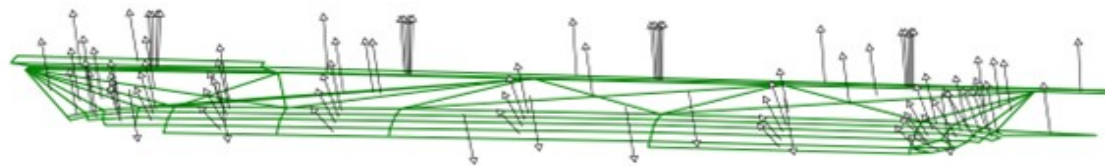
Rigid Body Mesh Check/Fix: *CONTROL_FORMING_AUTOCHECK

- **Element Normal Check / fix**
 - Mesh generators are not always reliable in giving high quality tool mesh (very long, overlapped elements, with inconsistent element normals)
 - Manual repair by user in pre-processor is time consuming and error-prone
 - Simulation with bad elements has high possibility to get unrealistic results
- **Physical offset of rigid tools**
 - In stamping simulation, it is common both upper and lower tools overlap each other in the home position
 - Negative offset is used (MST is negative)
 - With penetration, contact can be confused. Occasionally, unexpected results are obtained
- **Keyword: *CONTROL_FORMING_AUTOCHECK**
 - automatically check and fix the rigid body mesh
 - Automatically offset the rigid tool physically based on the MST values specified in contact definitions

Rigid Body Mesh Check/Fix



A severe, multiple overlapping case

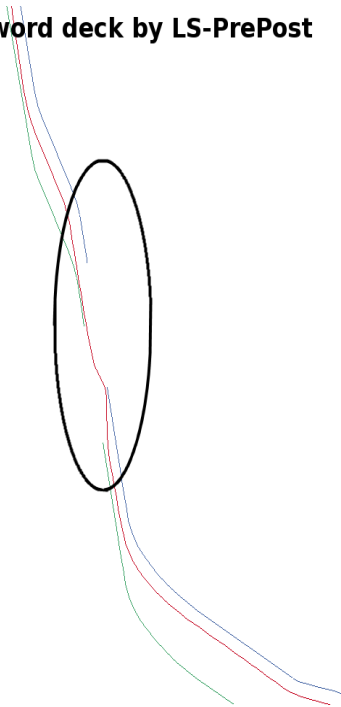


A case of typical incoming, inconsistent shell normals

Rigid Body Mesh Check/Fix

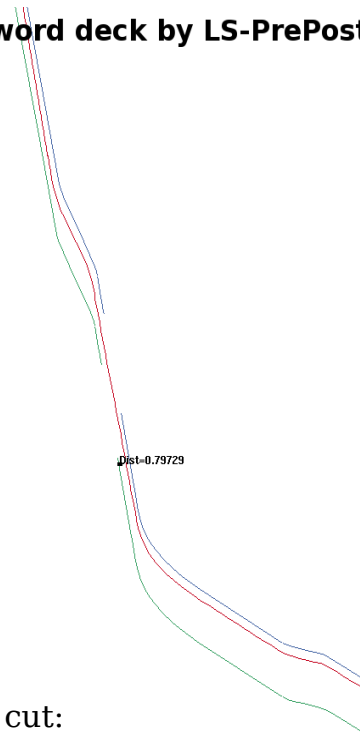
- Example of automatic mesh repair

word deck by LS-PrePost



Section cut:
contact problem found

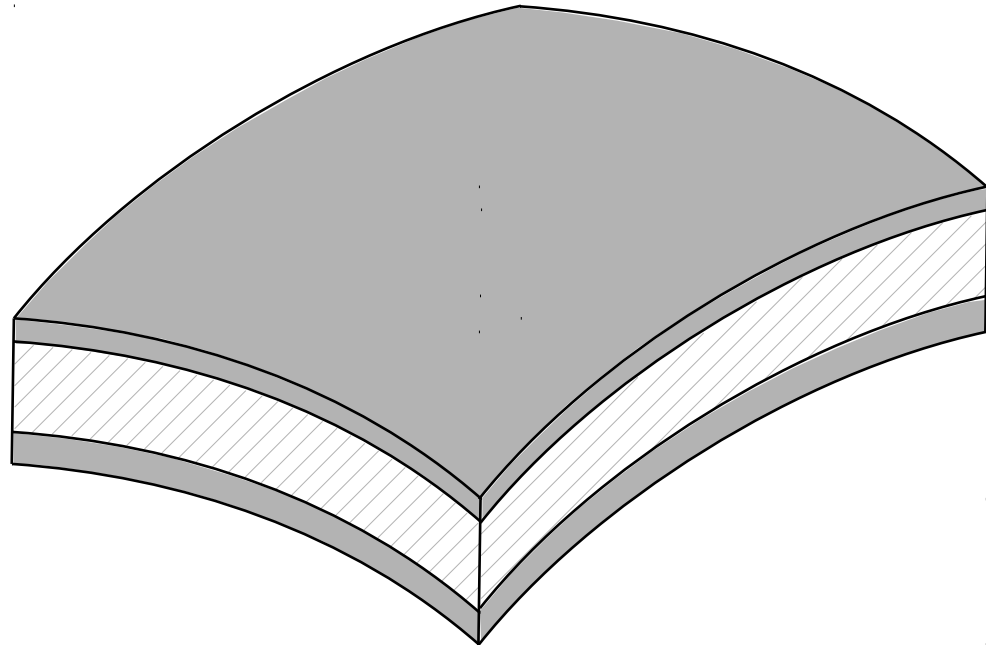
word deck by LS-PrePost



Section cut:
normal contact between the tools and the blank

Adaptivity for Sandwich Structures

- Example of sandwich part structure
- Top and bottom layers use shell element
- Middle layer use solid element
- Elements in top layer share nodes with solid element in top surface
- Elements in bottom layer share nodes with solid element in bottom surface

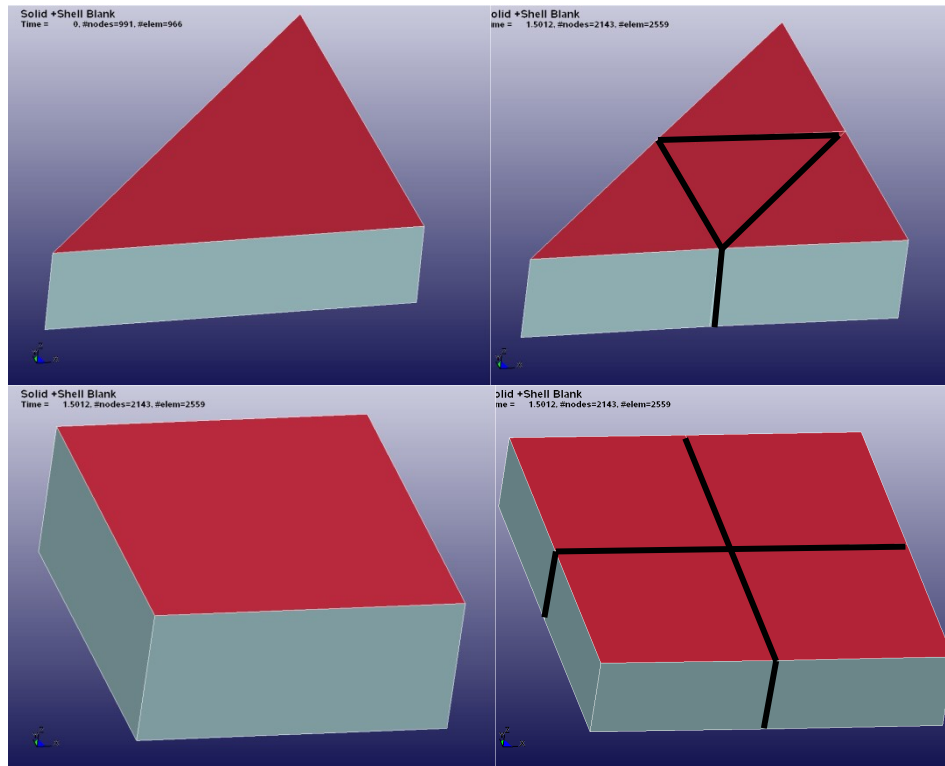


Adaptivity for Sandwich Structures

Adaptive algorithm

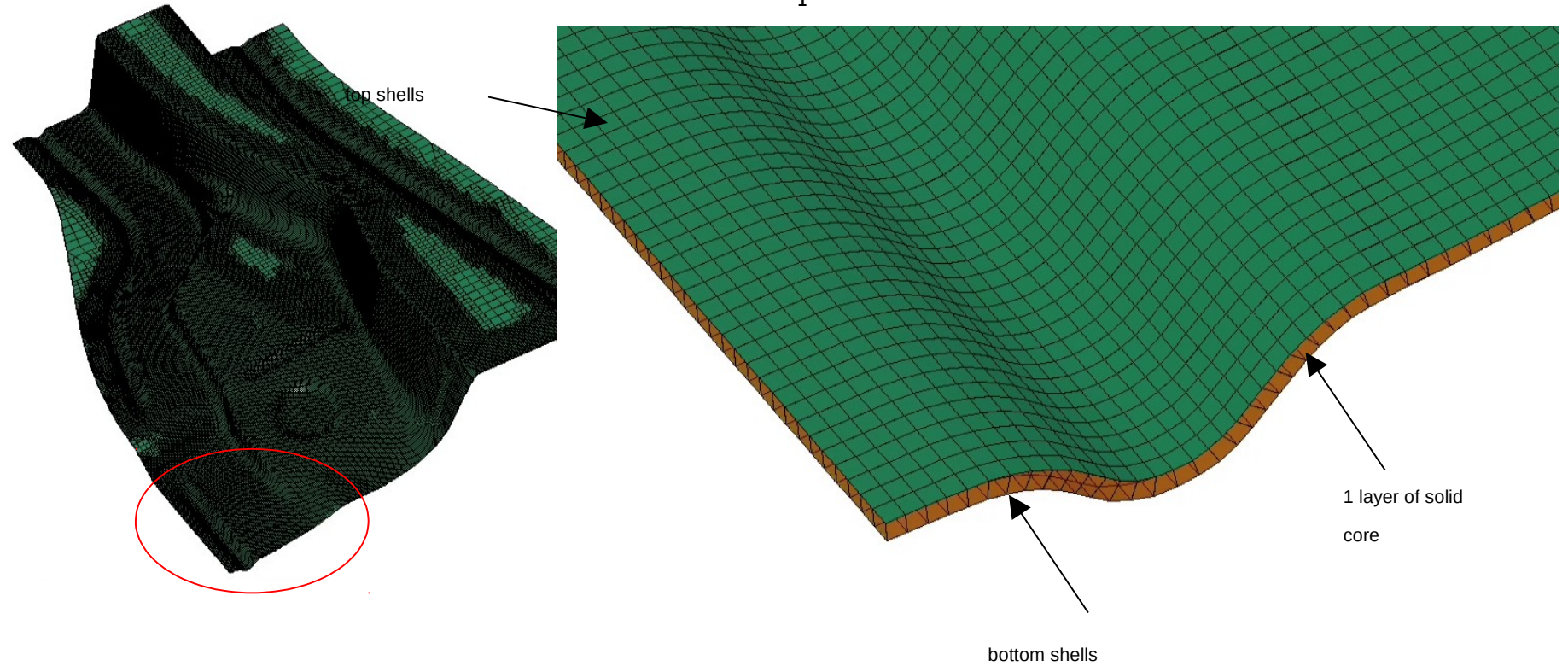
Mesh refinement in the plane

No refinement in the thickness direction



Adaptivity for Sandwich Structures

```
*CONTROL_ADAPTIVE
$# adpfreq  adpto1  adpopt  maxlvl  tbirth  tdeath  lcadp  ioflag
   &adpfq 4.0000E+00    1    4  0.0001.0000E+20    0    0
$# adpsize  adpass  ireflg  adpene  adpth  memory  orient  maxel
   0.90000    1    10.00000  0.000    0    0    0
$# ladpn90  ladpgh  ncfred  ladpcl  adpct1  cbirth  cdeath  lclvl
   -1    0    0    1  0.000  0.0001.0000E+20    0
$
                                     ifsand
                                     1
```



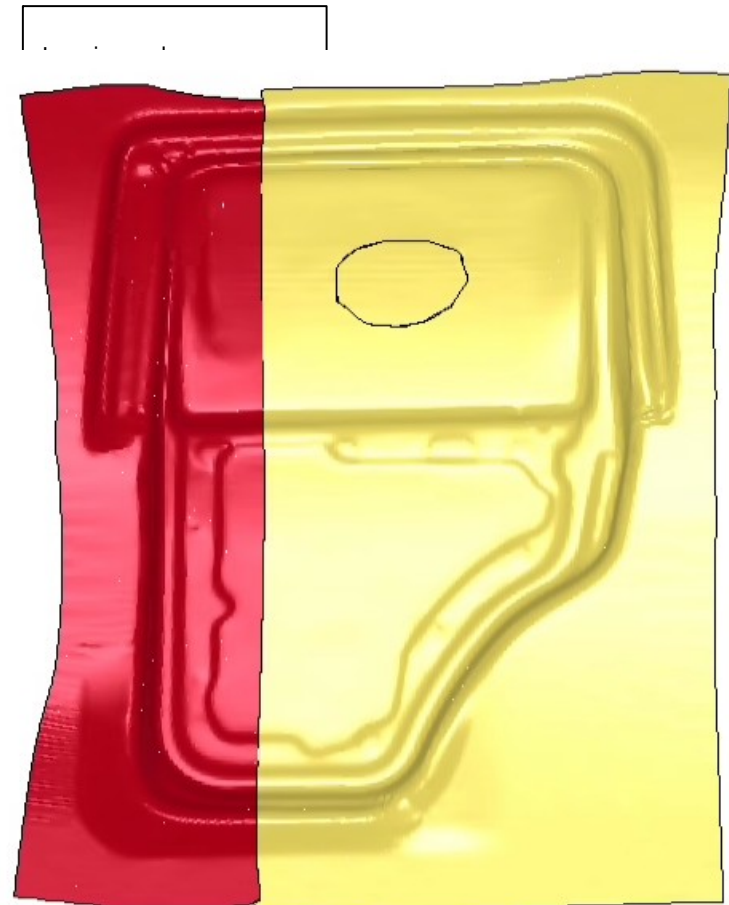
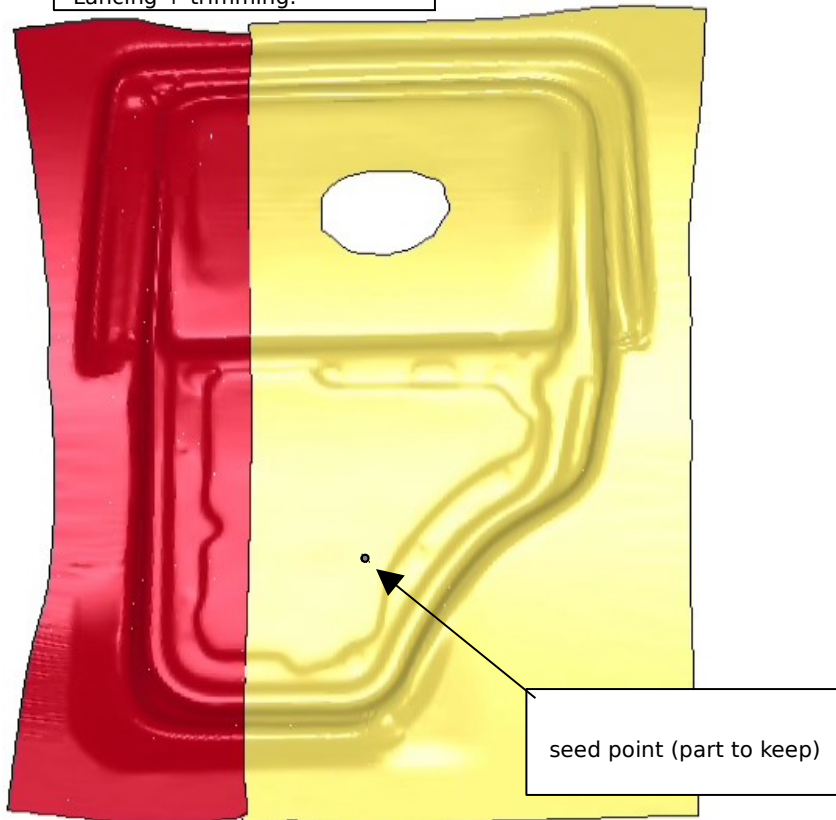
Removing Scrap after Lancing

```
*DEFINE_LANCE_SEED_POINT_COORDINATES
```

```
$ NSUM X1 Y1 Z1 X2 Y2 Z2  
1 -382.000 -17.000 76.0
```

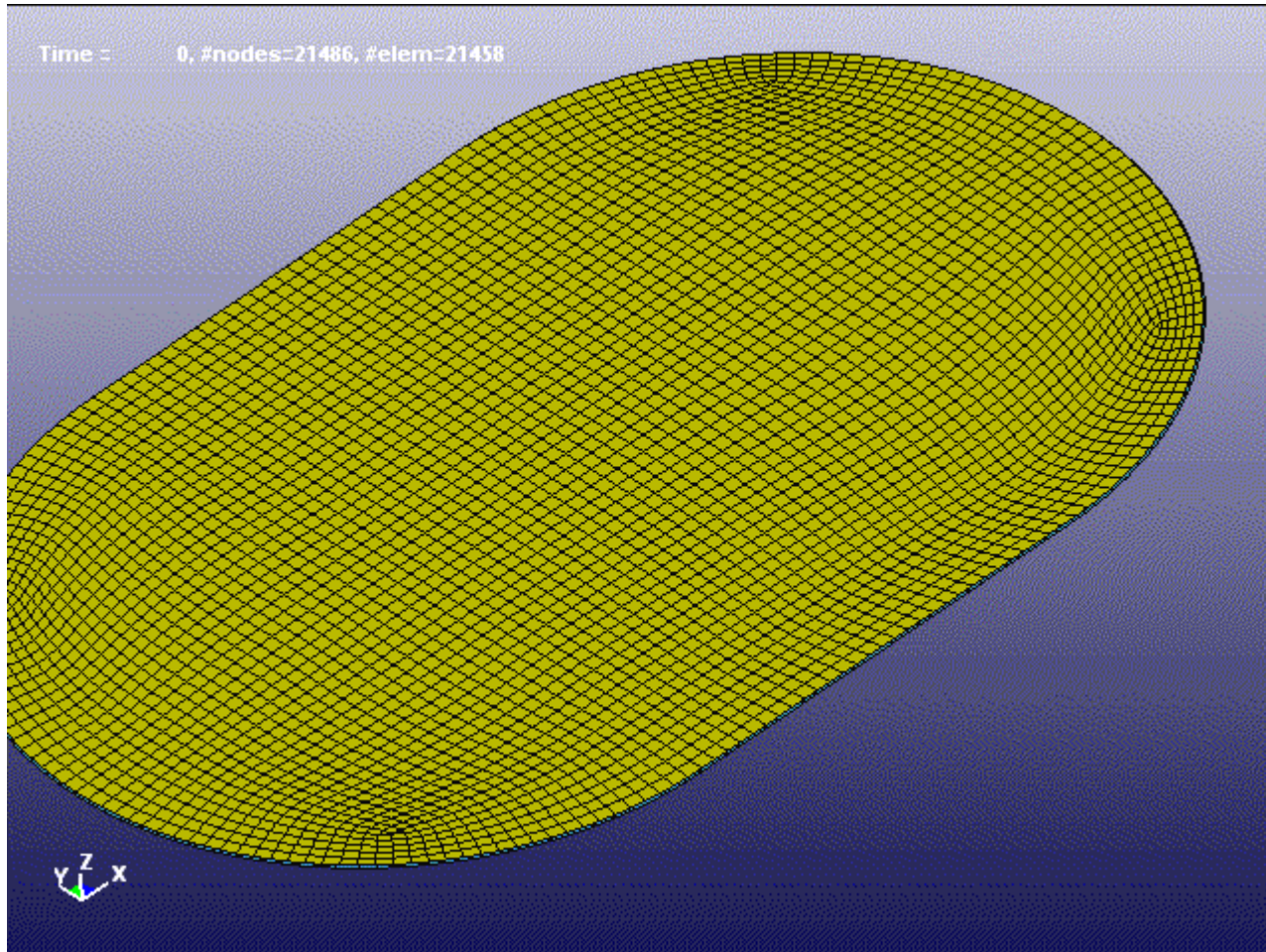
- Removes scraps after lancing.
- Maximum of 2 seed points can be defined.
- Lancing curve must be self-enclosed.

Lancing + trimming:



Removing Scrap after Lancing

Example: scrap removal after lancing

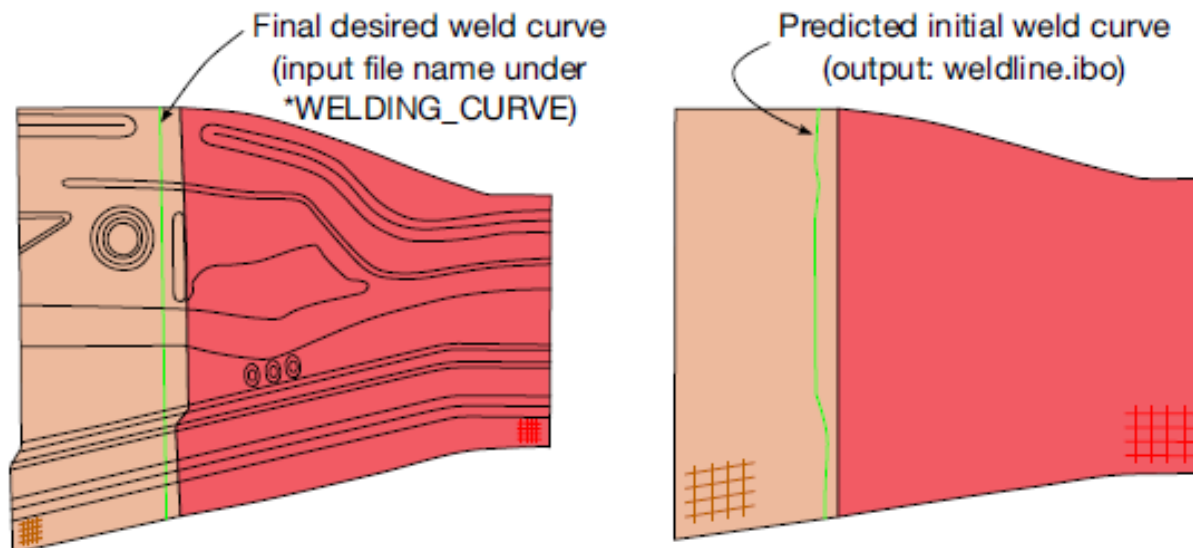


Conversion from shell element to TSHELL

- In certain situations, thick shell element is more accurate than thin shell element
 - For structure parts, the thickness can be large
 - For deformation under large normal stress, in the case of ironing
- New keyword `*CONTROL_FORMING_SHELL_TO_TSHELL`
 - Convert the shell model to thick shell model
 - It allow the offset to happen at the top, bottom or the middle surface
 - It automatically create segment sets for both the top and the bottom surface, to be used in segment based contact.
- After forming of thick shell, a trimming algorithm has been implement to trim the part
- The keyword is the same as those used to trimming shell parts

Weld Line Development

- For Taylor-Welded blank, if the weld line is defined for the final part, it is necessary to get the initial welding for the initial blank.
- New Keyword: `*INTERFACE_WELDING_DEVELOPMENT`



Trimming of Solid, laminated, and TSHELL parts



Trimming of solid



Trimming of laminate part

Enhancements in Adaptive Box

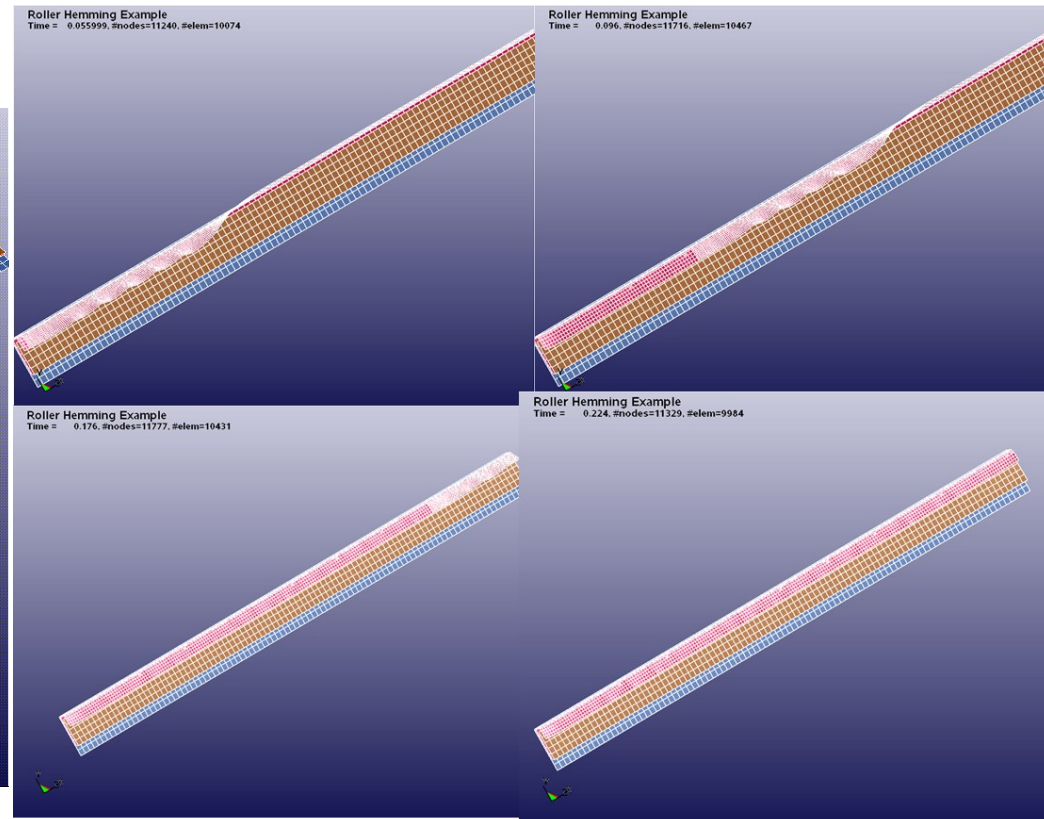
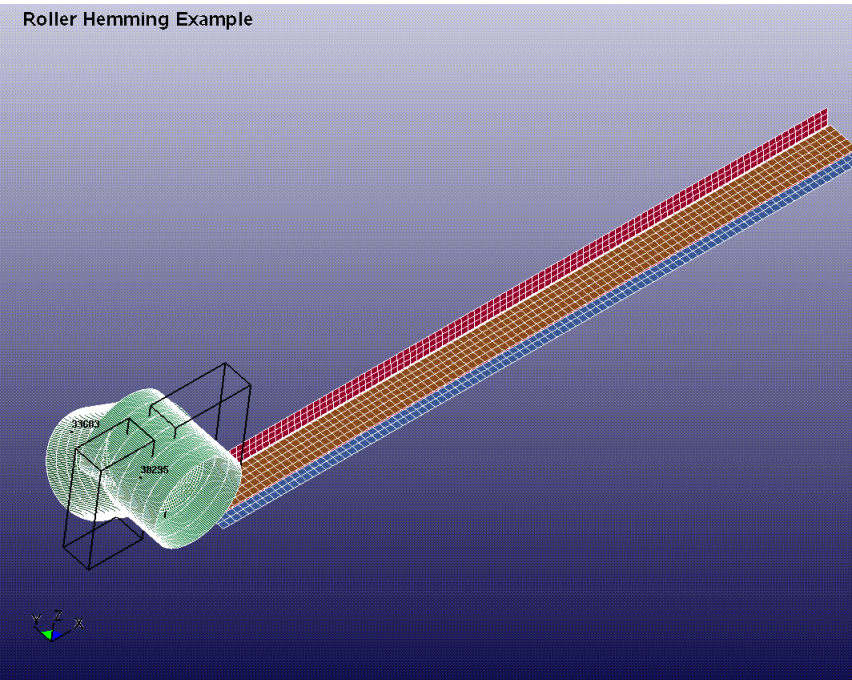
Example of adaptive box and fusion in hemming

One roller is for pre-hemming, and the other is for final hemming

Two boxes are defined, one for refinement and one for coarsening

Each box follow a node in the roller

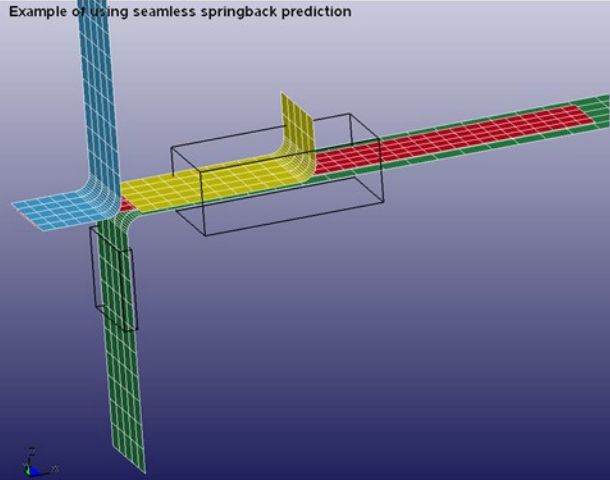
Roller Hemming Example



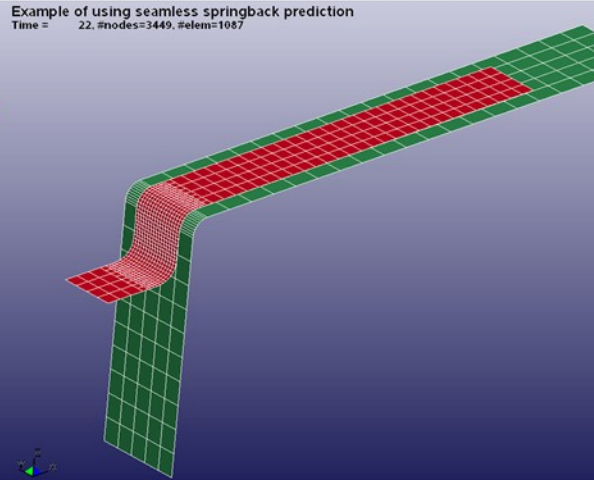
Enhancements in Adaptive Box

- Example of element fusion with adaptive box

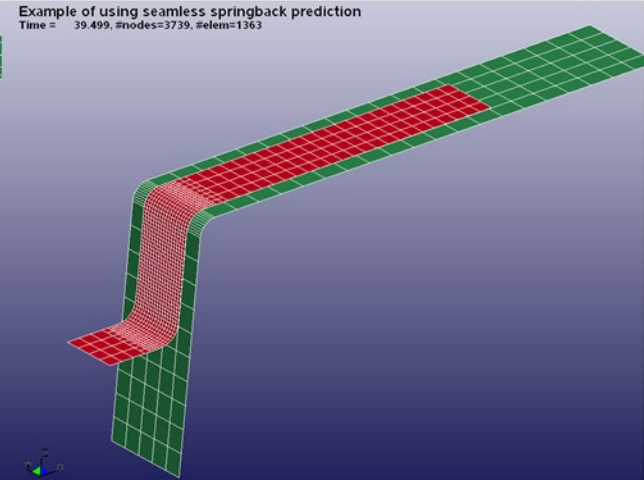
Example of using seamless springback prediction



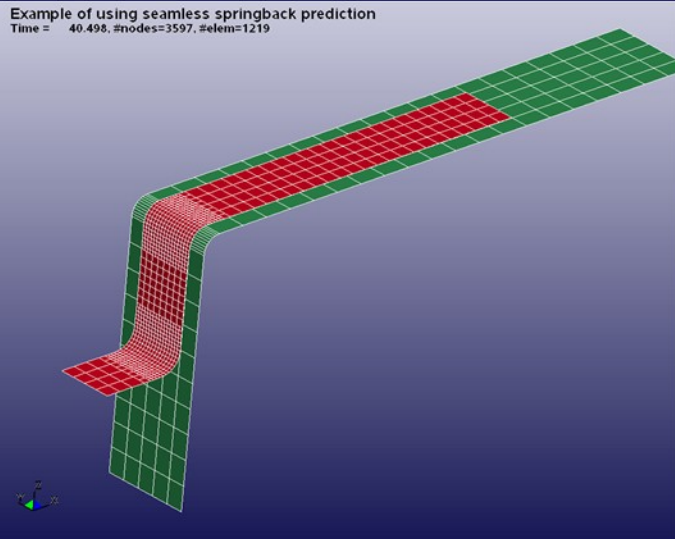
Example of using seamless springback prediction
Time = 22, #nodes=3449, #elem=1087



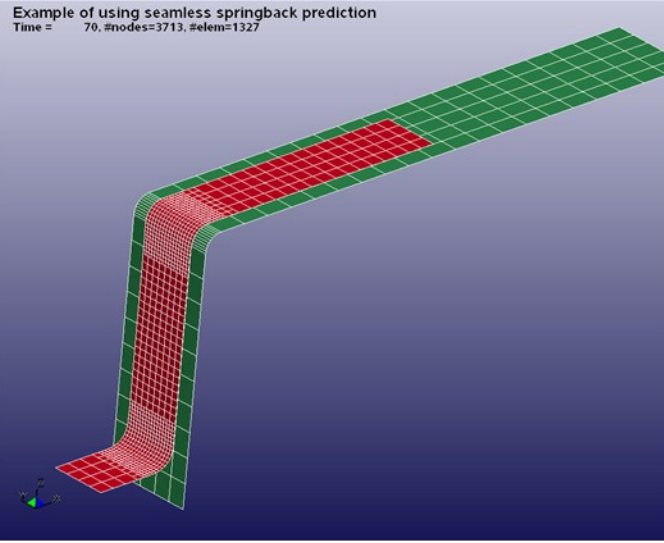
Example of using seamless springback prediction
Time = 39.499, #nodes=3739, #elem=1363



Example of using seamless springback prediction
Time = 40.498, #nodes=3597, #elem=1219



Example of using seamless springback prediction
Time = 70, #nodes=3713, #elem=1327



Enhancements in Adaptive Box

- **Advantages**

 - decrease the number of elements

 - Decrease the dynamic effect

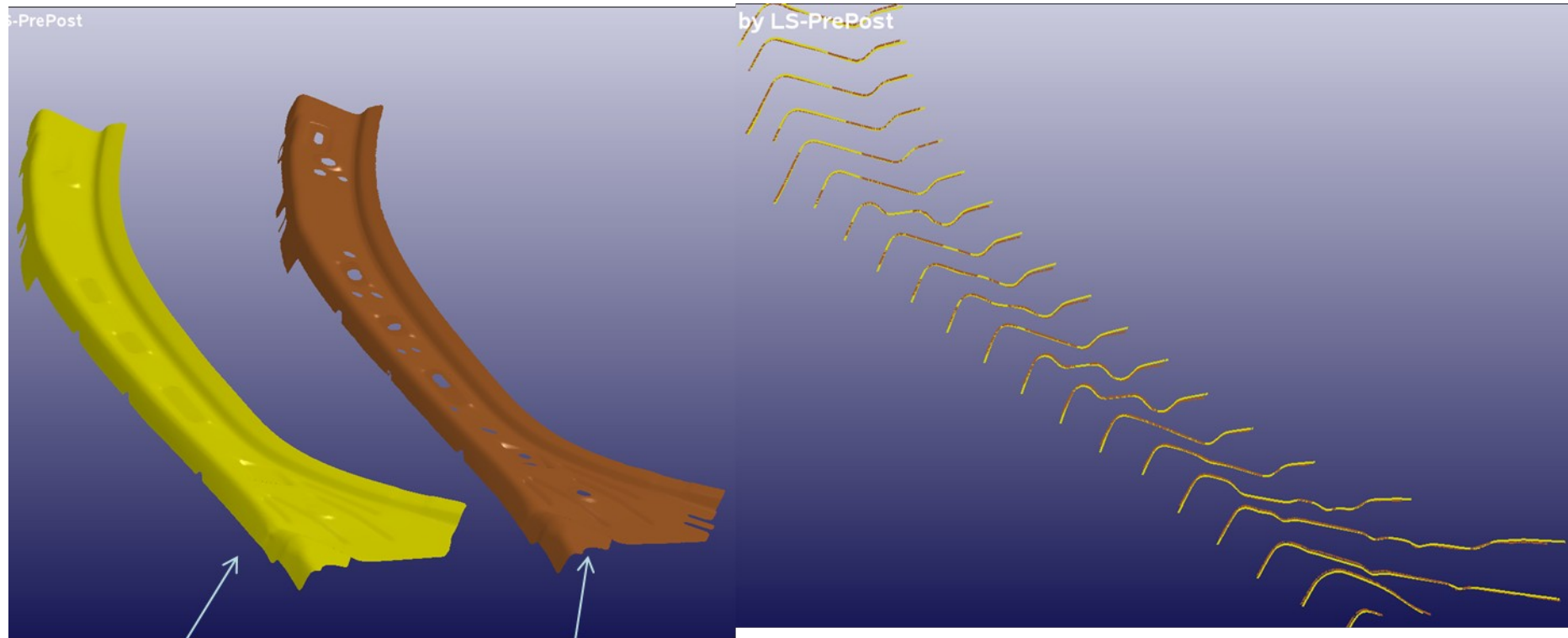
 - Improve calculation efficiency

- **The new adaptive box can be very important for certain applications**

 - Roller hemming

 - Incremental forming

Best Fit



Sprung shape scan data

Model info:

Scan data: 347359 elements, 730336 nodes
Sprung data: 106901 elements, 109300 nodes
Total CPU: 1 minute

Thickness Compensation for Thermal Forming

- After forming, the blank thickness is no-longer homogeneous
- The gap between the blank and the rigid tools are not homogeneous
 - The heat transfer between the die blank and the rigid tool will not be even
 - The cooling speed will be different for different location
- **New Keyword: *INTERFACE_THICKNESS_CHANGE_COMPENSATION**
 - Automatically modify the rigid tool surface, so that the gap between the blank and the tools are homogeneous
 - More efficient in cooling stage
 - More homogeneous mechanical property

MAT_260: Non-Associated Plasticity Model

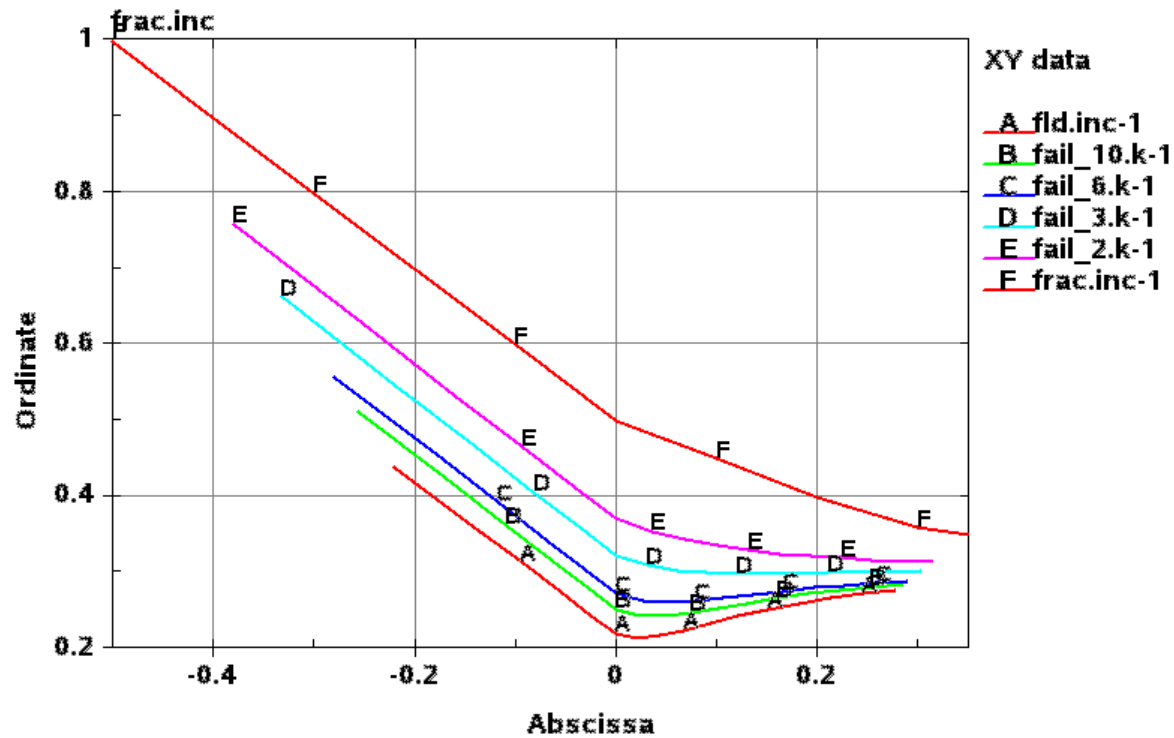
- Two non-associate plasticity models have been implemented:
 - MAT260A: *MAT_STOUGHTON_NON_ASSOCIATED_FLOW
 - MAT260B: *MAT_MOHR_NON_ASSOCIATED_FLOW
 - Yield function is not the same as flow potential
 - Hill's 1948 yield surface is used, different coefficients for yield function and flow potential
 - If the coefficients are the same for yield function and flow potential, then it degenerate into conventional plasticity
 - Available to both shell and solid elements
 - Strain rate sensitivity
 - Adiabatic heating effect, temperature is treated as an internal variable

*MAT_260B

- Special features for MAT_260B
 - Velocity scaling
 - This feature allow user to user faster speed in simulation, and scale down the strain rate, so as to speed up the simulation without losing accuracy
 - Rate dependent fracture model
 - The fracture strain depends on the deformation speed
 - User has the choice to input the fracture limit with a curve
 - Mesh size in-dependent fracture prediction
 - After necking, the deformation is not homogeneous and further deformation concentration in a narrow neck region
 - Strong strain gradients happens around the neck
 - Failure strain has to be the average limit strain over a length scale.

*MAT_260B

- The input fracture strain limit has to be associated to certain length scale.



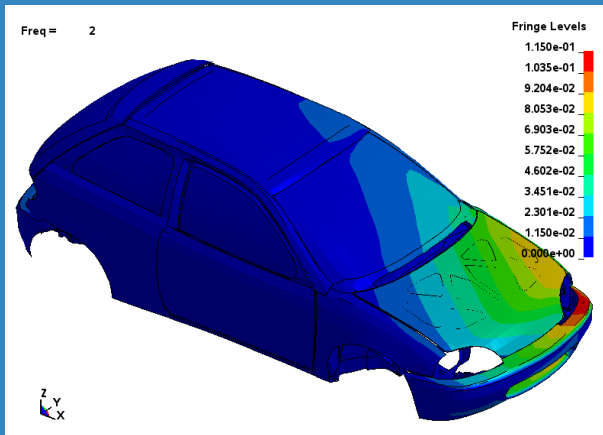
*MAT_260B

- Mesh size has significant effect on material failure prediction
 - The failure strain decreases with the increase of the element size and the necking strain is the lower limit
 - The effect of element size is significant when the element size is smaller than 5.0mm
- The width of the neck also affect the limit strain
 - The smaller the width, the less the limit strain
- Fracture strain and necking strain both affect the limit strain
 - The effect from fracture strain is not as big as the necking strain
 - The failure strain converges to necking strain with the increase of element size
- The mesh size effect also depends on the stress state.
- In application simulation, the limit strain should be significantly lower than the fracture strain
- Size independent method is only available to shell elements

Frequency

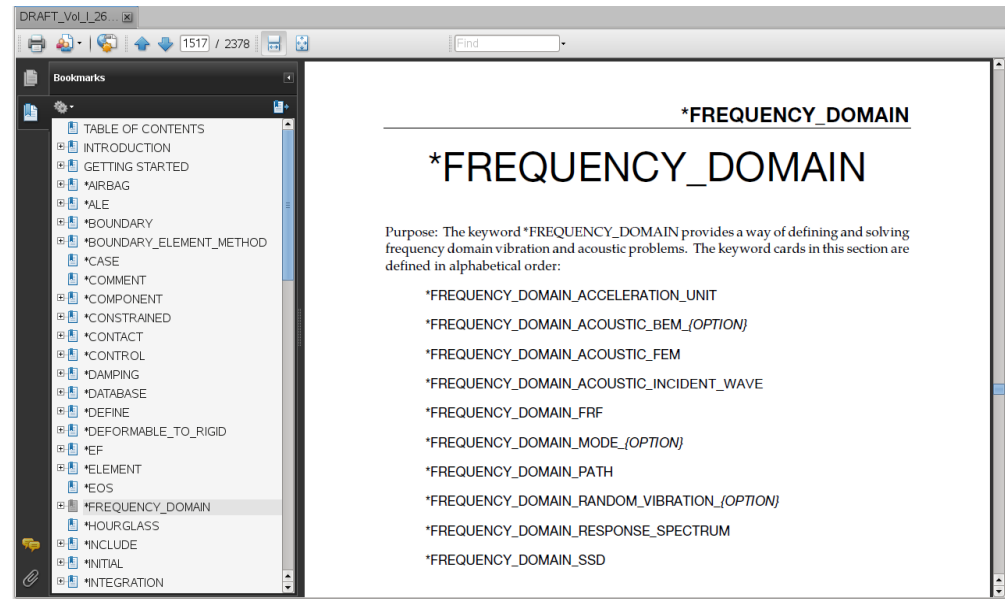
Domain Analysis

Yun Huang



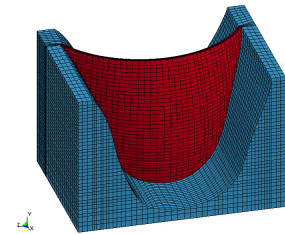
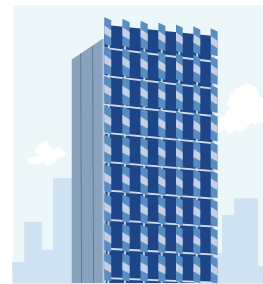
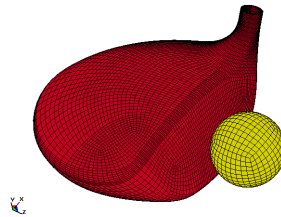
Frequency Domain Analysis

- FRF
- SSD
- Random Vibration
- Response Spectrum Analysis
- BEM Acoustics
- FEM Acoustics
- SSD Fatigue
- Random Fatigue



Applications

- NVH of autos and aircraft
- Acoustic design and analysis
- Defense industry
- Fatigue of machines and engines
- Civil and hydraulic engineering
- Earthquake engineering

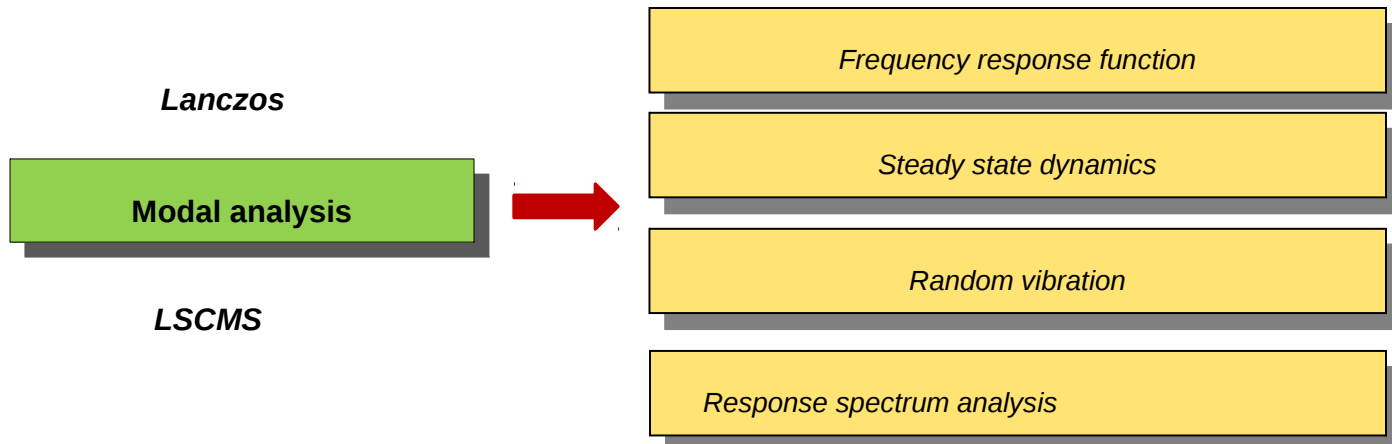
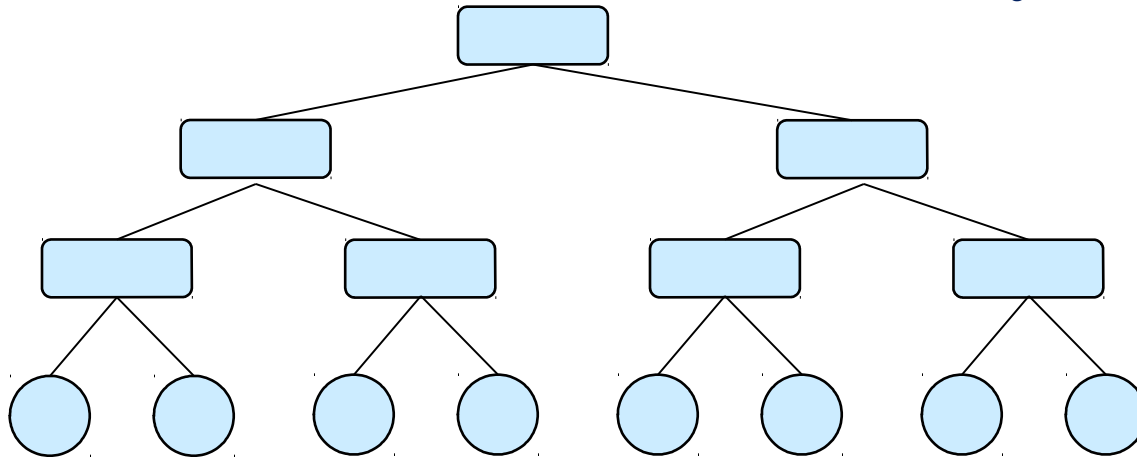


Using LSCMS in frequency domain analysis

LSCMS (Livermore Software Component Mode Synthesis)

Roger Grimes, LSTC

Chang-Wan Kim, Konkuk University, Korea



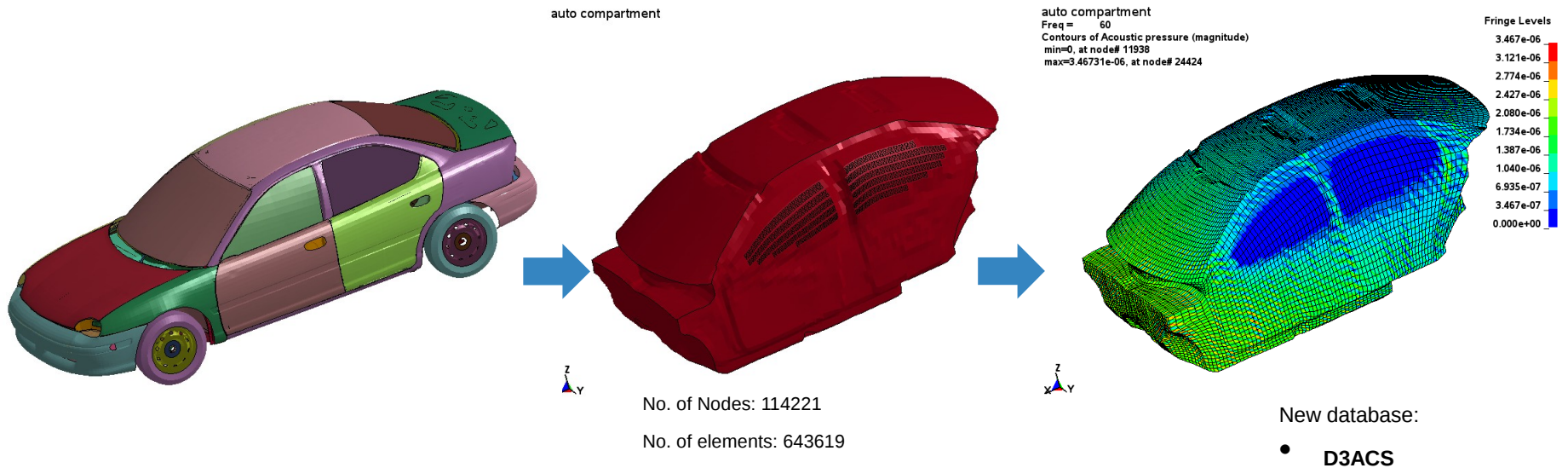
FEM Acoustics

New boundary conditions for FEM acoustic features

- Velocity
- Acoustic Impedance
- Pressure

- ✓ Vibration
- ✓ Sound absorbing material, damping
- ✓ Openings

In this example, the opened window is simulated using 0 pressure boundary condition. The blue area in the d3acs pressure plot clearly indicates the 0 pressure zones.



FEM Acoustics - Acoustic Eigenvalue Analysis

*FREQUENCY_DOMAIN_ACOUSTIC_FEM
_EIGENVALUE

$$\left([K_a] + j\omega[C_a] - \omega^2[M_a] \right) \{p_i\} = \{F_a\}$$

$$[K_a] \{\phi_i\} = \omega_i^2 [M_a] \{\phi_i\} \quad i = 1, \dots, N_a$$

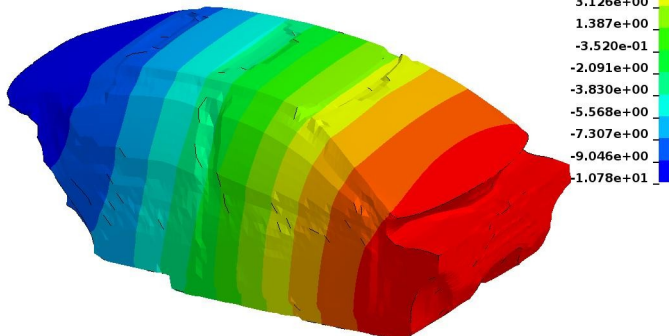
New databases:

- EIGOUT_AC
- D3EIGV_AC

A closed compartment model

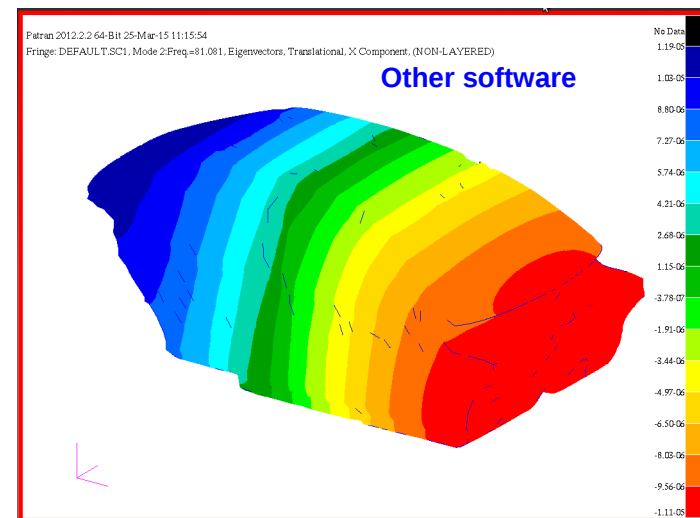
LS-DYNA keyword deck by LS-PrePost
Freq = 81.081
Contours of X-velocity
min=-10.7847, at node# 31
max=10.0807, at node# 7952

LS-DYNA

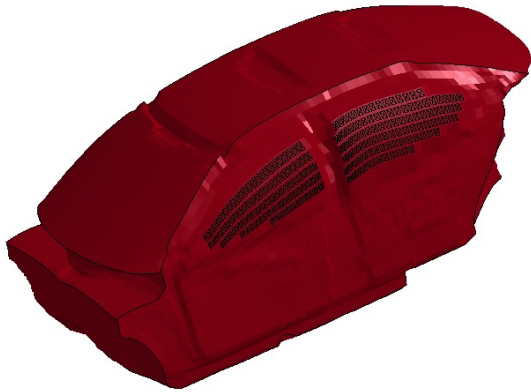


Eigenvector for the 2nd mode

Mode	LS-DYNA	Other software
1	3.93144E-06	6.698696E-06
2	8.10808E+01	8.108078E+01
3	1.25457E+02	1.254568E+02
4	1.47780E+02	1.477799E+02
5	1.52190E+02	1.521901E+02
6	1.72872E+02	1.728723E+02
7	1.98448E+02	1.984481E+02
8	2.08590E+02	2.085895E+02
9	2.14581E+02	2.145808E+02
10	2.23230E+02	2.232297E+02

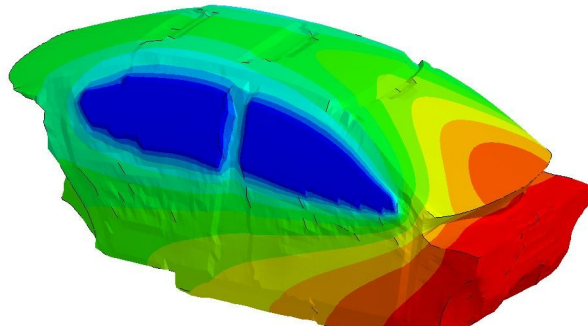


A compartment model with windows open
auto compartment



LS-DYNA keyword deck by LS-PrePost
Freq = 67.955
Contours of X-velocity
min=0, at node# 6198
max=9.83397, at node# 15903

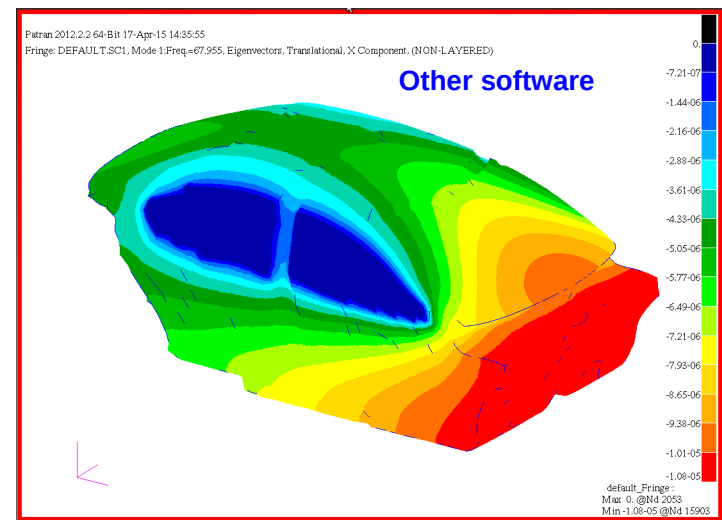
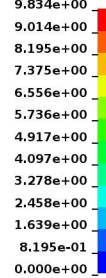
LS-DYNA



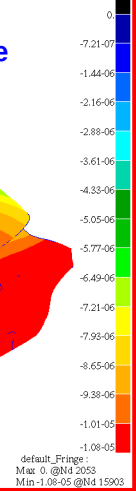
Eigenvector for the 1st mode

Mode	LS-DYNA	Other software
1	6.79551E+01	6.795506E+01
2	1.03346E+02	1.033460E+02
3	1.47853E+02	1.478530E+02
4	1.58211E+02	1.582106E+02
5	1.74781E+02	1.747807E+02
6	1.87460E+02	1.874595E+02
7	2.10906E+02	2.109057E+02
8	2.14993E+02	2.149934E+02
9	2.28861E+02	2.288609E+02
10	2.50667E+02	2.506669E+02

Fringe Levels



Patran 2012.2.2 64-Bit 17-Apr-15 14:35:55
Fringe: DEFAULT.SC1, Mode 1:Freq=67.955, Eigenvectors, Translational, X Component, (NON-LAYERED)



default_Fringe
Max: 0.0@N4 2053
Min: -1.08e-05@N4 15903

Acoustic fringe plot

*FREQUENCY_DOMAIN_ACOUSTIC_FRINGE_PLOT_{OPTION}

Purpose:

Define field points for acoustic pressure computation and use D3ACS binary database to visualize the pressure distribution.

Options:

PART

PART_SET

NODE_SET

SPHERE

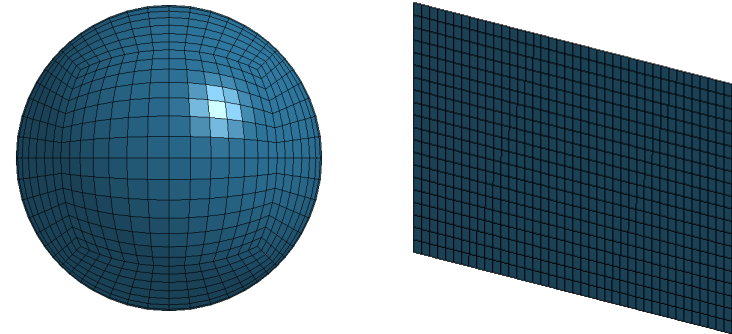
PLATE



Existing structure components



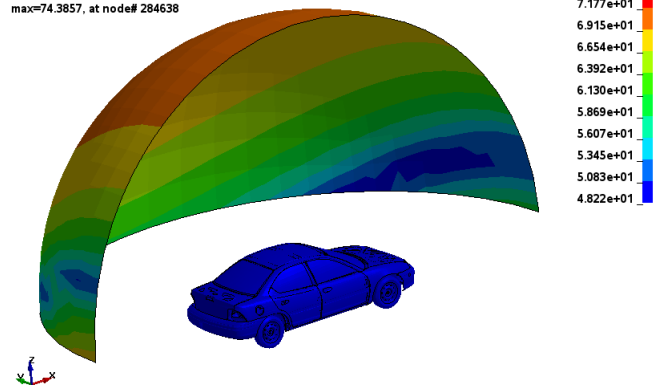
LS-DYNA generates mesh automatically



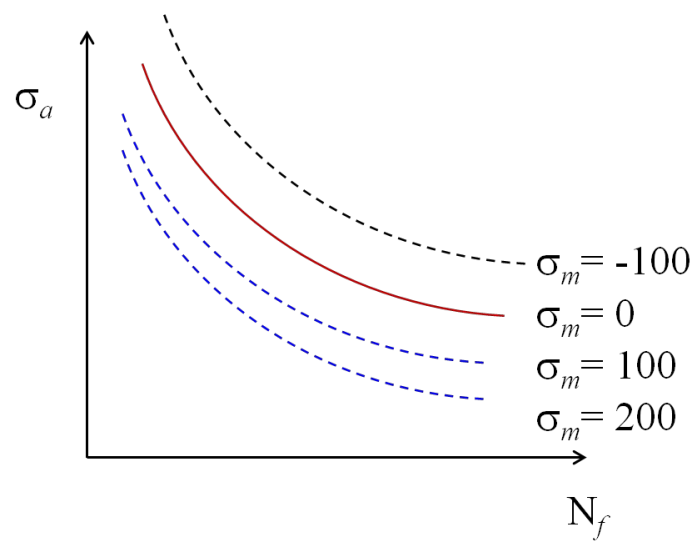
Results (D3ACS):

- Real part of acoustic pressure
- Imaginary part of acoustic pressure
- Absolute value of acoustic pressure
- Sound Pressure Level (dB)
- ✓ Supported by LS-PrePost 4.2 and above

Freq = 10
Contours of Sound pressure level (dB)
min=0, at node# 2297002
max=74.3857, at node# 284638



Mean stress correction on fatigue analysis



SN curves with different mean stress

Completely reversed tests

$$N \cdot S^m = a$$

Mean stress correction equations

Goodman

$$S = \frac{\sigma_a}{1 - \sigma_m / \sigma_u}$$

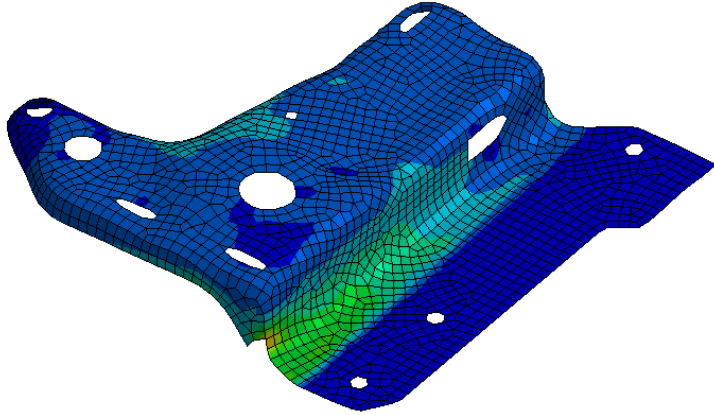
Soderberg

$$S = \frac{\sigma_a}{1 - \sigma_m / \sigma_y}$$

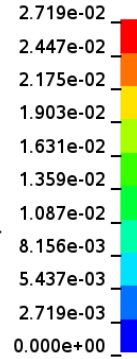
Gerber

$$S = \frac{\sigma_a}{1 - (\sigma_m / \sigma_u)^2}$$

Contours of Von Mises stress
max ipt. value
min=0, at elem# 479600
max=0.0271851, at elem# 479769

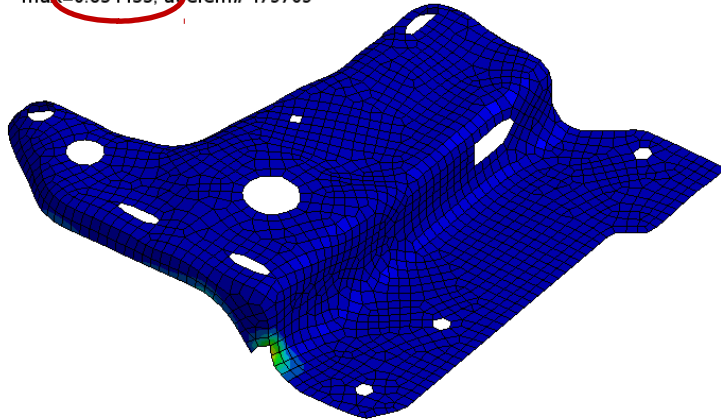


Von Mises stress

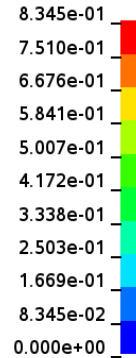


- ✓ Mean stress is introduced by
 - *INITIAL_STRESS_SHELL**
 - *INITIAL_STRESS_SOLID ...**
- ✓ Mean stress correction method is set by
 - *FATIGUE_MEAN_STRESS_CORRECTION**

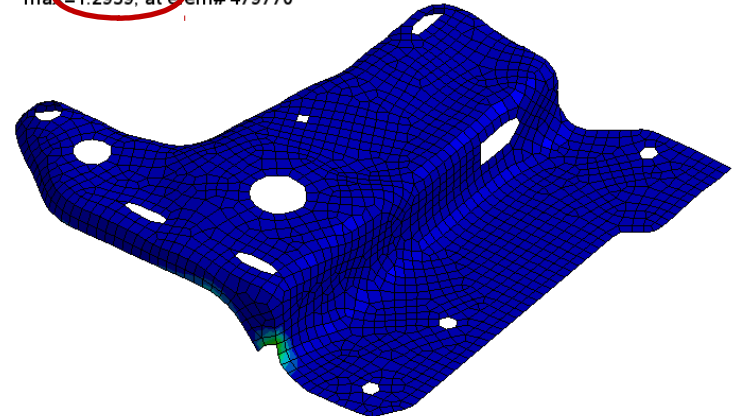
Contours of Cumulative damage ratio
max IP. value
min=0, at elem# 479601
max=0.834453, at elem# 479769



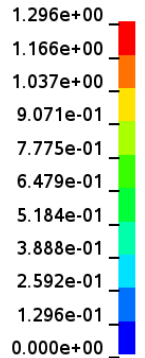
Cumulative damage ratio



Contours of Cumulative damage ratio
max IP. value
min=0, at elem# 479601
max=1.2959, at elem# 479770



Cumulative damage ratio



More damping options in SSD

*FREQUENCY_DOMAIN_SSD

Card 2	1	2	3	4	5	6	7	8
Variable	DAMP	LCDAM	LCTYP	DMPMAS	DMPSTF	DMPFLG		
Type	F	I	I	F	F	I		
Default	0.0	0	0	0.0	0.0	0		

*DAMPING_PART_MASS

*DAMPING_PART_STIFFNESS

*DAMPING_STRUCTURAL

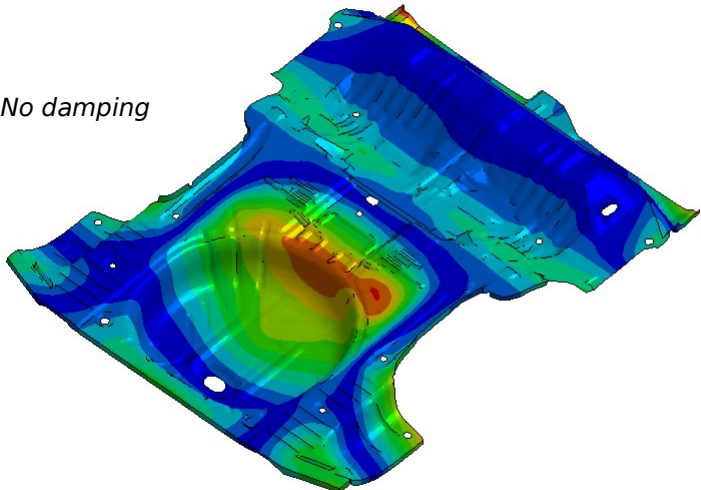
- Viscoelastic damping
- Structural damping

$$F_v = c \cdot v$$

$$F_s = i \cdot G \cdot k \cdot u$$

■ Freq = 50
 Contours of Z-velocity
 min=0.000494058, at node# 2149711
 max=149.872, at node# 2138219

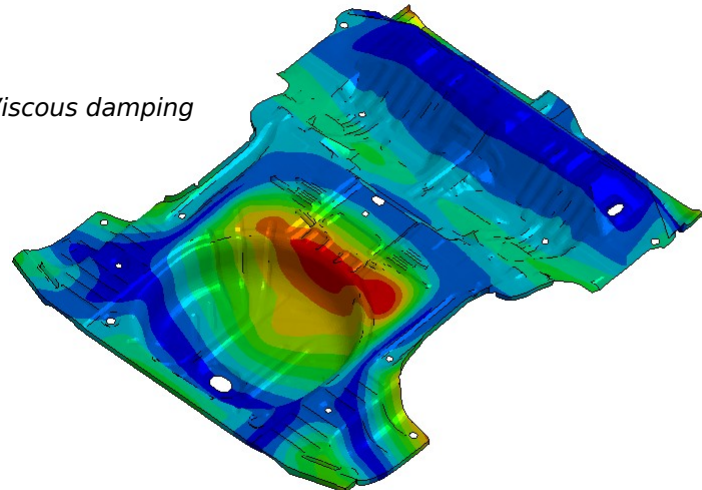
No damping



Z-velocity
 1.499e+02
 1.349e+02
 1.199e+02
 1.049e+02
 8.992e+01
 7.494e+01
 5.995e+01
 4.496e+01
 2.997e+01
 1.499e+01
 4.941e-04

■ Freq = 50
 Contours of Z-velocity
 min=0.0864911, at node# 2130455
 max=126.995, at node# 2134648

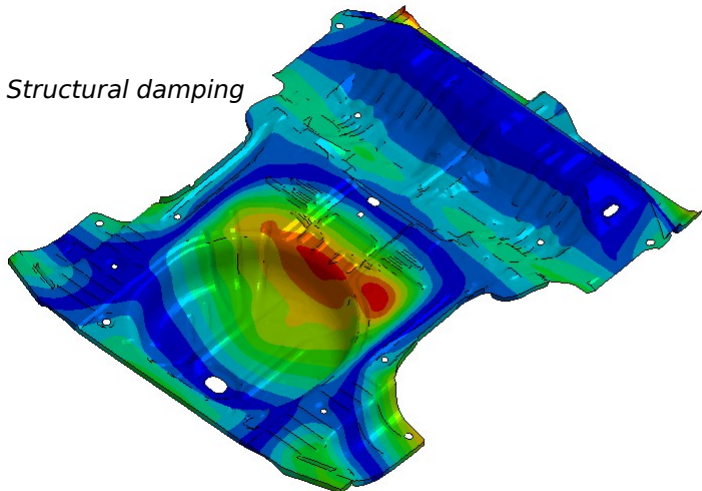
Viscous damping



Z-velocity
 1.270e+02
 1.143e+02
 1.016e+02
 8.892e+01
 7.623e+01
 6.354e+01
 5.085e+01
 3.816e+01
 2.547e+01
 1.278e+01
 8.649e-02

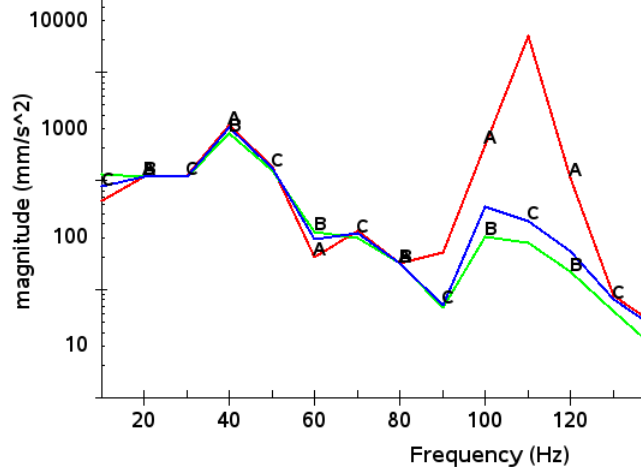
■ Freq = 50
 Contours of Z-velocity
 min=0.160948, at node# 2120159
 max=139.669, at node# 2138219

Structural damping



Z-velocity
 1.397e+02
 1.257e+02
 1.118e+02
 9.782e+01
 8.387e+01
 6.992e+01
 5.596e+01
 4.201e+01
 2.806e+01
 1.411e+01
 1.609e-01

Z-velocity response at node 2134648



A No damping
 B Viscous damping (0.05)
 C Structural damping (0.05)

Equivalent Radiated Power (ERP) calculation

*FREQUENCY_DOMAIN_SSD_{ERP}

The ERP density is defined as

$$ERP_{\rho} = \frac{1}{2} \rho_F c_F V_n \overline{V_n}$$

The ERP absolute is defined as

$$ERP_{abs} = \int_S ERP_{\rho} dS$$

The ERP in dB is defined as

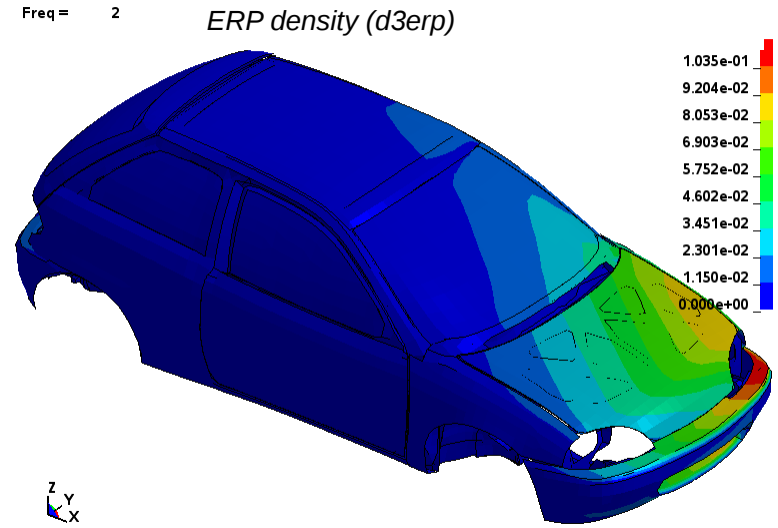
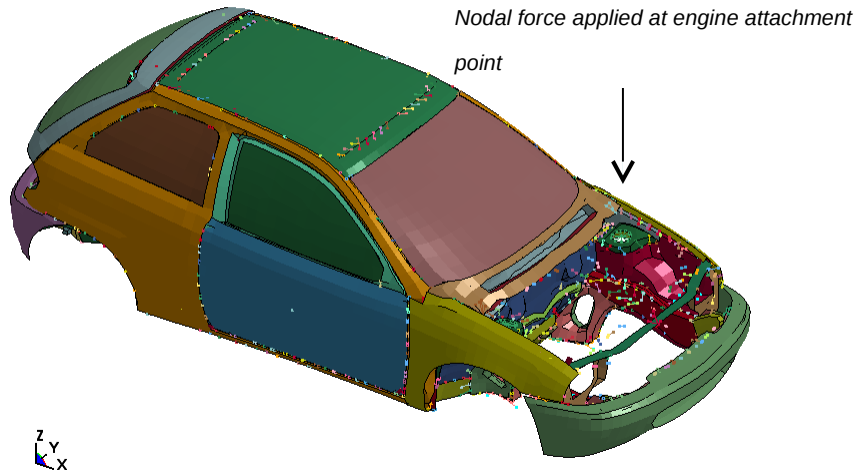
$$ERP_{dB} = 10 \log_{10} (ERP_{abs} / ERP_{ref})$$

Calculation of ERP is a simple and fast way to characterize the structure borne noise. It gives user a good look at how panels contribute to total noise radiation. It is a valuable tool in early phase of product development.

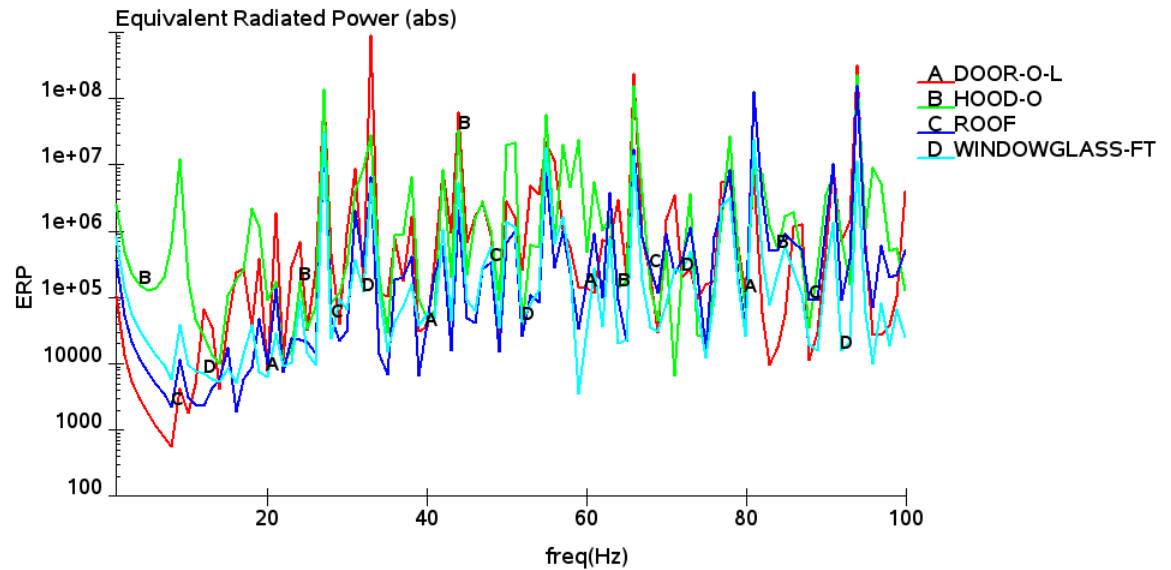
ERP calculation results are saved in

- Binary database
 - ✓ d3erp
- ASCII xyplot files
 - ✓ ERP_abs
 - ✓ ERP_dB

ERP calculation example (car model)

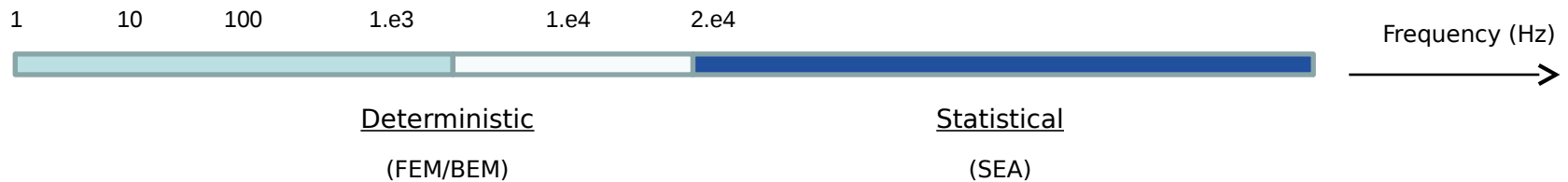


With ERP, one can study the contribution to the radiated noise from each panel.

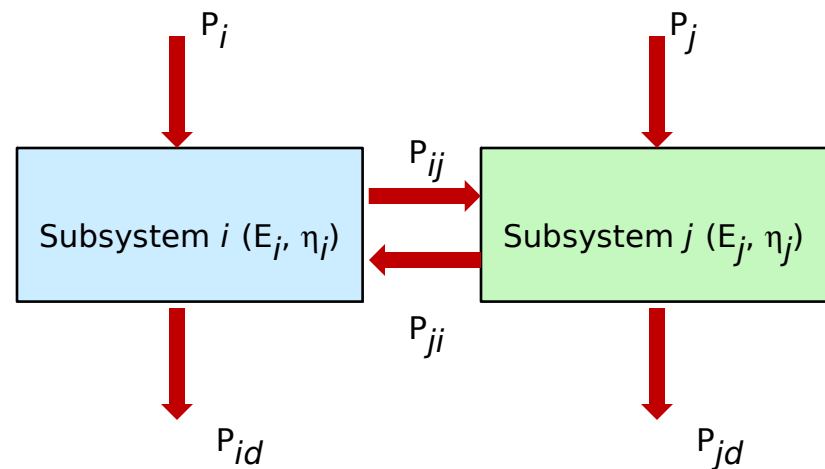


Statistical Energy Analysis

- *FREQUENCY_DOMAIN_SEA_SUBSYSTEM
- *FREQUENCY_DOMAIN_SEA_CONNECTION
- *FREQUENCY_DOMAIN_SEA_INPUT_POWER

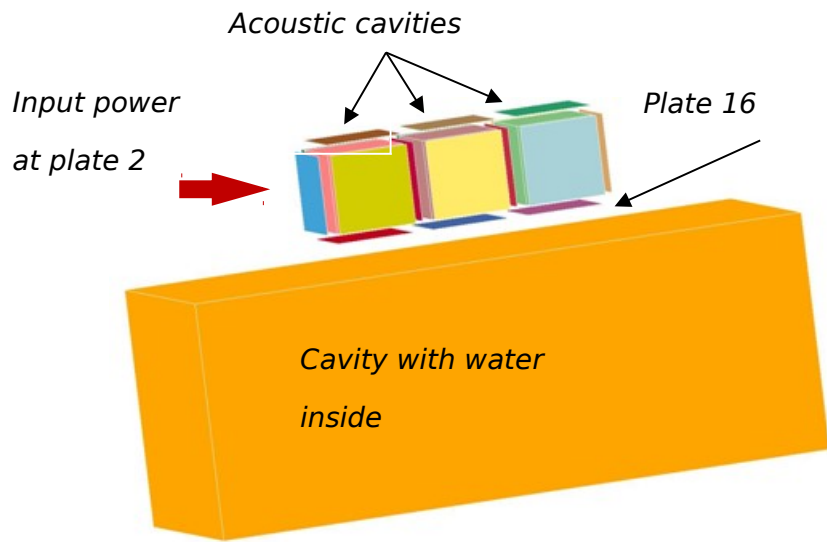


- SEA is a statistical method for studying vibration and acoustics in high frequency range, without using elements or mesh.
- In SEA a system is represented in terms of a number of coupled subsystems and a set of linear equations are derived that describe the input, storage, transmission and dissipation of energy within each subsystem.



SEA model of 2 subsystems

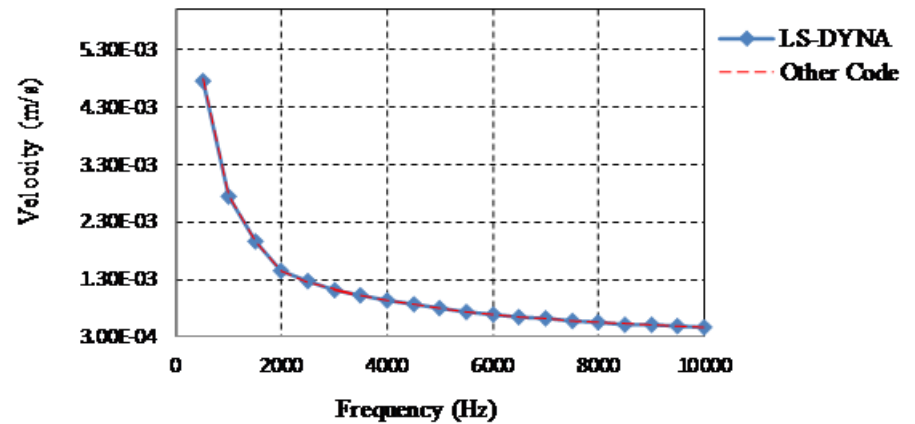
SEA example (a ship-water system)



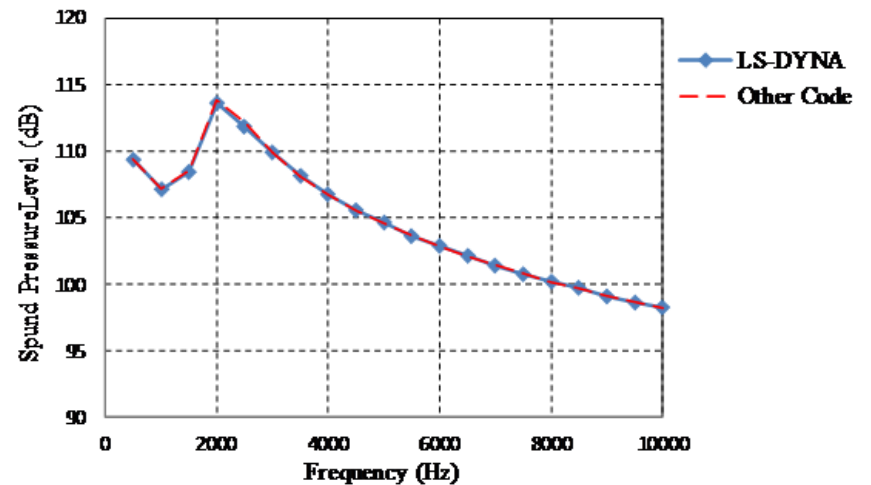
20 subsystems

- 16 steel plates
- 3 acoustic cavities (air)
- 1 acoustic cavity (water)

Velocity of plate 16



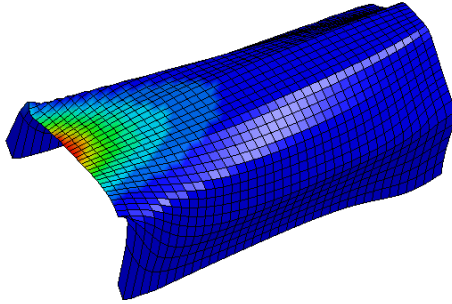
SPL of air cavity (next to plate 2)



Frequency domain analysis with IGA

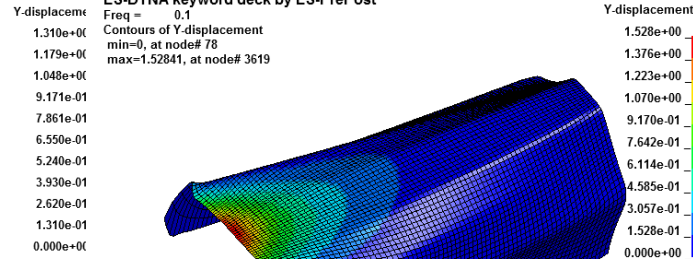
38×38=1444

LS-DYNA keyword deck by LS-PrePost
 Freq = 0.1
 Contours of Y-displacement
 min=0, at node# 41
 max=-1.31009, at node# 936



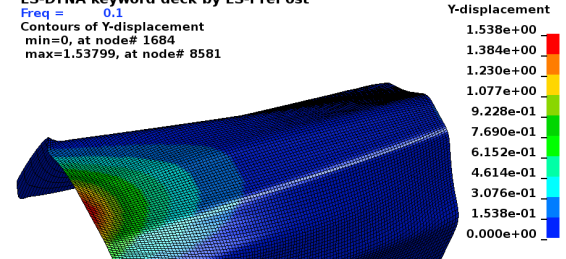
76×76=5776

LS-DYNA keyword deck by LS-PrePost
 Freq = 0.1
 Contours of Y-displacement
 min=0, at node# 78
 max=-1.52841, at node# 3619

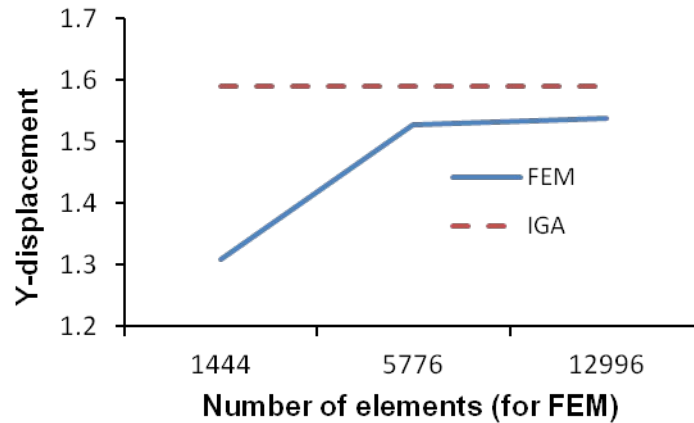
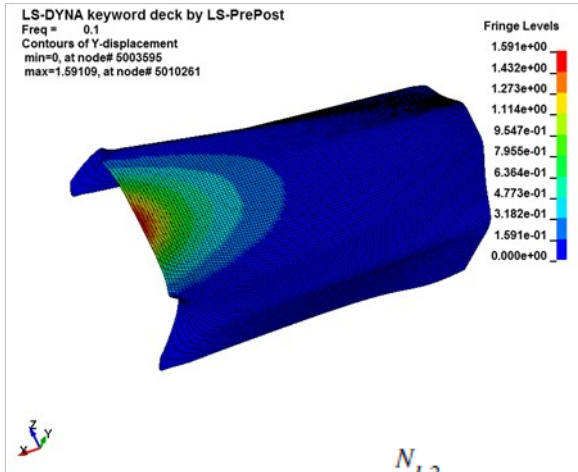


114×114=12996

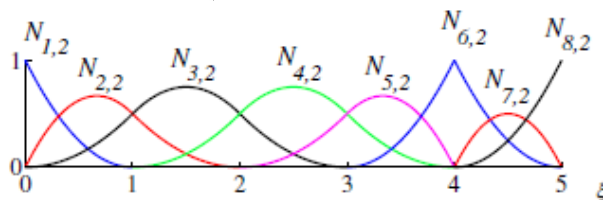
LS-DYNA keyword deck by LS-PrePost
 Freq = 0.1
 Contours of Y-displacement
 min=0, at node# 1684
 max=1.53799, at node# 8581



IGA

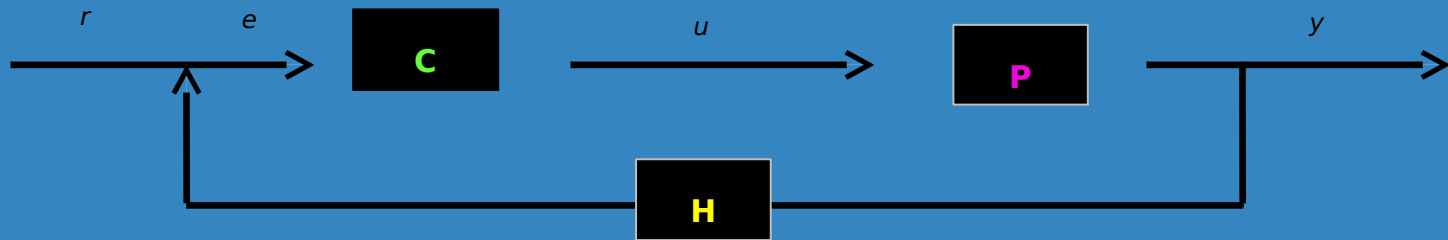


No. of elements	CPU time (sec.)
1444	6
5776	23
12996	54
IGA	47



Liping Li, LSTC

Control Systems



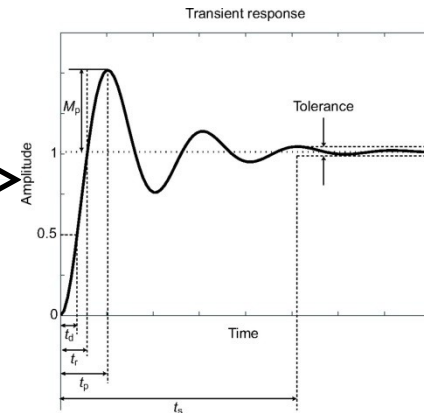
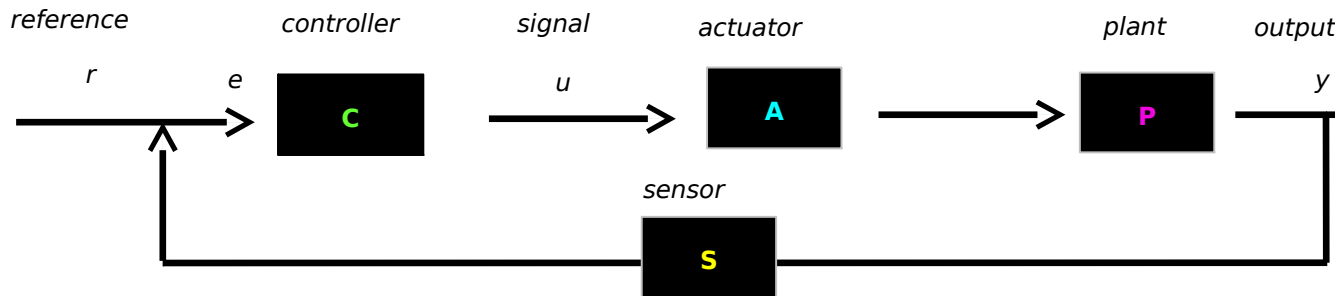
Isheng Yeh/ C. Keisser

Contents

- Introduction to Control System
- Overview of control capabilities in LS-DYNA
- Current status of
 - Controller design in LS-DYNA
 - Plant derivation in LS-DYNA
 - Piezoelectric material-based sensor and actuator
 - GUI
- Next step

Control System

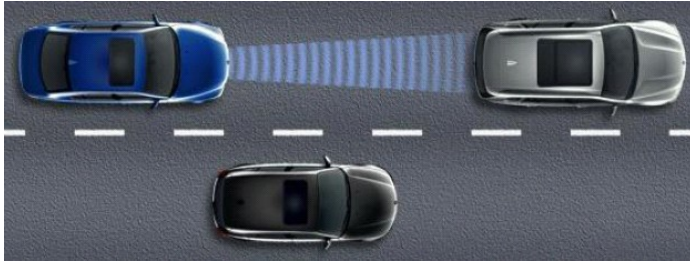
- Control is the process of making a system of design variables to conform to some desired values



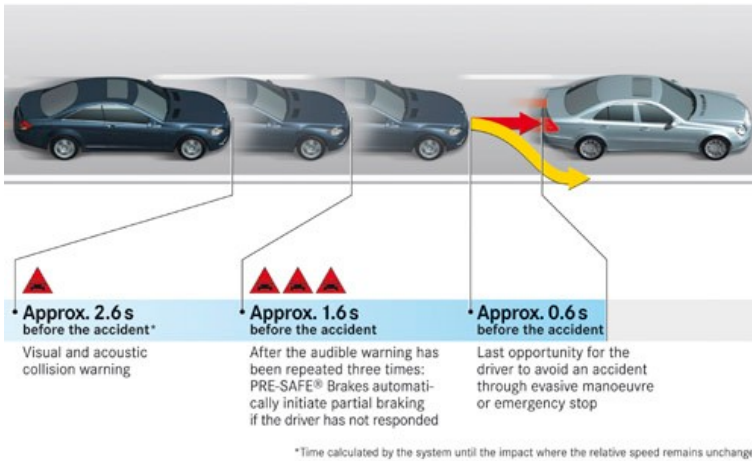
- Reference is the desired output
- Sensor provides the measurement of output
- Actuator converts the control signal to power signal
- Plant is the physical part to be controlled and can be in the form of a linear system (represented as a transfer function or state space), or FEA model

Control in Your Daily Life

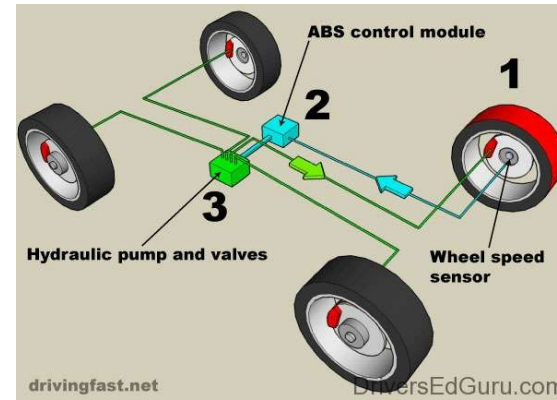
- Cruise control



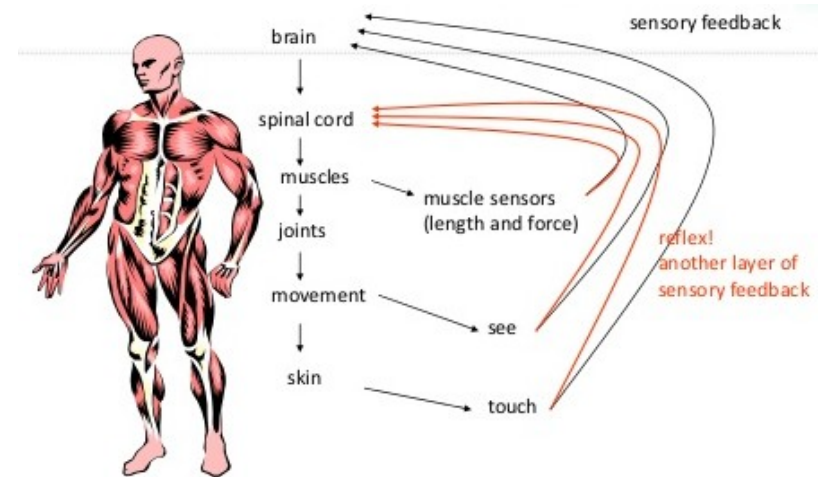
- Pre-crash system



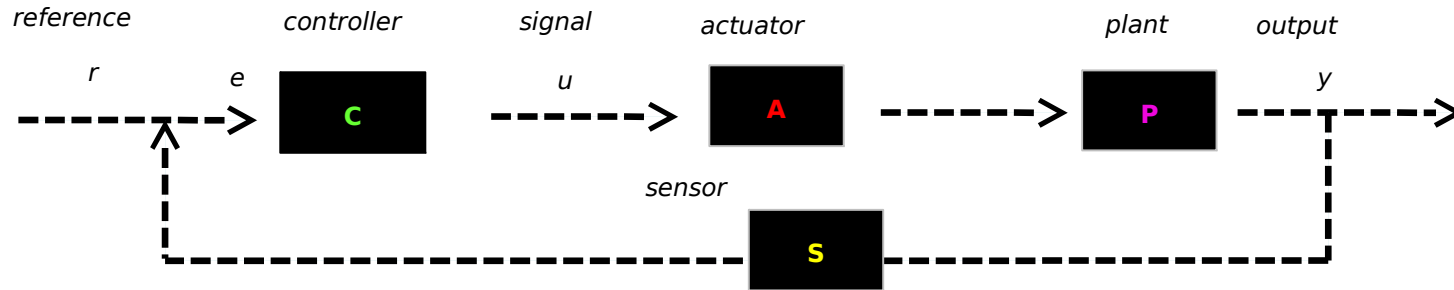
- ABS control



- Human closed loop system



Overview of Control Capabilities in LS-DYNA



- *CTRLER for controller design



- *MAT_PZELLECTRIC for piezoelectric material-based sensor and actuator
- PIDCTL and DLAY in *DEFINE_CURVE_FUNCTION for control force application



- *SENSOR



- *CTRLER_PLANT for plant model derivation based on modes truncation method



- A GUI is sunder development

Development status



*CONTRLLER for controller design



- System definition
 - *CONTRLLER_SYSLIN, TF, etc.
- Analysis
 - *CONTRLLER_RANK, ROOTS, SVD, EIG, PLZR, etc.
- Solver
 - *CONTRLLER_LSQ, ODE, CSIM, etc.
- Control tools
 - *CONTRLLER_PID, LQR, LQG, KALMAN, etc.
- Model Reduction
 - *CONTRLLER_BALANCMR, MINREAL, etc.
- System connections
 - *CONTRLLER_FEEDBACK, etc.

*CTRLER_PLANT for plant derivation



- A modes-reduction method for model order reduction, MOR

$$M\ddot{d} + C\dot{d} + Kd = F$$



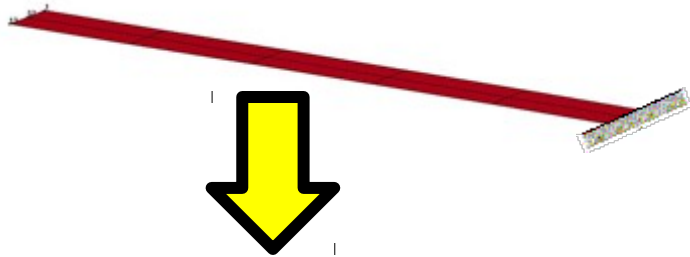
$$\begin{aligned} \dot{x}(t) &= Ax(t) + Bv(t) \\ y(t) &= Cx(t) + Du(t) \end{aligned}$$

State equation

Output equation

ID, I/O & Freq. modes	Card 1	1	2	3	4	5	6	7	8
	Variable	PLNTID	NINPUT	NOUTPUT	NMODE				
Output files	Card 2	1	2	3	4	5	6	7	8
	Variable	FMATLAB		FLSDYNA					
Frequency	Freq.	1	2	3	4	5	6	7	8
	Variable	freq1	freq2	freq3	freq4	freq5	freq6	freq7	freq8
Input DOF	INPUT	1	2	3	4	5	6	7	8
	Variable	IN1	IDOF1	IN2	IDOF2	IN3	IDOF3	IN4	IDOF4
Output DOF	OUTPUT	1	2	3	4	5	6	7	8
	Variable	ON1	ODOF1	ON2	ODOF2	ON3	ODOF3	ON4	ODOF4

Plant Model for Vertical Vibration Control



Matrix A

a =

0.	0.	0.	0.	0.	0.	1.	0.	0.	0.	0.
0.	0.	0.	0.	0.	0.	0.	1.	0.	0.	0.
0.	0.	0.	0.	0.	0.	0.	0.	1.	0.	0.
0.	0.	0.	0.	0.	0.	0.	0.	0.	1.	0.
0.	0.	0.	0.	0.	0.	0.	0.	0.	0.	1.
- 12774.	0.0000002	- 6.881D-08	0.0000002	5.576D-08	0.	0.	0.	0.	0.	0.
0.0000002	- 460440.	0.0000001	0.0000002	- 6.525D-08	0.	0.	0.	0.	0.	0.
9.658D-08	1.201D-08	- 3359300.	0.0000001	- 0.0000003	0.	0.	0.	0.	0.	0.
0.0000001	0.0000002	- 0.0000002	- 11739000.	5.851D-08	0.	0.	0.	0.	0.	0.
- 1.626D-08	- 4.630D-09	- 0.0000003	1.472D-08	- 25154000.	0.	0.	0.	0.	0.	0.

Matrix C

c =

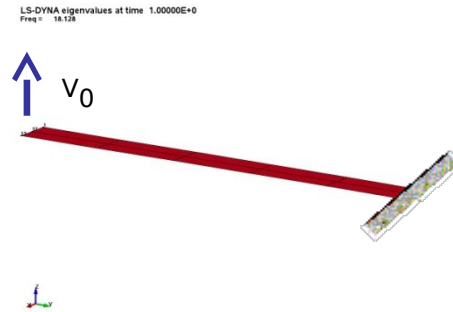
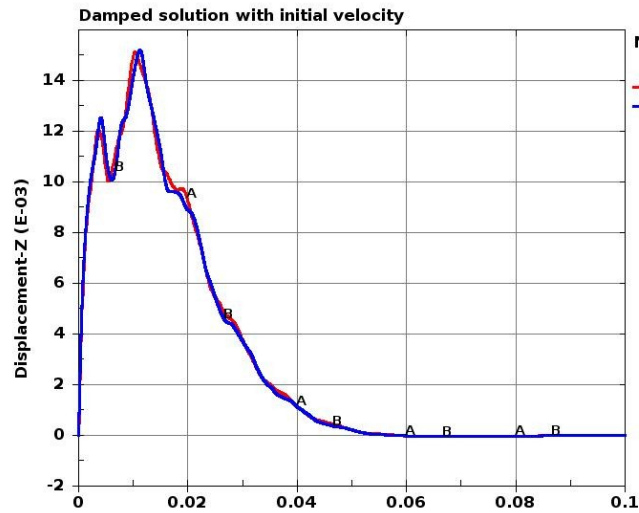
166.	149.56	118.58	74.446	- 31.458	0.	0.	0.	0.	0.
166.	149.6	118.93	75.458	- 32.592	0.	0.	0.	0.	0.
166.	149.56	118.58	74.446	- 31.458	0.	0.	0.	0.	0.
0.	0.	0.	0.	0.	166.	149.56	118.58	74.446	- 31.458
0.	0.	0.	0.	0.	166.	149.6	118.93	75.458	- 32.592
0.	0.	0.	0.	0.	166.	149.56	118.58	74.446	- 31.458

Matrix B

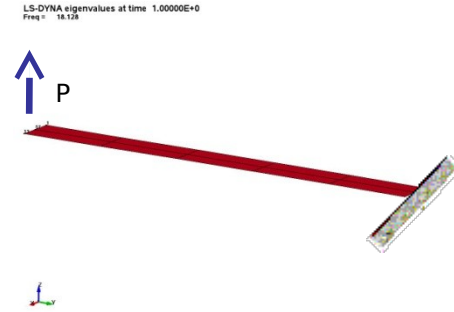
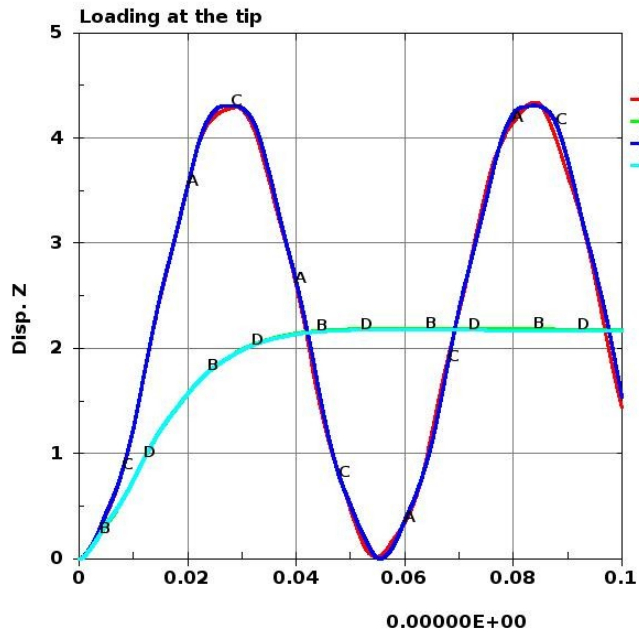
b =

0.	0.
0.	0.
0.	0.
0.	0.
0.	0.
- 166.	- 166.
149.56	149.56
- 118.58	- 118.58
- 74.446	- 74.446
- 31.458	- 31.458

Validation of Derived Plant Model



- Damped solution with initial vertical velocity



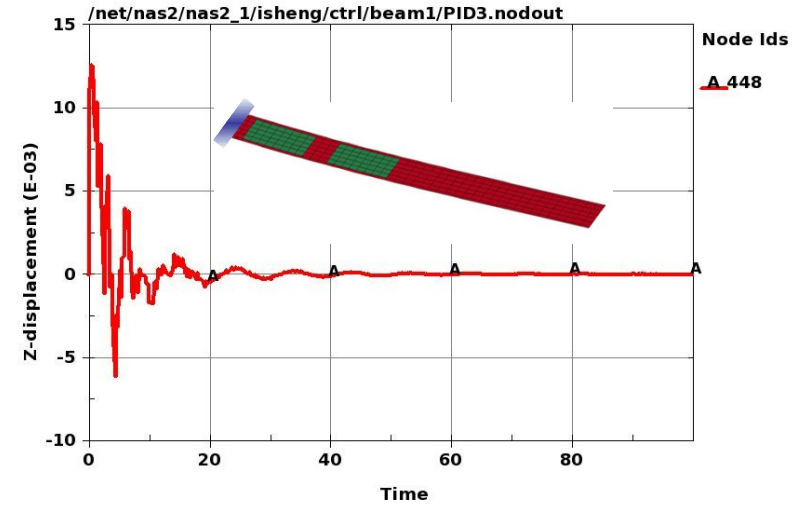
- Solution with initial step-loading

PIDCTL and DELAY for Control

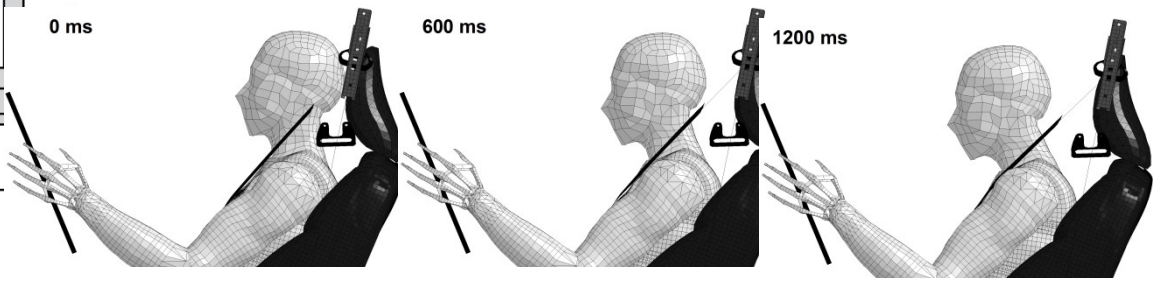
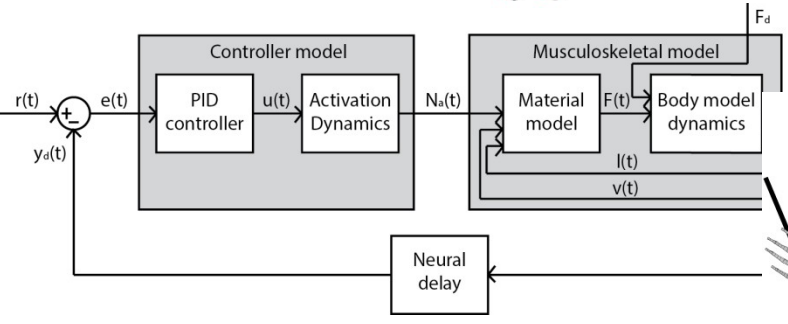
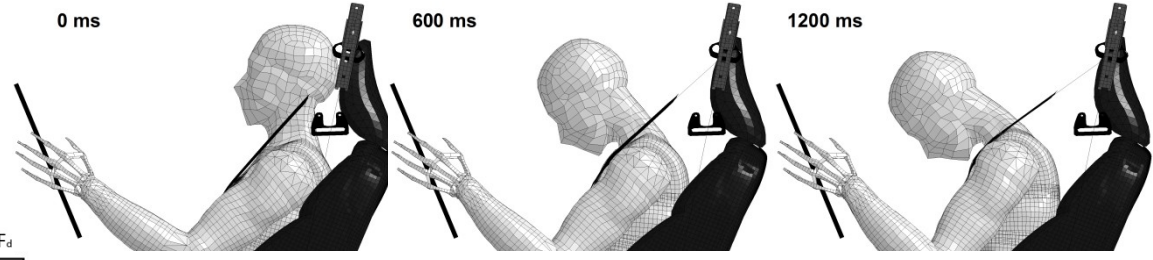
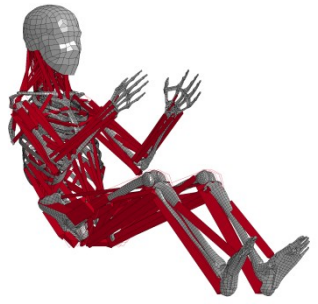


```

*DEFINE_CURVE_FUNCTION
$# lcid sidr sfa sfo offa offo dattyp
    201  0 1.000000 1.000000  0.000  0.000  0
DRX(1)
*DEFINE_CURVE_FUNCTION
$# lcid sidr sfa sfo offa offo dattyp
    1  0 1.000000 1.000000  0.000  0.000  0
PIDCTL(101, 0.,0, 14.273400,0,0.,0,  3.31570,0,0,0,0,0,0)+
PIDCTL(102, 0.,0, -0.951E+01,0,0.,0, -0.01200,0,0,0,0,0,0)+
PIDCTL(201, 0.,0, -42.910800,0,0.,0, -0.51480,0,0,0,0,0,0)+
PIDCTL(202, 0.,0, 367.32540,0,0.,0,  3.6699,0,0,0,0,0,0)
    
```

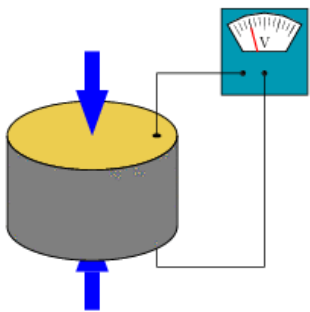


Vibration Control



- *Piezoelectric effects:*

- *Direct, sensor, effect:* Piezoelectric Material will generate electric potential when subjected to mechanical stress.
- *Inverse, actuator, effect:* Application of an electric field (voltage) results in mechanical strain.



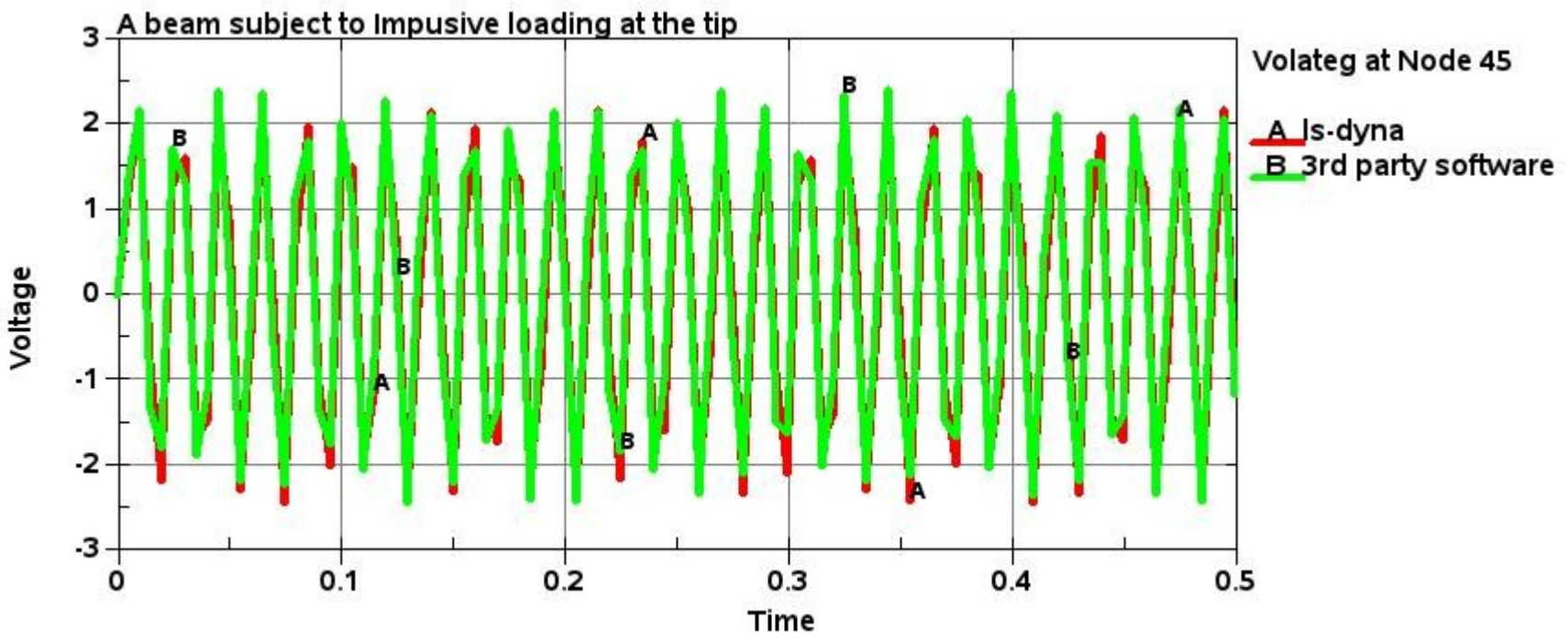
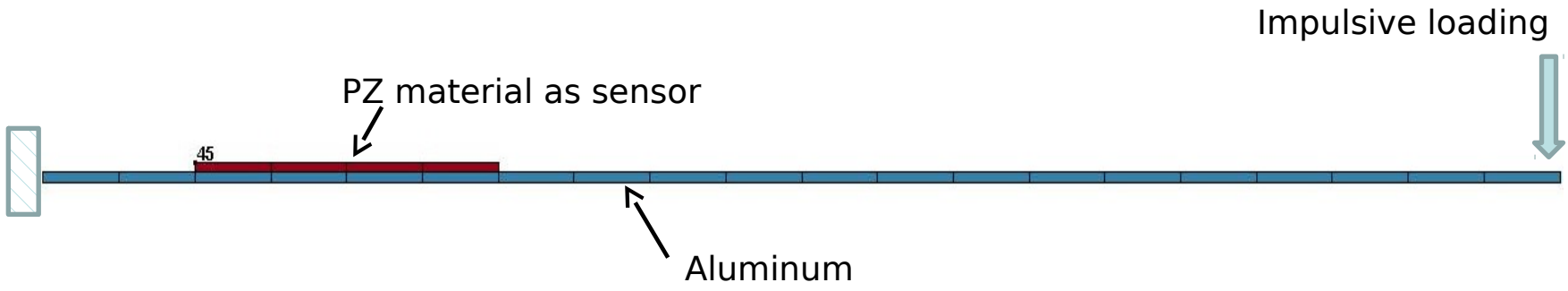
Sensor for wheel pressure

$$\begin{aligned} [\sigma] &= [c^E] \varepsilon - [e]^T E \\ \mathbf{D} &= [e] \varepsilon + [d^S] E \end{aligned}$$

- LS-DYNA

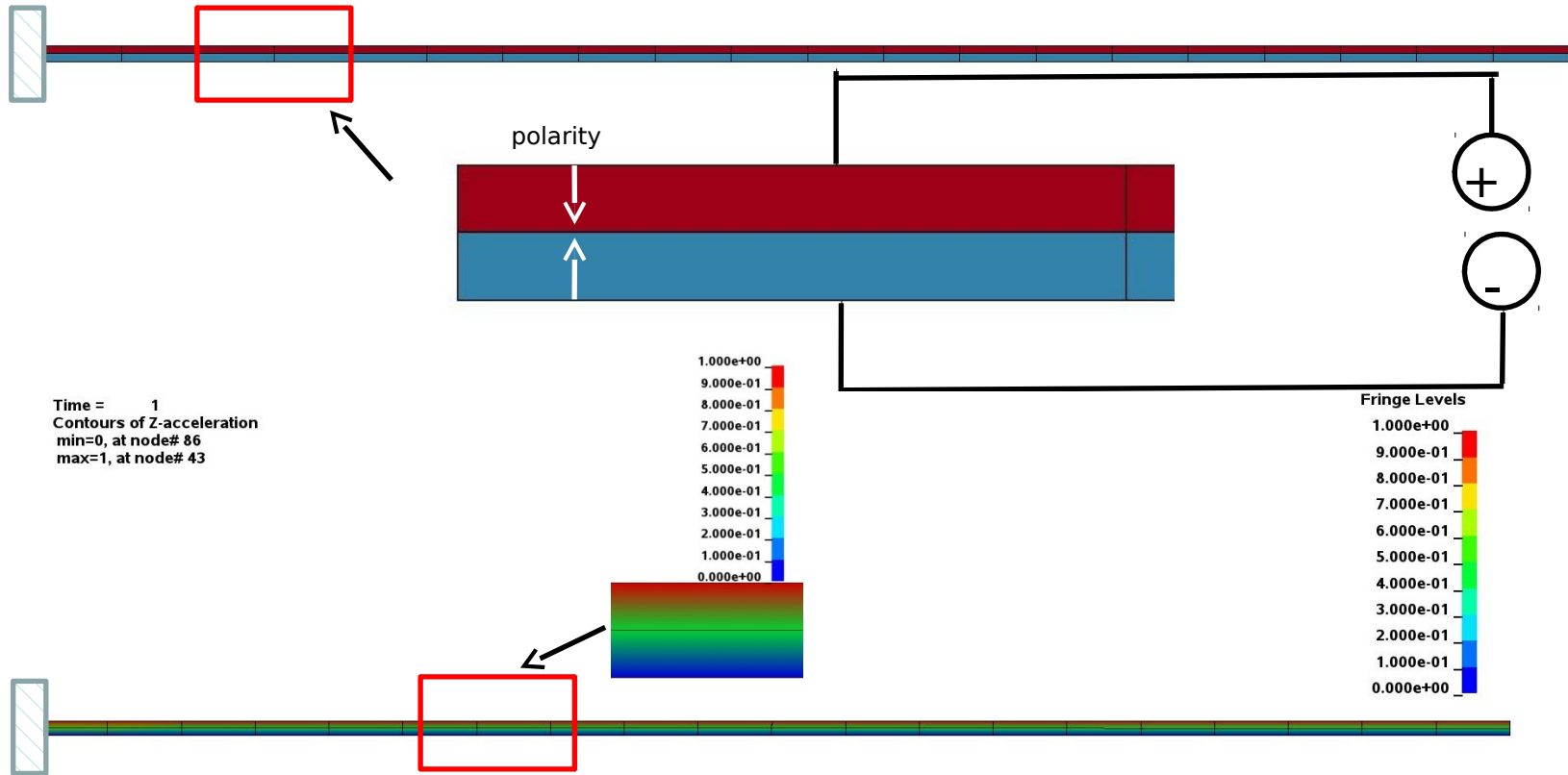
- *MAT_ADD_PZELECTRIC for PZ coefficients and dielectric coefficients
- *BOUNDARY_PZEPOT for electric potential specification

Validation of direct effect, sensor



Validation of inverse effect, actuator

- Bimorph beam subject to 1-V across the thickness



Voltage distribution

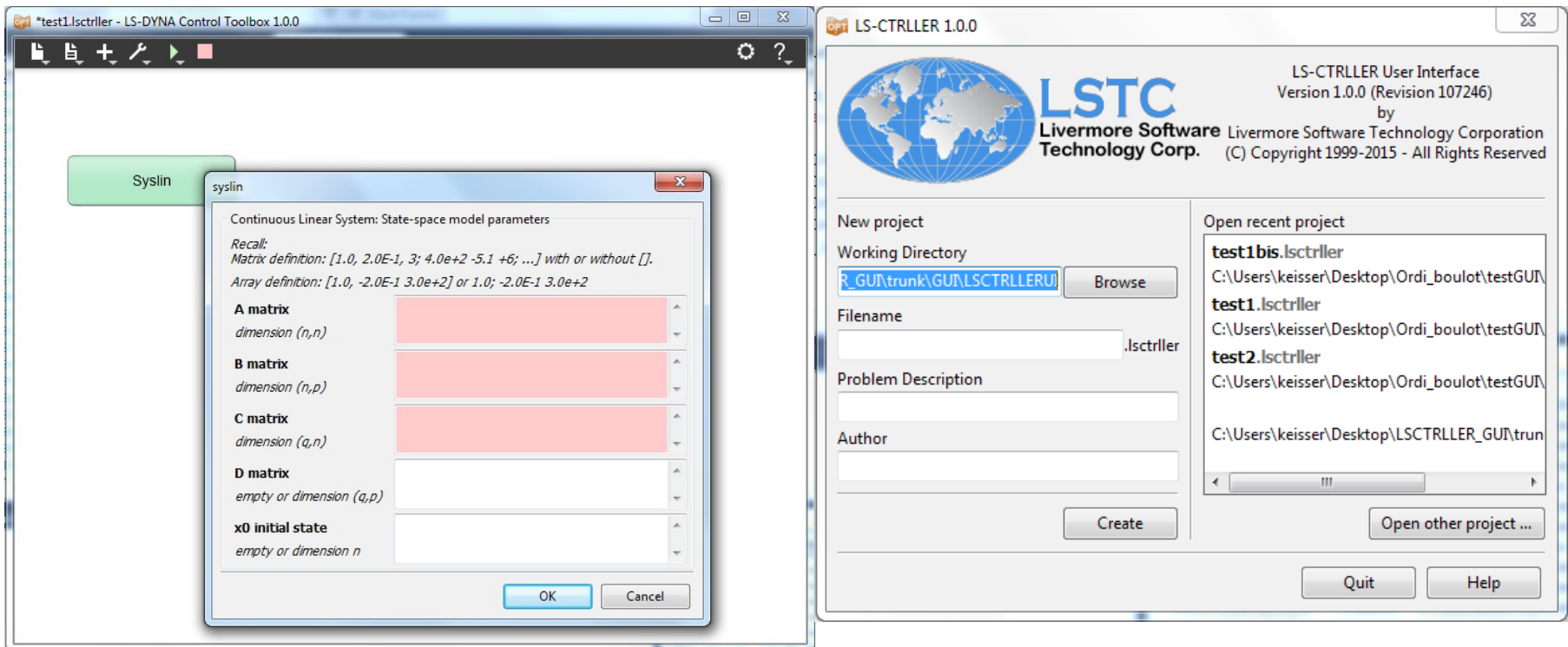
Tip displacement:

LS-DYNA: 3.33×10^{-7} vs. theoretical Sol. of 3.43×10^{-7}

Control System GUI

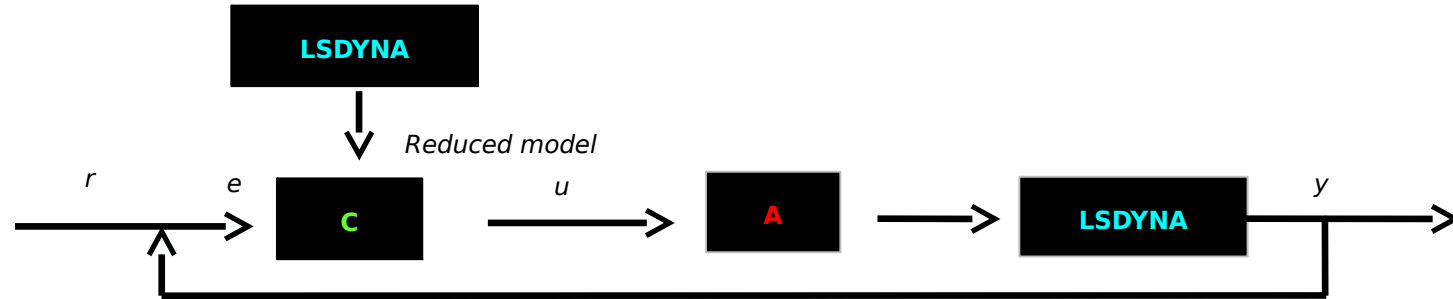


- Currently available: System definition
- To be available in 6 months: control tools, system connections, running ls-dyna solver
- To be available in one year: model reduction and analysis
- Long term: graphical result viewing



Next Step

- Achieve in two years



- Gather opinions from potential users
 - Improve currently implemented capabilities with more testing
 - More applications like MBS control, vibration control and acoustic control with piezoelectric material
 - More FEM model reduction methods and applications
- Thanks to
 - Katharina Witowski/Dynamore for guiding GUI implementation
 - François-Henri Rouet and Cleve Ashcraft for offering consultation for C. Keisser
 - Zhidong Han for enhancing PIDCTL implementation

Summary

Our ultimate goal is to deliver one highly scalable software to replace the multiplicity of software products currently used for analysis in the engineering design process. ***Only one model is needed and created.***

Capabilities

Multi-physics and Multi-stage

Structure + Fluid + EM + Heat Transfer

I mplicit + Explicit

Multi-scale

Accurate failure predictions

Multi-formulations

linear + nonlinear + peridynamics + ...

Future

- New features and algorithms will be continuously implemented to handle new challenges and applications
 - Electromagnetics,
 - Acoustics,
 - Compressible and incompressible fluids
 - Isogeometric shell & solid elements, isogeometric contact algorithms
 - Discrete elements
 - Peridynamics
 - Simulation based airbag folding and THUMS dummy positioning
 - Control systems and links to 3rd party control systems software
 - Composite material manufacturing
 - Battery response in crashworthiness simulations
 - Sparse solver developments for scalability to huge # of cores
 - Multi-scale capabilities are under development



Conferences



German LS-DYNA Forum 2016
October 10-12 Welcome Kongresshotel, Bamberg,
Germany



Nordic Users' Conference 2016



LSTC
Livermore Software
Technology Corp.

